

Plantwide control of an SO₂ abatement plant

by

Minèt Crafford

A dissertation submitted in partial fulfilment
of the requirements for the degree

Master of Engineering (Chemical Engineering)

in the

Department of Chemical Engineering
Faculty of Engineering, the Built Environment and Information
Technology

University of Pretoria
Pretoria

August 2023

Plantwide Control of an SO₂ Abatement Plant

Abstract

This study focused on an SO₂ abatement plant for a platinum group metal (PGM) smelting electric furnace. A systematic approach, using a simulated model of the plant, was followed to investigate plantwide control measures and thereby refine the plant's control philosophy. A steady-state model of a Wet gas Sulfuric Acid plant was developed using Aspen HYSYS software. The model was converted to a dynamic model to enable the evaluation of interactions within the process. This dynamic model was used while implementing a top-down, bottom-up plantwide control procedure. The results produced a control structure by which the first converter's inlet temperature controls the final SO₂ concentration. The feed gas heater's (second heater in the system) outlet temperature is controlled by varying the steam flow rate, which is used as a means of disturbance rejection.

Furthermore, using a dynamic model to implement a systematic plantwide control procedure eliminates the need to develop complex mathematical models while providing the opportunity to continuously validate the decisions made and selected manipulated and controlled variable pairings. Additional benefits of using a dynamic simulation model to implement a plantwide control model are:

- It provides a link between steady-state optimisation and process control.
- Self-optimising control is considered.
- Improved understanding of the process and interactions in the process.
- Provides a base model with the possibility to apply the solution to similar plants with minimal adjustment.
- The opportunity of implementing dynamic matrix control or model predictive control models to live plants (software dependent).
- Constant consideration of the control and operation of the plant as well as the overall (plantwide) control objective.

Keywords: plantwide control, acid plant, dynamic model, SO₂ abatement.

Acknowledgements

I sincerely thank my supervisor, Professor Philip de Vaal, for his valuable advice and support throughout my studies. I am also deeply indebted to Doctor Kevin Brooks, my co-supervisor, for his insight and extensive knowledge of control systems and HYSYS software. Without the guidance of my supervisors, completing this work would not have been possible.

I cannot begin to express my thanks to my husband for his unwavering support and encouragement and for granting me the time to complete this dissertation. I also wish to thank my parents, in-laws, brother, sister, and friends for their encouragement and patience throughout this project.

Contents

Abstract	ii
Acknowledgements	iii
List of Figures	vi
List of Tables	viii
Abbreviations	ix
1 Introduction	1
2 Literature	4
2.1 Processing of Platinum Group Metals	4
2.2 Acid Plants	6
2.2.1 Conventional	6
2.2.2 WSA Plant	8
2.2.3 Sulfacid®	8
2.3 Acid Plant Design	9
2.3.1 Process Parameters	9
2.3.2 Converter and Converting	9
2.3.3 Acid production	13
2.3.4 Condensation	14
2.3.5 Temperature Control	15
2.4 Plantwide Control	15
3 Methodology	20
3.1 Model Properties	20
3.2 Steady-State Model	25
3.2.1 Dust Removal	25
3.2.2 Wet Gas Cleaning	26
3.2.3 Auxiliary Areas	27
3.2.3.1 Cooling water	27
3.2.3.2 Effluent Treatment	29
3.2.4 Acid Plant Area	30

3.3	Dynamic Model	33
3.3.1	Model Conversion	33
3.3.2	Dynamic Controllers	36
4	Results and Discussion of the Plantwide Control Application	45
4.1	Choice of Methodology	45
4.2	Step 1: Identification of Process Variable	45
4.3	Step 2: Selection of Manipulated Variable	45
4.4	Step 3: Setting Production Rate	54
4.5	Step 4: Regulatory Control	54
4.6	Step 5: Supervisory Control	62
4.7	Step 6: Real-Time Optimisation	64
4.8	Step 7: Model validation	66
5	Conclusion and Recommendations	74
6	References	76

List of Figures

Figure 1: Typical SO ₂ abatement plant block flow diagram.....	1
Figure 2: Basic flow diagram of process considered.....	2
Figure 3: Basic flowsheet of PGM processing (Adapted from Mbohwa & Mabiza (2015), Figure 1).	4
Figure 4: SO ₂ conversion as a function of equilibrium temperature.	11
Figure 5: Equilibrium curve, heat-up path, and interbed cooling.	12
Figure 6: Example of reactor types tested.	22
Figure 7: Equilibrium reactor basis screen.	23
Figure 8: PFR specification requirements.....	23
Figure 9: Overall steady-state model.....	24
Figure 10: Hot gas cooling and cleaning flowsheet.	26
Figure 11: Wet gas cleaning process flowsheet.	27
Figure 12: Cooling water cycle flowsheet.	29
Figure 13: Neutralisation of effluent flowsheet.....	29
Figure 14: Traditional WSA flowsheet (Rosenberg (2006), Figure 4).....	30
Figure 15: Steady-state WSA flowsheet.....	32
Figure 16: <i>Adjust</i> used to control temperature.....	34
Figure 17: Steady-state to dynamic model by combining similar coloured (circled) heater-cooler pairs and connecting recycled stream (arrows).....	35
Figure 18: Feed gas flow controller – parameters.	38
Figure 19: Step test to tune a controller.....	39
Figure 20: Example of step test resulting in wave-type system response.....	39
Figure 21: Dynamic integrator parameters.	40
Figure 22: DMCplus Controller initial model test.....	41
Figure 23: Step test results – initial.	42
Figure 24: Step response – increased sampling frequency.	43
Figure 25: Step response – long time delay.	44
Figure 26: Steam valve nozzle parameters.	44
Figure 27: Dynamic model – variables used for control.....	47
Figure 28: Dynamics specification of blowers.....	49
Figure 29: Effect of step tests on final SO ₂ concentration.....	52
Figure 30: Total duty during step tests.	53
Figure 31: Final conversion response when stepping MVs while controlling converter inlet temperature.	55
Figure 32: Effect on Total Duty when controlling the final SO ₂ concentration.	56

Figure 33: Effect of disturbance variable on other process variables.....	57
Figure 34: Effect of disturbance variable, when controlling steam flow rate.....	58
Figure 35: Step response of CVs contributing to total duty to a disturbance change.	59
Figure 36: Effect of remaining 5 MVs on the total duty.	59
Figure 37: Effect of remaining 5 MVs on the final SO ₂ concentration.....	60
Figure 38: Effect of remaining DOFs on duty and HX-003's outlet temperature.....	61
Figure 39: Using MV FA-003 fan speed to control stream 8FG temperature.	61
Figure 40: Step tests when MV FA-003 fan speed is used to control 8FG's temperature. ...	62
Figure 41: Temperature control (above acid dewpoint) by changing hot air flow rate.	63
Figure 42: Block flow diagram of MPC.	64
Figure 43: Process control and optimisation levels (adapted from Seborg <i>et al.</i> (2010), Figure 19.2).	66
Figure 44: Parameter trial setup for open loop step responses.	67
Figure 45: Open loop step response of manipulated variables (SISO) – typical move disabled.	69
Figure 46: Open loop step response of manipulated variables (SISO) – typical move enabled.	70
Figure 47: Open loop step response of manipulated variables (SISO) – typical move enabled, only grades A-C.	71
Figure 48: Frequency uncertainty of the open loop step response using FIR parameter trials with 10 minutes to steady state.	72
Figure 49: Time uncertainty of the open loop step response using FIR parameter trials with 10 minutes to steady state.	73

List of Tables

Table 1: Key parameters of common acid plants Schlesinger <i>et al.</i> (2011).	9
Table 2: Components and fluid packages.	21
Table 3: Input and output parameters for various reactor types.....	23
Table 4: Steady state model inlet stream properties.....	25
Table 5: Key variables.....	46
Table 6: <i>DMCplus Controller</i> step test setup.	49
Table 7: Scaled steady-state gains.	50
Table 8: Dead time (in seconds).	51

Abbreviations

CSTR	Continuous Stirred Tank Reactor
CV	Controlled Variable
DMC	Dynamic Matrix Control
DOF	Degree of Freedom
EOS	Equation of State
ESP	Electrostatic Precipitator
FIR	Finite Impulse Response
GCT	Gas Cooling Tower
LLE	Liquid Liquid Equilibrium
LMTD	Log Mean Temperature Difference
LPG	Liquid Petroleum Gas
MIMO	Multiple-Input-Multiple-Output
MPC	Model Predictive Control
MV	Manipulated Variable
NRTL	Non-Random-Two-Liquid
OP	Output
PFHE	Plate and Frame Heat Exchanger
PFR	Plug Flow Reactor
PGM	Platinum Group Metals
PI	Proportional-Integral
PID	Proportional Integrating Derivative
PR	Peng-Robinson
PRBS	Pseudo Random Binary Sequence
PV	Process Variable
RFS	Radial Flow Scrubber
RTO	Real-time optimisation
SISO	Single-Input-Single-Output
SP	Set Point
SRK	Soave-Redlich-Kwong
VLE	Vapour Liquid Equilibrium
WESP	Wet Electrostatic Precipitator
WGCP	Wet Gas Cleaning Plant
WSA	Wet gas Sulphuric Acid
WSA-DC	Wet gas Sulphuric Acid Double Condensation

1 Introduction

South Africa is the world's largest producer of platinum group metals (PGM) worldwide (Jones, 2005). During the smelting process, SO₂ gas is liberated from the minerals. South African legislation dictates that sulphide smelting operations must comply with specific emission standards. These standards include ground-level concentrations¹ as well as point source emissions² associated with the respective plants. At PGM smelting facilities where low-concentration SO₂-containing off-gas is vented directly to the atmosphere, an SO₂ abatement plant is required to ensure compliance and prevent future penalties and/ or curtailments.

If the off-gas temperature is lower than the sulphuric acid dew point temperature, SO₂ in the off-gas can react with water (H₂O) and form corrosive sulphuric acid (H₂SO₄). Therefore, temperature control is of crucial importance in this plant.

A typical SO₂ abatement plant can effectively be grouped into three separate plants or plant areas:

- Hot gas cleaning area
- Wet gas cleaning area
- Acid plant.

Other supporting plant areas include a cooling water plant, effluent treatment plant, acid storage, instrument and plant air, fire protection, process and potable water, liquid petroleum gas (LPG) storage, and substations. A typical SO₂ abatement plant flowsheet, including key equipment per plant area, is shown in Figure 1.

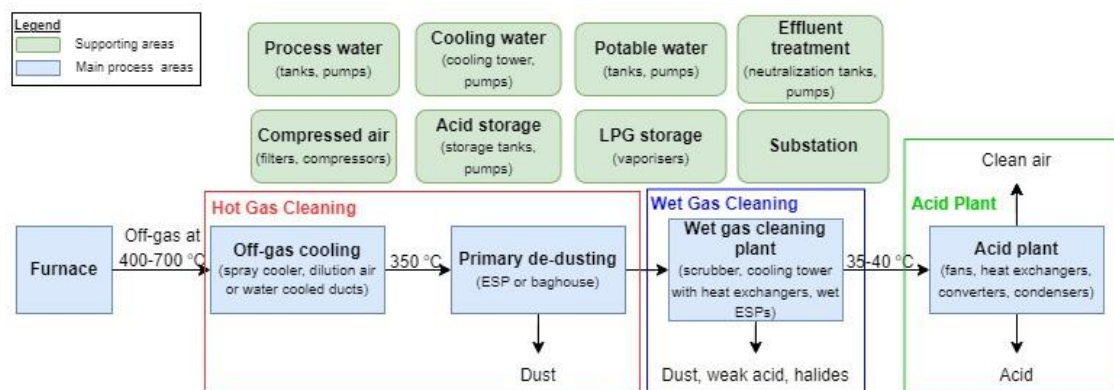


Figure 1: Typical SO₂ abatement plant block flow diagram.

¹ Section 9(1) of the NEM:AQA, 2004 (Act no. 39 of 2004) as established in Government Notice No. 1210, Gazette No. 32816, Section 3

² Section 21(1) (a) of the NEM:AQA, 2004 (Act no. 39 of 2004) as published under Government Notice No. 893, Gazette No. 37054, Subcategory 4.16: Smelting and Converting of Sulphide Ores

The plant considered for this study serves as a general approach to investigating plantwide control of an SO₂ abatement plant, focusing on control of the acid plant. This study can be expanded by evaluating the other plant areas and their interaction with the acid plant. The plant is based on similar SO₂ abatement plants at PGM smelting facilities in South Africa, with differences in operating and process conditions. Therefore, the study can be expanded by considering specific processes and cyclical conditions when converter cycles are present.

Topsoe developed the Wet gas Sulphuric Acid (WSA) process during the early 1980s to remove low concentrations (typically 0.2 – 6.5 %SO₂) of sulphur compounds from gas cost-effectively. The WSA process has impurity and dust inlet requirements similar to conventional acid plants, such as double contact double absorption (DCDA). However, the WSA plant has a higher saturated gas temperature since some water exits in the tail gas instead of being absorbed into sulphuric acid. This technology is desirable in the African environment as it utilises extensive heat integration, has lower water and power consumption requirements, and has the added benefit of producing steam. This technology has been installed at more than 100 sites across the globe (Rosenberg, 2006, Schlesinger, King, Sole *et al.*, 2011). A basic flow diagram of the process considered in this study is given in Figure 2.

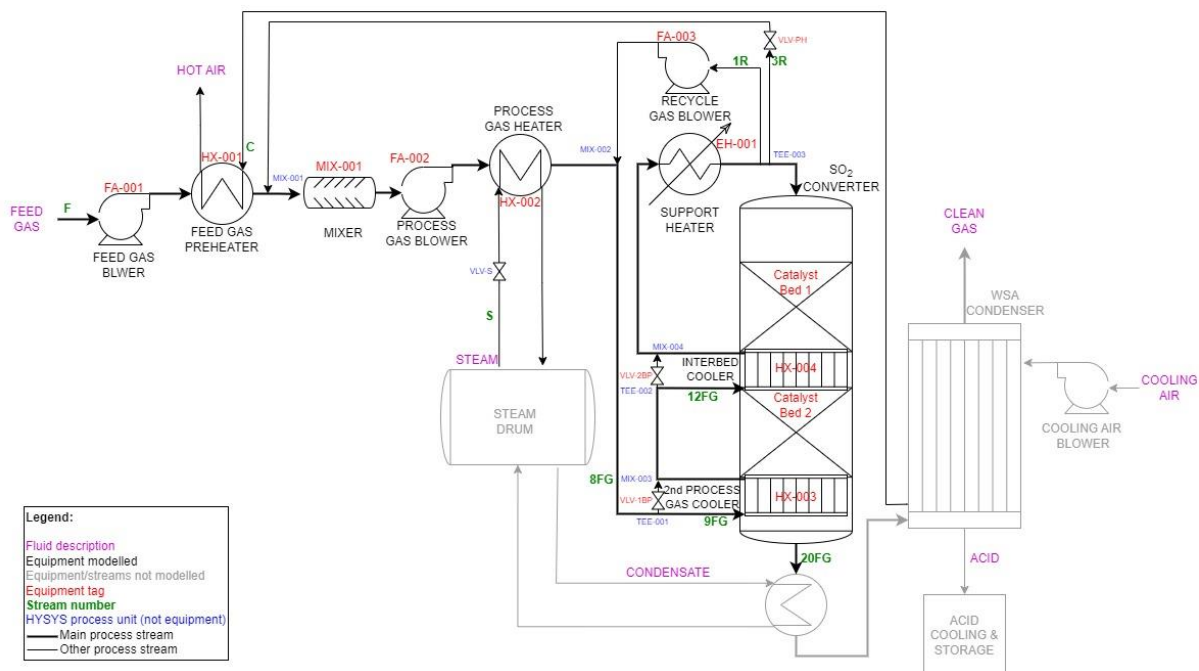


Figure 2: Basic flow diagram of process considered.

The overall plant consists of various areas, all involving multiple processing units that interact with each other both in a given plant area as well as interacting across plant areas. As previously mentioned, temperature control is important throughout the plant due to the off-gas

composition (presence of SO₂). These interacting units include multiple heat exchangers, pumps, and compressors.

The planned SO₂ abatement plant is designed to incorporate base and advanced regulatory controls, such as cascade, ratio, and feedforward control. Plantwide control and advanced process control measures (such as model predictive control – MPC) have not yet been considered or incorporated into the plant design. This research aimed to systematically investigate plantwide control measures, including using a simulated model of the plant, to enable refinement of the plant's control philosophy.

This study considered plantwide control strategies to evaluate the unit-to-unit interactions, choice of manipulated and controlled variables and overall control strategy (or philosophy) of the entire plant. In essence, this study aims to move from a traditional control system design approach to a model-based one (Seborg, Mellichamp & Edgar, 2010) by applying a plantwide control strategy to a digital plant model.

This model-based method required the development of a digital model of the process, consequently enabling evaluation of the unit-to-unit interactions and dynamic analyses of interactions throughout the plant. Furthermore, this dynamic digital model provided a simulated environment that could assist with the following (Larsson & Skogestad, 2000, Seborg *et al.*, 2010):

- Evaluation of the controllability of the plant.
- Providing a basis for model-based controller design methods.
- Incorporation of the control law.
- Assessment of alternative control strategies, including determining (preliminary) controller setting values.

2 Literature

2.1 Processing of Platinum Group Metals

South Africa is the world's largest producer of PGMs (Jones, 2005). Precious metals are the primary products of the platinum ores processed in South Africa, whereas platinum is often produced as a by-product of base metal, especially nickel, processing (Jones, 2005).

The original ore undergoes various processing steps to increase the grade of the valuable components, such as platinum. A basic flowsheet is provided in Figure 3. The particle size of the ore is reduced by crushing and milling. After that, the flotation step concentrates the sulphides. The sulphide concentrate is dried and treated in a smelting furnace, followed by converters. Each of the previously mentioned steps produces two layers: matte and slag. The slag contains the gangue, oxide- and silicate-rich minerals, and the matte contains the valuable PGM-containing copper-nickel product. The slag is granulated and sometimes subjected to flotation to increase PGM recovery before being discarded. The furnace matte undergoes further processing in the converter, and the converter matte is further refined to extract the precious metals from the base metals (Jones, 2005).

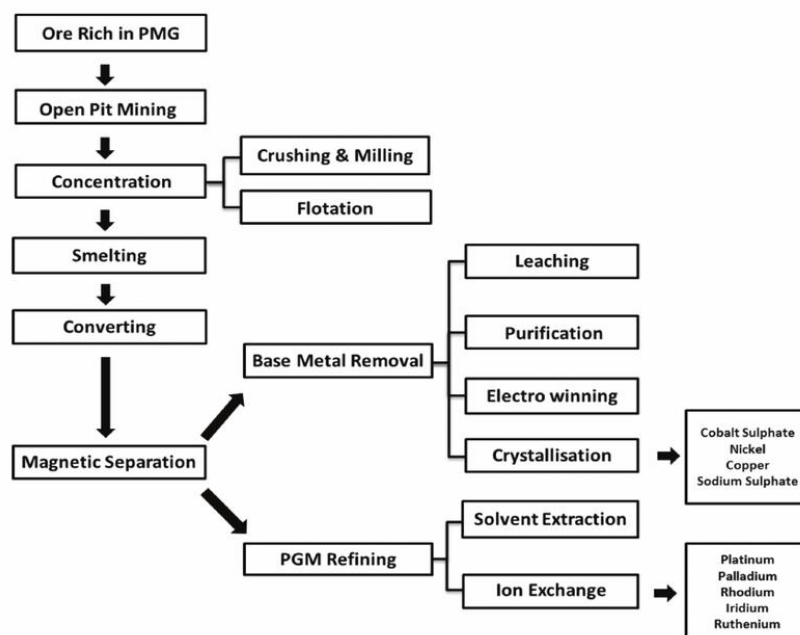


Figure 3: Basic flowsheet of PGM processing (Adapted from Mbohwa & Mabiza (2015), Figure 1).

During the smelting and converting process, the sulphide-containing ores are oxidised, and SO_2 is liberated from the material. The liberated SO_2 exits the smelter and converter in the off-gas stream and is eventually emitted to the atmosphere if not removed from the gas stream.

The off-gas is typically treated in an electrostatic precipitator and then emitted to the atmosphere via a stack. The low concentration of SO₂ in the furnace off-gas and the cyclical production from the converters make the conversion of the SO₂ to sulphuric acid challenging (Jones, 2005). However, removing SO₂ from the off-gas is becoming more critical in the overall attempt to reduce emissions in the platinum mining and production process in South Africa (Mbohwa & Mabiza, 2015).

South African legislation dictates that sulphide smelting and converting operations must comply with certain emission standards. These standards specify that point source emissions³ of SO₂ for processes where sulphide ores are roasted, smelted, calcined or converted must not exceed 1 200 mg / Nm³ and that such facilities must install equipment to treat them and reduce the sulphur content of the off-gases emitted to the atmosphere. Control of the point source emissions is the primary goal of the SO₂ abatement plant.

Typically, metallurgical complexes follow similar steps to treat their SO₂-containing off-gas (Schlesinger *et al.*, 2011):

1. If required, primary off-gas cooling to 350°C using a spray cooler or water-cooled ducts. The spray cooler has the added advantage of removing dust particulates whilst cooling the off-gas.
2. De-dusting in a baghouse or dry electrostatic precipitator (ESP). The off-gas exits this step between 300 °C and 350 °C.
3. Further conditioning in a wet gas cleaning plant. Usually, wet gas cleaning plants consist of comparable equipment starting with a scrubber for further de-dusting and removal of other impurities, such as HCl and HF, in the off-gas stream, a cooling tower for further cooling and wet electrostatic precipitators for final dedusting and removal of acid mist. The treated off-gas contains less than 1 mg / dNm³ (dry normal cubic meter) dust (King, Davenport & Moats, 2013).
4. The conditioned and cooled off-gas leaving the wet gas cleaning plant at 35°C to 40°C is treated in an acid plant to remove the SO₂ from the gas stream and ensure clean off-gas is emitted to the atmosphere. Different technologies for acid plants are available and discussed in Section 2.2.
5. Depending on the off-gas' SO₂ and acid mist content, a tail gas scrubber can be added for further conditioning prior to atmospheric emission.

³ Section 21(1) (a) of the NEM:AQA, 2004 (Act no. 39 of 2004) as published under Government Notice No. 893, Gazette No. 37054, Subcategory 4.16: Smelting and Converting of Sulphide Ores

As a rule of thumb, smelter or furnace off-gas usually equals $\sim 100 \text{ Nm}^3 / \text{h} / \text{m}^2$ of furnace area. Therefore, based on a compilation of furnace parameters from Jones (2005), nominal furnace off-gas flow rates of South African PGM smelters average $18\,660 \text{ Nm}^3 / \text{h}$. This value was used to define the nominal input flow rate of the feed gas in this study.

It is, however, essential to note that some of these smelters have combined furnace and converter off-gas streams, whilst others have either converter off-gas or smelter off-gas. Due to the cyclic nature of converter operation, off-gas streams combining the converter and furnace off-gas have additional complexities associated with the significant variation in process conditions such as flow rate and SO_2 concentration.

Electric furnaces typically produce off-gas with temperatures between 400 and $800 \text{ }^\circ\text{C}$ and SO_2 concentrations of $2\text{-}5 \text{ vol}\%$. Peirce-Smith converters generate off-gas with $8\text{-}15 \text{ vol}\%$ SO_2 concentrations at a significantly higher temperature of $1\,200 \text{ }^\circ\text{C}$ (Schlesinger *et al.*, 2011).

2.2 Acid Plants

2.2.1 Conventional

Conventional contact type acid plant is the most common technology for converting SO_2 gas to sulphuric acid. In this process, the off-gas is first cooled and cleaned (dust removed); thereafter, it is dehydrated by contact with 93% sulphuric acid to avoid the untimely sulphuric acid formation and corrosion in downstream equipment (King *et al.*, 2013, Schlesinger *et al.*, 2011). This step reduces the water content in the off-gas via absorption and is followed by catalytic oxidation at $420 \text{ }^\circ\text{C}$. A common catalyst used for this step is vanadium pentoxide (V_2O_5) which promotes the conversion of SO_2 to SO_3 . The newly formed SO_3 in the off-gas (at $\sim 200 \text{ }^\circ\text{C}$) is absorbed into a 98.5% sulphuric acid mixture and blended with the acid used in the drying stage. This acid product can either be used for leaching or sold (Schlesinger *et al.*, 2011).

In double-absorption plants, the off-gas goes through three catalyst beds before the first absorption step. It enters another set of heat exchangers and a catalyst bed before the final absorption of SO_3 into H_2SO_4 . Alternatively, the first absorption step occurs after the off-gas has passed through two catalyst beds, and the final absorption step occurs after the off-gas passes through the remaining two catalyst beds. A conventional double absorption plant will have an SO_2 capture efficiency greater than 99.7% . Lower capturing efficiencies are achieved in single absorption acid plants due to a lower SO_2 to SO_3 conversion rate. As the name implies, a single absorption plant has only one absorption step following the three to four catalyst beds (Schlesinger *et al.*, 2011).

The primary purpose of the acid plant is to remove the toxic SO_2 (greater than 100 ppm) from the off-gas stream. Key equipment in a typical acid plant is the main blower(s) used to move the off-gas through the wet gas cleaning plant and direct it to various heat exchangers and the converter(s). In the converter, the off-gas passes through a catalyst bed where the SO_2 is oxidised to SO_3 . If the entering off-gas has a volumetric ratio of O_2 to SO_2 less than 1, additional air is added to ensure near-complete conversion (Schlesinger *et al.*, 2011).

The catalyst required to speed up the oxidation reaction generally consists of V_2O_5 , K_2SO_4 , Na_2SO_4 , inert SiO_2 , and sometimes Cs_2SO_4 . Catalyst is usually manufactured in a ring or star-ring shape with a 10 mm diameter and 10 mm long. This shape and size promote longevity by minimising dust pollution, leading to a smaller pressure drop in the catalyst bed. The temperature of the off-gas entering the catalyst bed is controlled to above the ignition temperature of $360\text{ }^\circ\text{C}$ to promote a faster reaction rate. However, if the temperature exceeds $650\text{ }^\circ\text{C}$, the catalyst can be damaged and deactivated; therefore, the temperature is typically controlled to between $400\text{ }^\circ\text{C}$ and $440\text{ }^\circ\text{C}$ to achieve the optimal conversion rate (Schlesinger *et al.*, 2011).

An additional temperature consideration for the catalytic oxidation reaction is the equilibrium curve. The SO_2 - SO_3 reaction achieves a higher conversion rate at lower temperatures albeit with a slower reaction rate; therefore, the off-gas is cooled between catalyst beds to ensure an overall higher conversion (King *et al.*, 2013). The heat exchangers between the catalyst bed utilise the energy from the heat of the reaction to heat the incoming gas from the wet gas cleaning plant (King *et al.*, 2013, Schlesinger *et al.*, 2011). Schlesinger *et al.* (2011) state that the reduced concentration of N_2 in off-gas with higher SO_2 content results in higher catalyst bed temperatures, and similarly, the highest catalyst temperature is obtained in the first catalyst bed, where the highest concentration of SO_2 is.

The gas-to-gas heat exchangers used in acid plants generally transfer heat between $10\ 000\ \text{MJ / h}$ and $80\ 000\ \text{MJ / h}$ (about 2.5 to 10 MW). Due to the high variation of off-gas flow rates and SO_2 concentration experienced by acid plants, especially when batch-type converting is used, heat exchangers must be designed and sized to accommodate these variable off-gas conditions.

The acid plant tail gas often contains an acid mist which can be scrubbed with a calcium hydroxide (lime) or sodium carbonate hydroxide solution before emission to the atmosphere (Schlesinger *et al.*, 2011).

2.2.2 WSA Plant

Conventional acid plants are generally designed to treat off-gas streams with higher SO₂ concentrations, typically obtained during copper smelting and converting activities. However, the lower concentration of SO₂ in PGM smelting facilities' off-gas requires some adjustment to conventional technologies. Topsoe developed the Wet gas Sulphuric Acid process to treat wet off-gas with lower concentrations of SO₂: 0.2 – 6.5 vol% (Rosenberg, 2006). The key difference between the WSA and conventional acid plants is the higher saturated gas temperature due to the presence of water – the water is not absorbed into sulphuric acid but remains present in the gas. The wet off-gas requires a specifically formulated catalyst for the oxidation reaction in the converter but is otherwise similar to the conventional acid plant process. The oxidation reaction is accomplished in two to three catalyst beds, utilising interbed cooling to cool down the off-gas before entering the subsequent catalyst bed.

The interbed cooling is achieved by indirect heat exchange with either a molten salt circulation system, a steam boiler or incoming process gas. A hydration reaction occurs at temperatures below 290 °C, and SO₃ reacts with water to form sulphuric acid. Temperature control is therefore important to hinder the untimely formation of sulphuric acid. A glass tubed condenser is positioned after the converter to indirectly cool the sulphuric acid gas with air. The condensed concentrated sulphuric acid drops out at the bottom of the condenser and is further cooled with recycled concentrated acid via a plate and frame heat exchanger. The clean gas exits at the top of the condenser at about 100 °C. Acid mist can be removed from the clean gas via a wet ESP or candle filter before emission to the atmosphere, increasing the sulphur-capturing efficiency even further (Schlesinger *et al.*, 2011).

2.2.3 Sulfacid®

Sulfacid® produces weak sulphuric acid (10 – 20 %) from off-gas with SO₂ concentrations of less than 1 vol%. Although these concentrations are not often experienced by PGM smelting and converting facilities, a high-level review of the technology is provided below.

The off-gas is cleaned (de-dusted) and cooled before undergoing an activated carbon catalytic reaction to produce sulphuric acid. The 30 °C to 80 °C saturated off-gas reacts with water and oxygen, and the produced acid is occasionally washed from the catalyst, producing the weak 10 % to 20 % acid. Usually, Sulfacid® plants are installed where a nearby operation can utilise the produced weak acid (Schlesinger *et al.*, 2011).

2.3 Acid Plant Design

2.3.1 Process Parameters

Table 1 summarises the key parameters of the acid plants mentioned above. Of the acid plants considered, it is evident that the WSA plant is best suited for the typical concentrations observed at PGM smelting and converting operations. Should the WSA plant be required to process off-gas with higher concentrations of SO₂, it can be altered to have two acid condensation stages. This altered Wet gas Sulphuric Acid-Double Condensation (WSA-DC) plant can process off-gas streams with up to 15 % SO₂ (Schlesinger *et al.*, 2011).

Table 1: Key parameters of common acid plants Schlesinger *et al.* (2011).

Parameter	Unit	Conventional single absorption	Conventional double absorption	WSA	Sulfacid®
Minimum SO ₂ concentration	vol%	4.5	6	0.6	0.5
Maximum SO ₂ concentration	vol%	10	14	6.5	1.0
Product acid concentration	%H ₂ SO ₄	93-98.5	93-98.5	98	10-20
SO ₂ capture efficiency	%	98-99	99.7-99.95	98-99	65-90

2.3.2 Converter and Converting

As previously mentioned, the converters used in acid plants consist of two to four catalyst beds. These catalyst beds are typically 500 mm to 1 000 mm thick, with an average of 620 mm for the first bed, 720 mm for the second bed, and 840 mm for the third bed. The increase in bed thickness provides longer residence times, enabling better conversion of the off-gas containing less SO₂ and more SO₃ than the gas into the initial bed. Due to the presence of interbed coolers, converters with four catalyst beds can be up to 20 m tall, with diameters ranging between 8 m and 16 m (King *et al.*, 2013). Generally, these converters and the supporting internal structures are stainless steel. King *et al.* (2013) provide graphs for estimating converter diameters, residence times, interbed temperatures, and catalyst beds required based on the feed-gas characteristics.

Gas flow through the catalyst beds is typically downward and in the range of 25 Nm³ / (min m²) of the top surface of the catalyst bed. The SO₂-bearing feed gas into the catalyst bed is required to be above the activation temperature to ensure that it does not deactivate the catalyst. However, as previously mentioned, the gas needs to be cooled between the different catalyst beds to obtain better overall conversion and ensure that the catalyst is not damaged. Typically, the feed gas is cooled to 425 – 440 °C. The most important control objective at the converter is to maintain the required constant inlet gas temperatures (King *et al.*, 2013).

The SO₂ to SO₃ equilibrium constant depends on temperature, feed gas composition (SO₂, O₂, and SO₃) and pressure. As previously mentioned, the equilibrium conversion of SO₂ is low at high temperatures. The oxidation reaction for SO₂ to SO₃ is shown in Equation 1 and the associated equilibrium equation in Equation 2, where PE_x is the equilibrium partial pressure, in bar, of component x calculated by multiplying the equilibrium mole fraction of component x with the total equilibrium gas pressure. Generally, it is safe to assume that the gas behaves as an ideal gas due to the low pressures (~100 kPa) in industrial converters (King *et al.*, 2013).



$$K_E = \frac{P_{SO_3}^E}{P_{SO_2}^E * P_{O_2}^E} \quad 2$$

Furthermore, the equilibrium constant's temperature dependency is given in Equation 3, with $-\Delta G^\circ_T$ as the Gibbs free energy of the reaction at the equilibrium temperature T_E , and R is the ideal gas constant. King *et al.* (2013) analysed published data on ΔG°_T as a function of temperature. They concluded that ΔG°_T , the standard free energy of change, could accurately be estimated with a linear, temperature-dependent equation, as shown in Equation 4. Rearranging Equation 3 and Equation 4 gives Equation 5, which can, in turn, be rearranged to calculate the equilibrium temperature, T_E (in Kelvin), A and B in Equations 4 and 5 are 0.09357 MJ / (kmolSO₂ K) and -98.41 MJ / kmolSO₂, respectively.

$$\ln(K_E) = \frac{-\Delta G^\circ_T}{RT} \quad 3$$

$$-\Delta G^\circ_T = AT + B \quad 4$$

$$\ln(K_E) = \frac{-AT_E - B}{RT_E} \quad 5$$

King *et al.* (2013) go on to rewrite the equilibrium constant, Equation 2, in terms of the equilibrium percentage of SO₂ converted/ oxidised (ϕ) and then combine it with Equation 5 to express the equilibrium temperature as a function of the percentage of SO₂ converted, shown in Equation 6, with α the volume percentage of SO₂ in the feed gas and γ the volume percentage of O₂ in the feed gas.

$$T_E = \frac{-B}{A + R \ln \left(\left(\frac{\phi^E}{100 - \phi^E} \right) \left(\frac{100 - 0.5\alpha \frac{\phi^E}{100}}{\gamma - 0.5\alpha \frac{\phi^E}{100}} \right)^{0.5} P_t^{-0.5} \right)} \quad 6$$

The equilibrium conversion as a function of temperature can now be visualised in Figure 4. For the low concentrations of SO₂ observed in the feed gas of PGM smelting facilities, varying concentrations of inlet gas composition have little effect on the equilibrium temperature and an increase in O₂ content results in a small increase in the equilibrium temperature or an increase in SO₂ conversion for similar temperatures.

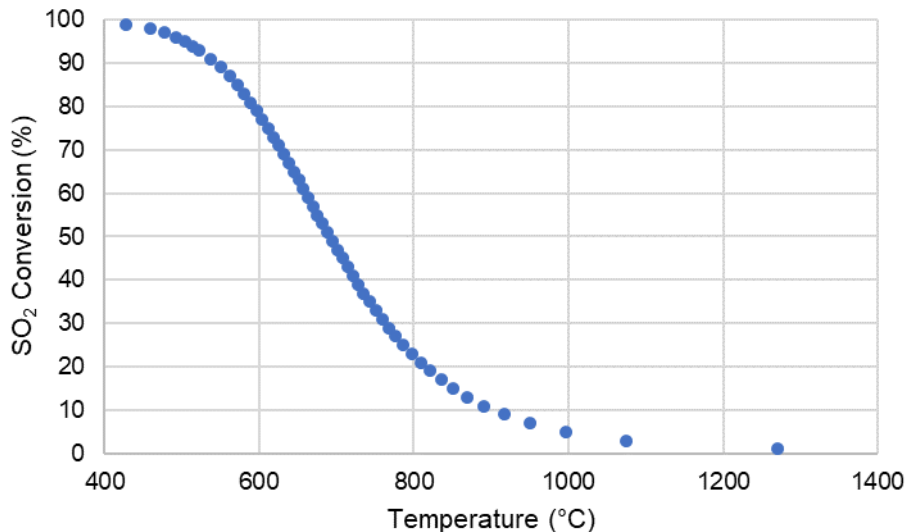


Figure 4: SO₂ conversion as a function of equilibrium temperature⁴.

As reaction 1 occurs, heat is generated, and consequently, the gas temperature increases as the gas travels through the converter bed. The gas follows a specific heat-up path before reaching the equilibrium curve temperature (Figure 4) and achieving equilibrium conversion. The heat-up path is dependent on the feed gas temperature and feed gas composition. The heat-up path can be determined by utilising component/mole balances for each of the elements in the feed gas (such as S, O, N, H, C), an enthalpy balance (enthalpy in feed gas = enthalpy in gas exiting converter bed), and the reaction 1 equation. It is assumed that H₂O, N₂ and CO₂ are inert; therefore, the N, H, and C balance is straightforward, and the amount of H₂O, N₂ and CO₂ in the exiting gas can easily be determined. The S, O, and enthalpy balance, along with Reaction 1, can then easily be used to determine the amount of SO₂ reacted (oxidised). These steps can be used to determine the amount of SO₂ oxidised for various feed gas compositions and temperatures. It will then become evident that higher conversion is achieved for lower feed gas temperatures. Decreased SO₂ oxidation percentage occurs for increased SO₂ concentrations in the feed gas, and the heat-up path exhibits a smaller gradient

⁴ For calculation of this equilibrium curve, the following assumptions were made using Equation 6: ambient pressure is 0.89 bar, inlet SO₂ and O₂ concentrations at 2 vol%, and 15 vol%, respectively.

(heating rate). Increased SO_2 concentrations in the feed gas also result in higher temperatures in the gas exiting the catalyst bed.

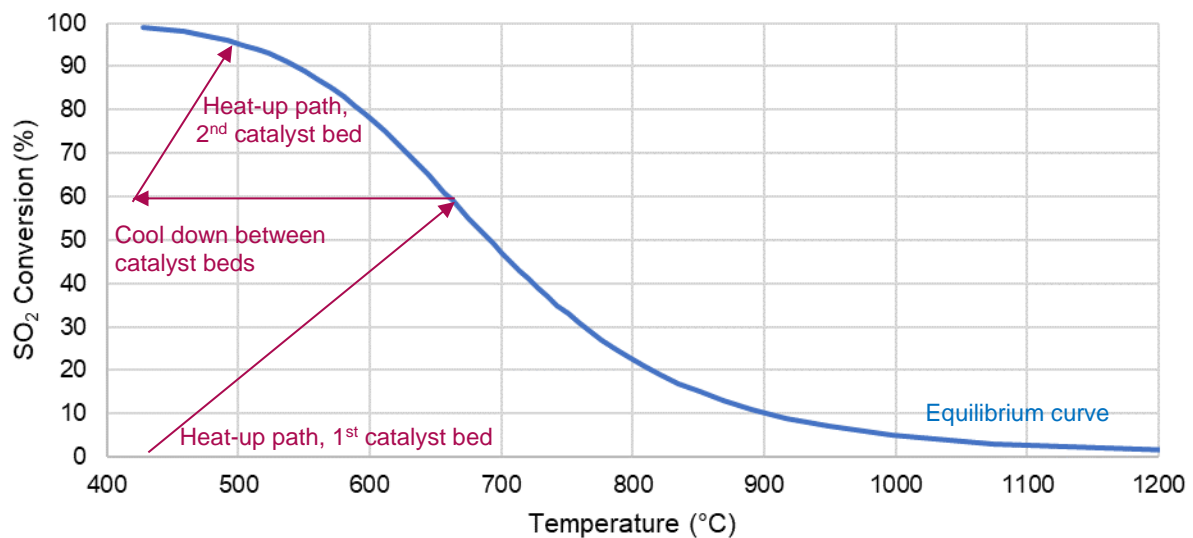


Figure 5: Equilibrium curve, heat-up path, and interbed cooling.

The maximum conversion of SO_2 that can be achieved is where the heat-up path and equilibrium curve intersect, given that the catalyst bed is thick enough. The first catalyst bed is typically 500 – 1 000 mm thick and cannot achieve SO_2 conversion greater than 80 %. One or two additional catalyst beds are required, with cooling between catalyst beds to promote increased oxidation. A frequently used target cooling temperature between catalyst beds is 700 K (427 °C). Figure 5 illustrates the increased final conversion that can be achieved if the gas is cooled and passed through a second catalyst bed. Depending on the feed gas conditions, consequent heat-up paths, and equilibrium curves, two or more catalyst beds can be installed to increase SO_2 oxidation. The lower SO_2 and O_2 and higher SO_3 concentrations in the gas entering the second or third catalyst beds results in a slower conversion reaction. The slower conversion reaction is compensated for by increasing the second catalyst bed thickness and using a higher inlet temperature. Methods of cooling interbed gases include: making or superheating saturated steam from a boiler, heating boiler water in an economiser, or using gas-gas heat exchangers to preheat incoming gas. The metallurgical industry normally uses the latter to heat the feed gas to the first catalyst bed. The economiser is generally used before the absorption step (production of H_2SO_4). The gas-to-gas heat exchangers provide the opportunity to use heat integration and heat the incoming gas while cooling the gas in the converter. The cooling requirements (King *et al.*, 2013), as well as operational considerations dictate the choice of interbed cooling employed.

King *et al.* (2013) investigated the effect of pressure on the heat-up path and SO₂ conversion and concluded that pressure does not significantly influence these parameters. A similar conclusion was drawn regarding the effect of CO₂, O₂ and N₂ on the extent of reaction and equilibrium temperature. Of the abovementioned parameters, the feed gas temperature has the most distinct effect on the conversion of SO₂ to SO₃.

As previously mentioned, catalyst degradation can also occur if the catalyst is operated above the degradation temperature for long periods. King *et al.* (2013) found that the typical degradation temperature of these catalysts is 900 K, correlating to a feed gas with a composition of about 13 %. As these concentrations are not typical for the industry considered, the catalyst is not expected to degrade due to continuous high-temperature operation. However, should this become a problem, diluting the gas with air is a possible solution. The downside of dilution air is increased capital cost (larger ducts and equipment) and increased operating costs (e.g., increased fan sizes lead to increased power consumption). Another alternative is feeding the gas to the catalyst beds at a lower temperature. A caesium-enhanced catalyst bed can be fed with gas at a temperature of 387 °C without the catalyst being deactivated (King *et al.*, 2013).

The following assumptions are typical for acid plants:

- Near steady-state operation, which indicates that the process gas heat is not used to heat the catalyst
- No heat loss due to good insulation and short residence times in catalyst beds. This assumption does not hold for smaller plants; the heat loss per kilomole of gas should be accounted for.
- Equilibrium conversion is achieved in every catalyst bed.

2.3.3 Acid production

Double contact acid making is often used to improve the oxidation of SO₂ to SO₃ since the feed gas is passed through a series of catalyst beds, SO₃ is converted to H₂SO₄ (first contact step), thereafter the remaining SO₂ in the feed gas is oxidised via another set of catalyst beds and the newly formed SO₃ is converted to acid (second contact step) (King *et al.*, 2013). This study assumed that the extent of conversion of SO₂ to SO₃ is sufficient in the first set of catalyst beds, and therefore, the double contact acid-making procedure will not be followed.

The feed gas to the acid plant can be preheated via heat exchange with hot air (200 °C) from the condenser, heat exchange with hot molten salt, or indirect heating via the combustion of hydrocarbon fuels. In some processes, further heating can occur via indirect heat exchange

with the reacted process gas. Depending on the feed gas temperature, one or more of these techniques can be used to heat the gas to the required 420 °C.

The heated gas is cooled between catalyst beds using molten $\text{KNO}_3\text{-NaNO}_3\text{-NaNO}_2$ salt or steam. The number of catalyst beds and cooling steps, catalyst types and cooling temperatures are selected to ensure the required SO_2 to SO_3 conversion is achieved.

Concentrated sulphuric acid can be produced by contacting the SO_3 -containing gas with water in a strong sulphuric acid solution. However, the WSA process uses the moisture already in the *wet gas* to form the acid, as shown in Equation 7. King *et al.* (2013) stipulate that metallurgical acid plants can contain 5 – 8 % H_2O in the feed gas, and therefore, little to no water addition is required. However, if the process gas contains too much moisture, the produced acid will be less concentrated (diluted) due to the excess moisture.



The formation of sulphuric acid (Equation 7) is promoted by cooling the produced SO_3 gas stream to 270 – 290 °C. The temperature of the sulphuric acid gas stream must be kept sufficiently high (220 – 265 °C, depending on the acid concentration) to ensure that acid condensation will not happen in equipment ill-suited to handle liquid acid.

2.3.4 Condensation

Condensation of the sulphuric acid is achieved by counter-currently sending the sulphuric acid gas stream to a glass tube condenser utilising a cold inlet air stream to cool the acid stream to 110 °C. The heated air (~200 °C) can preheat the SO_2 gas feeding into the converter. Solid nanoparticles (2 – 100 nm diameter) are inserted into the gas stream as nuclei for sulphuric acid condensation. Other than promoting acid condensation, the particles enable the formation of larger acid mist particles which can be easily removed from the gas stream. These nanoparticles are the product of fuel gas and silicone oil combustion.

The condensed sulphuric acid droplets are collected in filters at the top of the glass tube condenser. The accumulated droplets flow down the glass tubes, where the droplets are collected and can be pumped, cooled and sent to storage. Typical glass tubes used in industry are 6.8 m tall, have an outside diameter of 40 mm and a thickness of 4.6 mm, with a flow rate of 15 Nm^3/h of gas per tube (Schlesinger *et al.*, 2011).

Depending on the environmental and legislative requirements, a secondary filter system can capture the remaining acid mist in the cleaned off-gas after exiting the condenser.

2.3.5 Temperature Control

The amount of heat to be removed between catalyst beds and during acid-making can easily be determined by calculating the difference in enthalpies required for the gas to be cooled to the specified temperature. The catalyst bed temperatures can further be controlled by bypassing the gas around the equipment used for heat transfer. The bypassed stream is not cooled; therefore, the combined stream after the heat exchanger will be warmer than when the entire stream is cooled. This bypass property is seen in most acid plant heat exchangers (King *et al.*, 2013). Suppose the heat exchanger is designed to achieve a certain amount of heat transfer (final outlet temperature) for a specified inlet gas flow rate. In that case, the bypass flow rate can be determined by calculating the amount of excess gas or energy.

The effect of inefficiencies should, however, be accounted for in industrial applications. Inefficiencies occur due to the slower linear velocity of gas going through the heat exchanger and, thereby achieving a longer residence time, increasing heat transfer (King *et al.*, 2013)

2.4 Plantwide Control

Like most other industrial processes, this plant has a complex flow sheet containing multiple unit operations, recycle streams and relies on energy integration. Therefore, a plantwide control strategy is required to ensure that the entire process can be operated and controlled efficiently and economically while meeting the design objectives. Luyben, Tyreus & Luyben (1997) suggest that plantwide control is based on eight fundamental principles, including but not limited to economic or process optimisation, energy management, production rate and consideration of safety, operational, and environmental constraints. Luyben *et al.* (1997) propose a heuristic nine-step procedure to produce a plantwide control strategy. It is important to note that this strategy is for an open-ended design problem and will not generate a single (unique) solution. This nine-step procedure to design a plantwide control strategy is summarised as follows:

1. Determine the control objectives, including steady-state, dynamic control objectives, and process constraints.
2. Discern the control degrees of freedom (quantify variables that can be controlled).
3. Consider the system's energy management measures, including heat integration between unit operations and evaluation and mitigation of possible energy disturbances due to the increased use of heat integration.
4. Confirmation of the production rate and where it will be fixed within the process. This is either predetermined by the presence of certain constraints, or it can be set at a valve that ensures smooth (stable) transitions of production rate and rejection of disturbances.

5. Control constraints and product quality. These constraints refer to environmental, safety, and operational constraints. As these quantities are important from an operational and economic point of view, tight control is cardinal. The choice of manipulated variables should ensure that their dynamic relationship with the controlled variables exhibits large steady-state gains with small dead times and time constants.
6. If possible, control gas pressure and liquid level (inventories) with the manipulated variable that has the greatest effect on the respective inventory variable within a specific unit. Luyben *et al.* (1997) suggest that:
 - 6.1. Proportional-only control is implemented for cascaded units in series (in non-reactive level loops) and can improve downstream flow rate disturbances in reactor level control.
 - 6.2. All liquid recycle loops be equipped with a flow controller, except in some cases when a composition analyser is available.
 - 6.3. The maximum recirculation rate (limited by compressor capacity) is used for gas recycle loops to maximise yields.
7. Perform component balances and include purge and make-up streams, where required.
8. Develop individual unit operation control loops.
9. Optimise and improve either dynamic controllability or the process's economics by utilising the additional degrees of freedom (left after the regulatory requirements have been satisfied).

This nine-step procedure inspired the development of many other similar procedures, where different ordering or importance of the main heuristics have been proposed. The following heuristics or topics are typically present in process-oriented approaches (Juliani & Garcia, 2017):

- Degrees of freedom analysis (for both control and optimisation).
- Production rate – often the largest disturbance.
- Dominant variables and partial control.
- Decomposition of the problem.

Plantwide control aims to define and assess the overall plant's control philosophy, where attention can be drawn to the structural decisions (Larsson & Skogestad, 2000, Skogestad, 2002). These structural decisions are widely (Juliani & Garcia, 2017, Larsson & Skogestad, 2000, Skogestad, 2002) understood to involve the selection of the following:

1. Controlled variable, c .
2. Manipulated variable, m , (physical degrees of freedom).

3. Extra measurements, v - for other control purposes, such as stabilisation.
4. Control configuration.
5. Controller type.

In essence, the structural decisions during plantwide control consider what to measure and manipulate and how these variables can be linked to form control loops (Larsson & Skogestad, 2000, Skogestad, 2002). These structural methods are also referred to as the mathematically oriented approach to solving the plantwide control problem (Larsson & Skogestad, 2000).

The plantwide control procedure can also be approached via a top-down and bottom-up analysis (Juliani & Garcia, 2017, Larsson & Skogestad, 2000, Skogestad, 2002), requiring some iteration at each step to achieve convergence at a control structure. This approach describes a process-oriented strategy for solving the plantwide control problem (Larsson & Skogestad, 2000).

A seven-step (process-oriented) procedure was proposed by Skogestad (2002) and inspired by Luyben *et al.* (1997) (Juliani & Garcia, 2017). The top-down steps focus on steady-state economics, while the bottom-up steps are focused on loop-pairing and stabilisation (Juliani & Garcia, 2017). The top-down approach identifies the (primary) variables that should be controlled, selects the manipulated variables to achieve that control (degrees of freedom analysis) and determines where the production rate should be set in the process. The bottom-up approach considers the concepts of dominant variables and partial control. This approach uses the controlled and manipulated variables selected in the top-down approach as input to determine/select secondary controlled variables. These secondary variables are used in the regulatory control layer to stabilise the plant and provide some measure of local disturbance rejection; in other words: they improve the control (Larsson & Skogestad, 2000). After the regulatory control layer has been established, the supervisory control layer is developed. This layer utilises the unused manipulated variables and setpoints from the regulatory layer as input. Two options for structural control exist within this layer: decentralised and multivariable control. The last two steps of the bottom-up design consist of real-time optimisation and the validation of the model. As mentioned above, different methods assigning different degrees of importance to the various steps, exist (Larsson & Skogestad, 2000) and this top-down bottom-up approach has been applied to some large-scale processes (Juliani & Garcia, 2017). Inventory (regulatory level control) control is one example of this. When viewed from only an operational view, it is often considered the most important step whereas, when considered purely from a design perspective, it is deemed of lesser importance.

The third control technique encountered in plantwide control design is a hybrid between the two techniques already mentioned, i.e., a combination of mathematical and process-oriented methods. Juliani & Garcia (2017) summarises the major techniques proposed for plantwide control; these techniques include ones already discussed (Luyben *et al.*, 1997, Skogestad, 2002) as well as some other techniques that touch on topics such as self-optimising control, mixed-integer linear programming, decentralised plantwide control, decomposition techniques, and dynamic vs steady-state models. Some of these topics are briefly discussed below.

Designing a plantwide control system is difficult; therefore, the problem is often divided into smaller, more manageable portions. Larsson & Skogestad (2000) mention four frequently encountered methods to decompose the problem: process units, process structure, control objectives, or timescale. Usually, a combination of these methods is used to solve the plantwide control problem. Decomposition based on process units provides a decentralised or horizontal technique to break the problem into simpler parts. However, this technique can become impractical when numerous recycle streams and increased heat integration are present in a system. The other methods provide hierarchical decompositions. One of the major advantages of a hierarchical approach is that optimisation procedures can be applied at various stages without generating an unsolvable problem. Process structure-based decomposition allows the simultaneous development of the control system and process. Decomposition based on control objectives follows a bottom-up design procedure, and one example of such a procedure is the nine-step plantwide control strategy mentioned above (Larsson & Skogestad, 2000, Luyben *et al.*, 1997, Skogestad, 2002). The last decomposition method, based on timescales, generally focuses on controllability analyses to select outputs. However, this can be problematic as variables that are easier to control can be selected instead of those that are more important (Larsson & Skogestad, 2000).

Formulation of the operational (and economic) objectives generally receives precedence when following a systematic approach to plantwide control. It should, however, be emphasised that plantwide control is a multi-objective problem (Larsson & Skogestad, 2000) and that both operational (e.g. good disturbance rejection) and economic (cost) objectives need to be considered. The review completed by Juliani & Garcia (2017) highlights that the assumption that process economics are only determined by steady-state plant behaviour can present an oversimplified model. This model considers the effect of disturbances and dynamics on process operating costs negligible, consequently restricting the model and failing to provide a model that presents optimal process behaviour. It is emphasised that dynamics due to, for

example, disturbances and process variability should be taken into account as they can have a considerable effect on process economics.

Multivariable vs decentralised control is discussed by multiple authors (Juliani & Garcia, 2017, Skogestad, 2002, Skogestad, 2004). Using multivariable control such as MPC is advantageous when frequent reconfiguration of loops is required but is more complex than decentralised control methods (Skogestad, 2002). Instead of only implementing an MPC system, it is proposed to implement MPC on top of a regulatory control layer. This alternative ensures that no loss in terms of performance occurs, given that the multivariable control policy has access to the setpoints of the regulatory controllers (Juliani & Garcia, 2017, Skogestad, 2002).

Self-optimising control is the control philosophy that achieves an acceptable loss by implementing a constant setpoint policy. This policy focuses on identifying the best variables to keep constant rather than obtaining the optimal setpoints of controlled variables (Skogestad, 2000, Skogestad, 2002). Skogestad (2000) proposed a seven-step process to identify and select the controlled variables to achieve self-optimising control. Juliani & Garcia (2017) stated that not much more research, development, or practical applications of this concept can be found in the literature. However, Shen, Ye, Guan *et al.* (2023) used enhanced design techniques to determine manipulated and controlled variable pairings that will reduce the economic loss in a roaster. Martínez-Sánchez, Gómez-Castro & Ramírez-Corona (2022) used Aspen to simulate a biodiesel production process and devolved a plantwide control structure to handle variations in feed composition.

Currently, most plantwide control techniques focus on small to medium-scale processes. Few (published) methods apply to the design of plantwide control systems for large-scale systems or complete processes (Juliani & Garcia, 2017).

3 Methodology

The methodology followed by Lausch, Wozny, Wutkewicz *et al.* (1998) to develop a (decentralised) plantwide control concept for an industrial process used dynamic simulation and a controllability analysis. Their model was validated with existing data from the process. However, no plant data was used for the study on SO₂ abatement, and the results should apply to the plantwide control of WSA plants in general.

Skogestad (2004) stated that a generic model is usually sufficient for control structure design as it is mostly insensitive to parameter changes. Furthermore, Skogestad (2004) recommended that a theoretical model of the entire plant, based on first-principle mass and energy balances, should be used for such an analysis. When controller design is desired, a specific model of the plant will be required to tune the control loops.

The following phased approach was used to build a digital model of the plant:

- Phase 1: Setup a steady-state model of the overall plant
- Phase 2: Use the steady-state model to build and analyse a dynamic simulation of the plant.
- Phase 3: Develop a digital control model of the plant by following the 7-step top-down, bottom-up procedure developed by Skogestad (2002), incorporating advanced process control if and where required.
- Phase 4: Evaluate the control structure and strategy and optimise or adjust if required.

Should plant data be available, process parameters can be used to calibrate the model (as far as practically possible). However, for this study, the model is not based on an actual operating plant; therefore, the model cannot be implemented at a plant.

3.1 Model Properties

The steady-state model of the hot gas cleaning plant, wet gas cleaning plant and acid plant was built in *Aspen HYSYS V11* (Aspen Technology, 2019a). The first step in setting up the model was to define the properties of the model. This included adding the components, identifying fluid package requirements, and defining the possible reactions. The components required for the steady-state model are listed in Table 2, where the two data sources of the components are listed in separate columns. Components indicated with an asterisk (*) were only used in the steady state model as they were not required in the dynamic model where only the acid plant was modelled and an electric heater was used instead of a LPG-fired heater. The first thermodynamic equation of state (EOS), Peng-Robinson (PR), was described

in the HYSYS Help as ideal for Vapour-Liquid-Equilibrium (VLE) calculations and efficient in solving single- to three-phase systems over a wide range of pressures and temperatures. The PR package also provides improved binary interaction parameters for components anticipated to be present in this model (N₂, H₂, CO₂, H₂O). The PR package was chosen as the equation of state for this model. Another commonly used EOS fluid package is the Soave-Redlich-Kwong (SRK) model. However, HYSYS Help explicitly states that this EOS model should not be used for acids, eliminating it as an option for modelling an acid plant. The Non-Random-Two-Liquid (NRTL) model can be used for VLE and LLE of nonideal solutions, indicating that it can be used in cases where multiple fluids are present.

Additionally, the NRTL model can calculate the heat of mixing, becoming useful when modelling neutralisation reactions in the effluent treatment area. When modelling the condensing of the acid vapour exiting the converter, it was noticed that the concentrated acid vapour's temperature reduced, but the vapour did not condense to form a liquid. The root of this problem lies in the chosen fluid package. The Peng-Robinson fluid package works adequately for the process up to this point but is insufficient for the liquid phase. A constant enthalpy stream splitter was inserted before the condenser to allow changing the fluid package to the NRTL package.

Table 2: Components and fluid packages.

Component	Overall Package 1	Overall Package 2
H ₂ O	HYSYS (Peng-Robinson, NRTL)	Aspen Properties (NRTL (Water))
SO ₂	HYSYS (Peng-Robinson, NRTL)	Aspen Properties (NRTL)
H ₂ SO ₄	HYSYS (Peng-Robinson, NRTL)	Aspen Properties (NRTL (Sulfuric Acid))
Calcium*	HYSYS (Peng-Robinson, NRTL)	Aspen Properties (NRTL)
Oxygen	HYSYS (Peng-Robinson, NRTL)	
CO ₂	HYSYS (Peng-Robinson, NRTL)	
Carbon*	HYSYS (Peng-Robinson, NRTL)	
Air*	HYSYS (Peng-Robinson, NRTL)	
Nitrogen	HYSYS (Peng-Robinson, NRTL)	
SO ₃	HYSYS (Peng-Robinson, NRTL)	
Propane*	HYSYS (Peng-Robinson, NRTL)	
CO	HYSYS (Peng-Robinson, NRTL)	
i-Butane*	HYSYS (Peng-Robinson, NRTL)	
Calcium-Sulfate*		Aspen Properties (NRTL)
Calcium-Hydroxide*		Aspen Properties (NRTL)
Calcium-Carbonate- Calcite*		Aspen Properties (NRTL)

Three reactions were defined: the oxidation reaction of SO₂ to SO₃ (Equation 1), the hydration of SO₃ to sulfuric acid (Equation 7), and the neutralisation of sulfuric acid with lime (calcium hydroxide) to form calcium sulphate. The catalytic reaction prompted defining the reaction as Heterogeneous Catalytic, which requires defining the reaction rate (Equation 8) and using a

Plug Flow Reactor (PFR) type converter. In Equation 8, A is -11.25 and β is 11836 K. and T is in Kelvin.

$$k = A \exp\left(-\frac{E}{RT}\right) T^\beta \quad 8$$

To accurately define the reaction rate, information on the catalyst properties is required. As mentioned in Section 2.2.1, the catalyst's composition, shape and size can vary and influence the conversion achieved.

However, based on the previous discussions (Section 2.3.2), it is generally accepted or assumed that the reaction in each catalyst bed intercepts the equilibrium curve, thereby reaching equilibrium. Information on the equilibrium curve is also available (refer to Equations 3 to 6). The equilibrium reaction can be defined via the equilibrium constant (K_{eq}) or using Gibbs Free Energy. Therefore, an equilibrium reaction in either the equilibrium reactor or the Gibbs reactor is also a plausible option. The extent of the reaction can also be manually defined by using a conversion reaction and a conversion reactor.

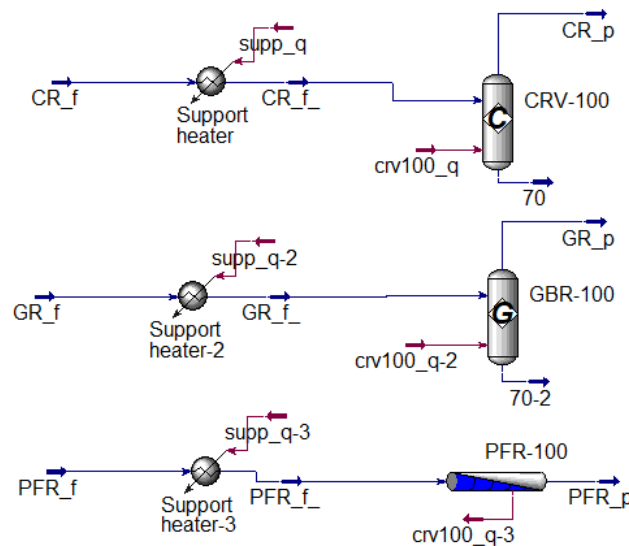
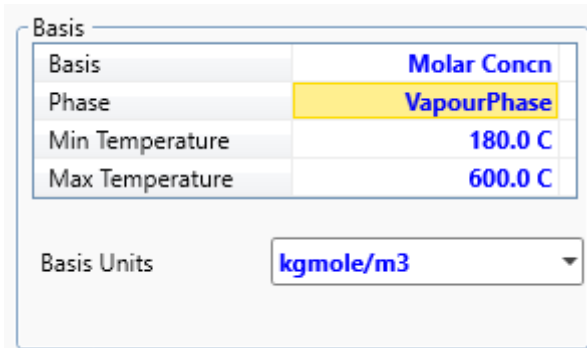


Figure 6: Example of reactor types tested.

The reaction was modelled in each reactor with the same inlet parameters for each listed reactor. The outlet temperature and extent of reaction achieved in each type of reactor are documented in Table 3. It was noted that for the equilibrium reactor, the definition of the *Basis* and *Basis Units* (Figure 7) significantly affects the extent of reaction. Table 3 gives three examples using the Equilibrium reactor: for both examples, the molar concentration was chosen as the *Basis*, with the *Basis Units* as kmol / m^3 and $\text{gmol} / \text{cm}^3$, respectively. Selecting *Partial Pressure* with MPa units resulted in a 93.5 % conversion and a temperature of 462.3 °C.

Table 3: Input and output parameters for various reactor types.

Parameter	Unit	Equilibrium Reactor (kmol / m ³)	Equilibrium Reactor (gmol / cm ³)	Equilibrium Reactor (MPa)	Gibbs Reactor	PFR	Conversion reactor
Outlet temperature	°C	461.7	434.9	462.3	465.2	456.4	465.2
Conversion achieved	%	85.5	26.17	93.5	97.3	80.19	100

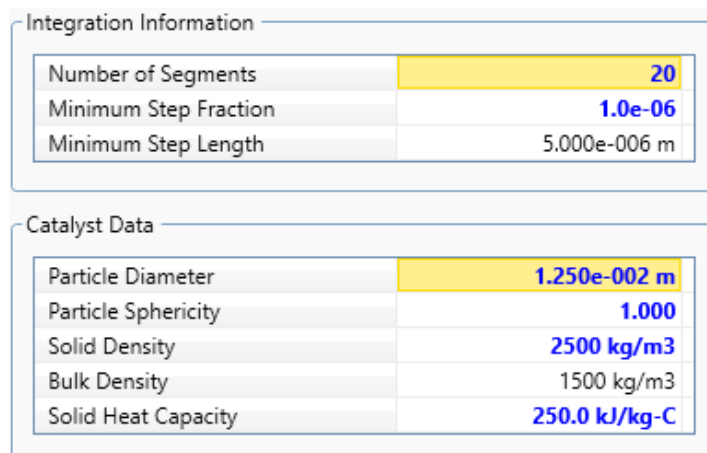


Basis	
Basis	Molar Conc
Phase	VapourPhase
Min Temperature	180.0 C
Max Temperature	600.0 C

Basis Units: kgmole/m³

Figure 7: Equilibrium reactor basis screen.

The *Conversion Reactor* is ruled out as an option since defining the conversion achieved in the reactor removes any dependency on variables (temperature, pressure, concentration) that would normally impact the extent of reaction. The *PFR* would be the ideal reactor as it resembles a catalytic converter bed the closest. However, the *PFR* requires various inputs (Figure 8) or knowledge of the catalyst as well as the definition of a reaction rate. The *Gibbs Reactor* requires little input if the *Gibbs Reaction Only* option is selected. However, the conversion achieved in a single reactor is much higher than expected – it is expected that only after multiple converter beds will a conversion of ~98 % be achieved. The *Equilibrium Reactor* was therefore selected for this model. The *Basis Units* of kmol / m³ were used as the achieved conversion and outlet temperature aligns with that of the other reactors and what is expected in an actual converter.



Integration Information	
Number of Segments	20
Minimum Step Fraction	1.0e-06
Minimum Step Length	5.000e-006 m

Catalyst Data	
Particle Diameter	1.250e-002 m
Particle Sphericity	1.000
Solid Density	2500 kg/m ³
Bulk Density	1500 kg/m ³
Solid Heat Capacity	250.0 kJ/kg-C

Figure 8: PFR specification requirements.

The flowsheet was subdivided into smaller sub-flowsheets according to typical plant areas, similar to Figure 1. This division had the dual benefit of visual simplification of the flowsheet layout and the ability to build and analyse portions of the flowsheet separately. The steady-state model is subdivided similarly, as shown in Figure 9. However, during the definition and building of the steady-state model, it became evident that converting the entire off-gas treatment plant (including dust removal, wet gas cleaning, acid cooling, effluent treatment, and cooling water) to a dynamic model would require more effort than initially anticipated. Therefore, the initial steady-state model was a coarse model of the entire plant, but the focus eventually shifted to the acid plant. The steady-state model is discussed below, highlighting some of the complexities and issues encountered during the development of the model in HYSYS.

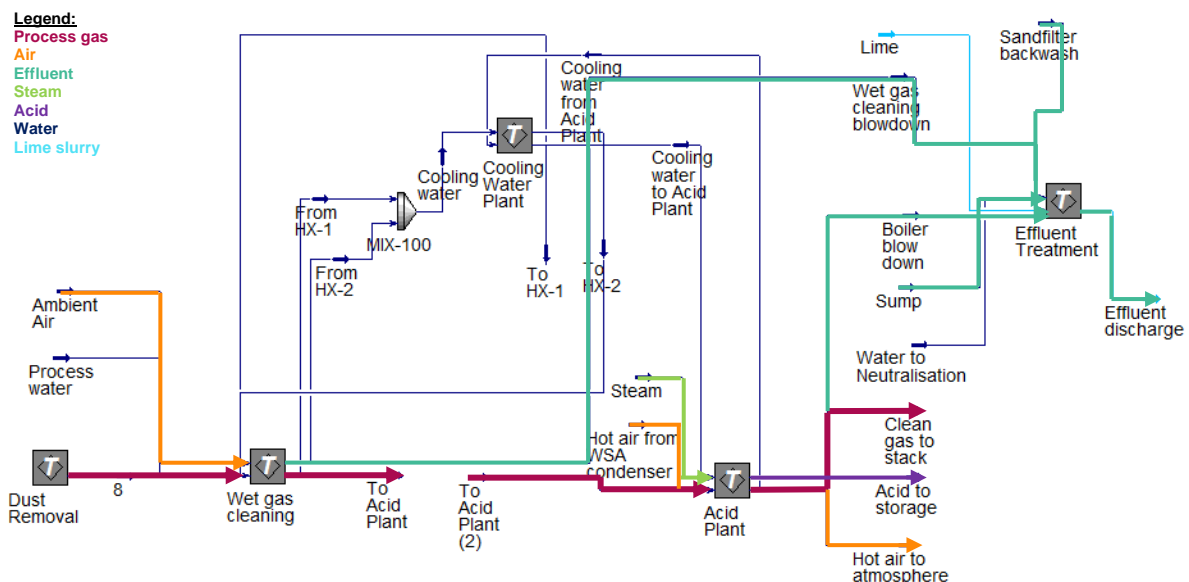


Figure 9: Overall steady-state model.

The properties and compositions of the inlet streams were used as specified in Table 4 for the initial base case of the model. This model represents a nominal case, with fixed inputs, which was used to validate the model based on expected temperatures and operation as discussed in Section 2.3. These were derived from the typical and average properties of furnace off-gas from PGM smelters, as discussed in Section 2.1. In practice, the feed gas properties can be measured by online gas analysers, pitot tubes, flow meters, and thermocouples, and the composition can be determined through isokinetic and other testing. Furthermore, these values will vary to some degree, and a dynamic model will be the best method for evaluating the effect of these changes on the plant's performance.

Table 4: Steady state model inlet stream properties.

Parameter	Unit	Furnace off-gas	Air	Water
Temperature	°C	500	20	20
Flow rate	Nm ³ /h	18 660	-	-
Pressure	kPa (a)	90	-	-
Composition:				
H ₂ O	Vol%	6.5	1.5	100
SO ₂	Vol%	3.5		
SO ₃	Vol%	0.0008		
H ₂ SO ₄	Vol%	-		
O ₂	Vol%	15.2	21.0	
CO ₂	Vol%	2.37		
CO	Vol%	-		
N ₂	Vol%	72.43	77.5	

This coarse model represented the plant adequately and highlighted possible problem areas. Section 3.2.1 discusses the cooling of the furnace off-gas and the removal of dust from the furnace off-gas. Typically, furnace off-gas is conditioned in a wet gas cleaning plant to ensure the off-gas sent to an acid plant has sufficiently low dust levels to minimise damage or plugging of the catalyst. Auxiliary plant areas (Section 3.2.3), such as cooling water towers and effluent treatment, are also required when installing an acid plant.

3.2 Steady-State Model

3.2.1 Dust Removal

The first two plant areas: dust removal (hot gas cleaning) and wet gas cleaning, are mainly concerned with removing dust (particulate matter) from the off-gas stream. In these plant areas, the off-gas is kept above the dewpoint temperature of SO₂ to hinder the formation of acidic condensate and consequently inhibit corrosion.

In the hot gas cleaning plant, the bulk of the dust is removed by using a spray cooler (cooling the off-gas to the allowable ESP inlet temperature) and ESP. As the off-gas exits the ESP, it is directed to the wet gas cleaning area via fans. However, the primary purpose of the fans is to control the furnace freeboard pressure. In cases where the downstream plant is unavailable, these fans divert the off-gas to a bypass stack. Other cooling and dust removal techniques could be water-cooled ducts, a baghouse, or a wet scrubber system. Various configurations for wet gas cleaning plants are possible, although these plants typically consist of scrubbers, gas cooling towers and wet ESPs.

Including solid components (dust) in the off-gas stream introduced an unwanted complexity into the HYSYS model. Given the requirement that gas with a dust content below 1 mg / dNm³ (King *et al.*, 2013) is fed into the downstream plant areas, it was assumed that all of the dust

would be removed in the spray cooler and ESP and dust was therefore excluded from the off-gas stream. This exclusion is further justified by the assumption that dust is an inert component of the off-gas stream and should not impact the HYSYS model results. Inadequate removal of dust from the off-gas stream can lead to plugging or damaging of the catalyst, but for this study, the assumption is that the equipment functions as designed. Consequently, modelling of the dust removal steps was not required.

A simple *Mixer* unit accounted for the change in off-gas composition due to the water added by the spray cooler. Atomizing air is used to split the water into fine droplets and achieve optimal cooling. The water flow rate to the *Mixer* was adjusted to achieve a temperature of 350 °C for the off-gas exiting the spray cooler and entering the ESP. The new gas composition can be determined from the *Cooled Gas* stream in Figure 10.

The dust removal process, therefore, does not resemble an actual plant, but as previously mentioned, the goal is to apply plantwide control following a model-based approach. The model can be expanded and changed to resemble an industrial plant in a future study.

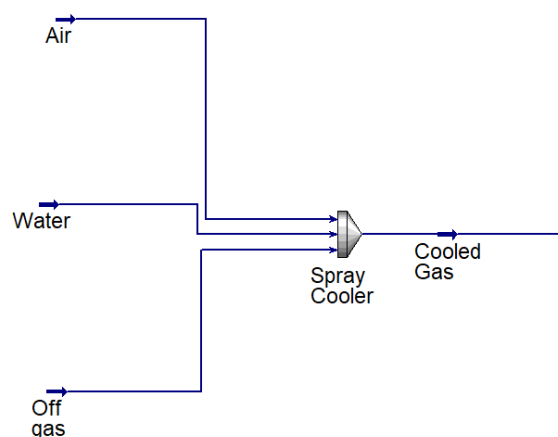


Figure 10: Hot gas cooling and cleaning flowsheet.

3.2.2 Wet Gas Cleaning

The steady-state model included a rough model of the wet gas cleaning process (WGCP) as shown in Figure 11. At this portion of the plant, the first recycle streams and heat exchangers were introduced into the model. Recycle streams were treated as separate streams, i.e., an inlet and outlet stream with the same properties. When downstream material is recycled and mixes with upstream material in a steady-state HYSYS model, a *Recycle* operation is required to join two streams. This *Recycle* operation transfers one stream's conditions to the other by performing iterative calculations and is a key unit to ensure the HYSYS model converges (Aspen Technology, 2019a). HYSYS's *Simple End Point Plate and Frame Heat Exchangers*

(PFHE) were used to model the weak acid and water heat exchangers as two heat exchangers in parallel. Pressure drops were assumed for both the cold and hot sides. The overall heat exchange coefficient and heat transfer area were specified to adequately cool the weak acid.

Tees and *Mixers* were used to split and combine the various gas and liquid streams as and when required. *Separators* were used when gas and liquid phase systems had to combine or split into the respective phases. Therefore, *Separators* were used to model the scrubbers, wet ESPs and gas cooling towers as they allowed for splitting the condensed liquid from the gas streams. *Pumps* with an estimated adiabatic efficiency of 75 % were used to circulate the liquid between the gas cooling tower and the heat exchangers.

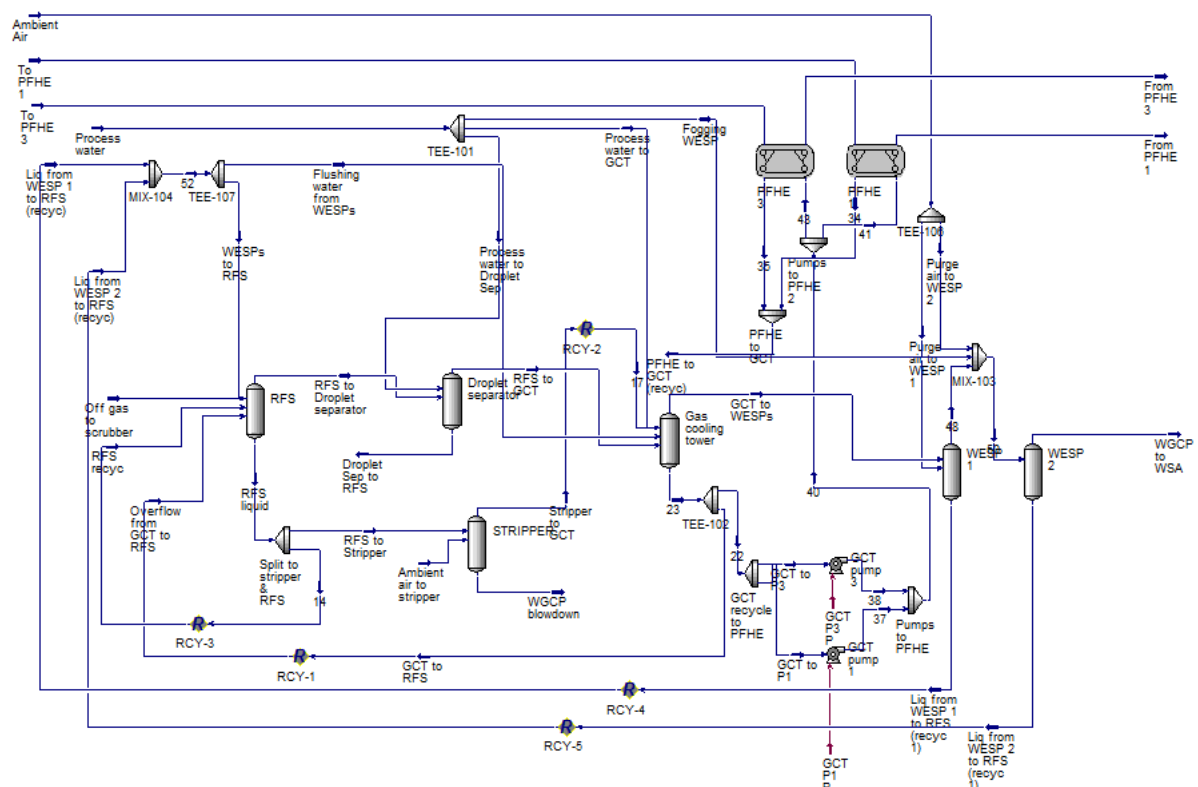


Figure 11: Wet gas cleaning process flowsheet.

The off-gas exiting the WGCP and entering the acid plant is at a lower temperature of 35 – 40 °C, with a slightly lower SO₂ concentration, due to the introduction of water and ingress air.

3.2.3 Auxiliary Areas

3.2.3.1 Cooling water

Inlet water streams were defined as the outlet streams from the wet gas cleaning and acid plant areas. In the wet gas cleaning area, cooling water is used in parallel plate and frame heat exchangers to cool weak acid gas from the gas cooling tower. Cooling water is also used

to cool the acid produced in the acid plant after it has been condensed and before it is sent to storage. These streams are combined in HYSYS using a standard *Mixer*. After that, the combined return cooling water is sent to a cooling tower, modelled as an *Air Cooler*. The *Air Cooler* was chosen as it is the best representation of a cooling tower: an air mixture is used as a cooling medium where the cool air is circulated through the tower employing one or more fans to cool the hot water. However, it should be noted that the HYSYS *Air Cooler* models the air flow through tube bundles, similar to closed-circuit cooling towers. In contrast, the cooling towers in an operating plant can also be open-circuit cooling towers, where the water and air are not separated by tube bundles, meaning the cooling water circuit is not closed.

Open circuit cooling towers generally have less equipment (lower capital and maintenance costs) and lower operating costs due to the use of less equipment. The downside of these types of towers is that they generally have a poorer cooling water quality than closed-circuit cooling towers. As this plant does not represent an actual plant, the change in cooling water quality is not modelled and therefore, the details of the choice of cooling water plant were not considered.

The cooling water is distributed to the various heat exchangers via pumps. Standby pumps are often used to offer redundancy in case one pump fails. However, to simplify the model, no standby pumps were modelled in this study. The supply pressure of the pump is layout dependent, so an assumption regarding the supply pressure had to be made. It was assumed that the pressure drop (*Delta P*) over the pump is 300 kPa, with an adiabatic efficiency of 78 %, to achieve a supply pressure of 600 kPag.

Since the cooling water is recycled between the heat exchangers and the cooling tower, the stream exiting the cooling water pumps is used to specify the recycle stream (cooling water supply) specifications. This method of 'hardcoding' can be removed when the model is switched to *Dynamic Mode*, as discussed later in Section 3.3. Two *Tees* supply cooling water to the acid plant and the two *Plate and Frame Heat Exchangers* in the wet gas cleaning area. The modelling of this plant area is illustrated in Figure 12.

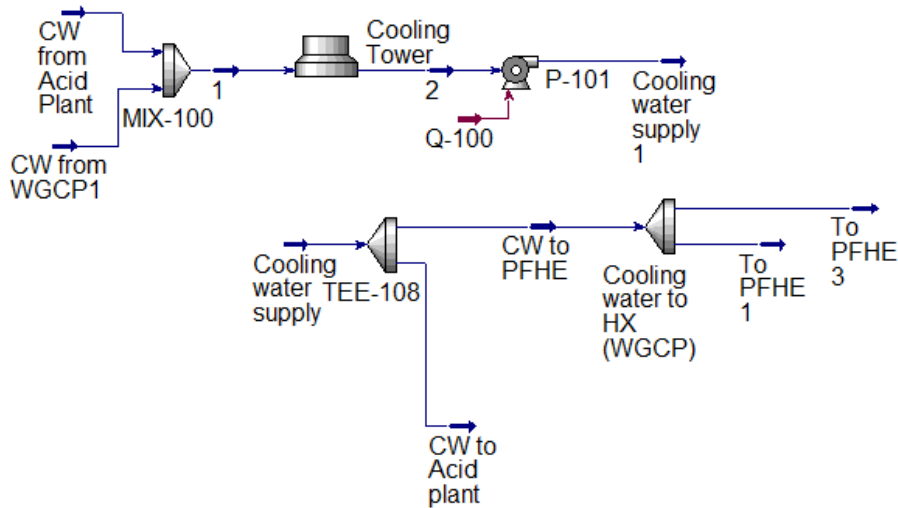


Figure 12: Cooling water cycle flowsheet.

3.2.3.2 Effluent Treatment

The effluent generated in the wet gas cleaning plant (weak acid) and blowdown from the cooling towers and other plant areas should be sent to an effluent treatment area where the weak acid can be neutralised, and the neutralised mixture recycled into the greater plant (such as the process water circuit). This was modelled as a *Continuous Stirred Tank Reactor* (CSTR) in the steady-state model, where calcium hydroxide was used to neutralise sulfuric acid.

However, this part of the plant would operate as a semi-batch process where neutralised slurry will be recycled until the tank reaches a certain capacity (high level). The effluent will then be discharged to a predetermined area until the tank reaches a minimum level.

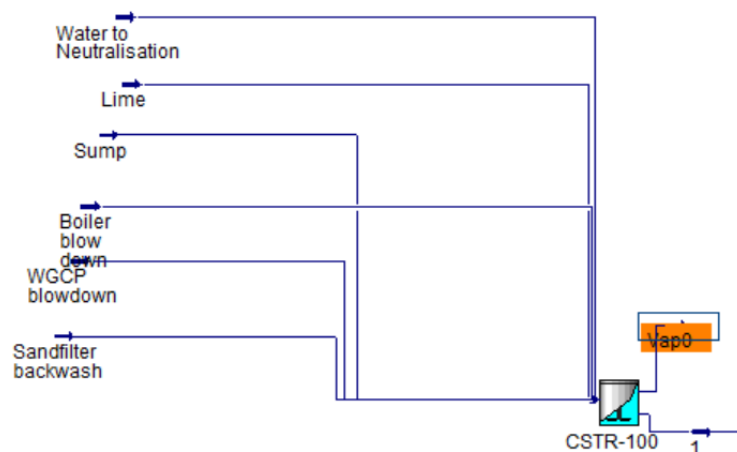


Figure 13: Neutralisation of effluent flowsheet.

3.2.4 Acid Plant Area

The methodology and concepts discussed in Sections 2.2 and 2.3 were applied to develop a steady-state model of the acid plant, largely based on the traditional WSA flowsheet described by Rosenberg (2006), shown in Figure 14.

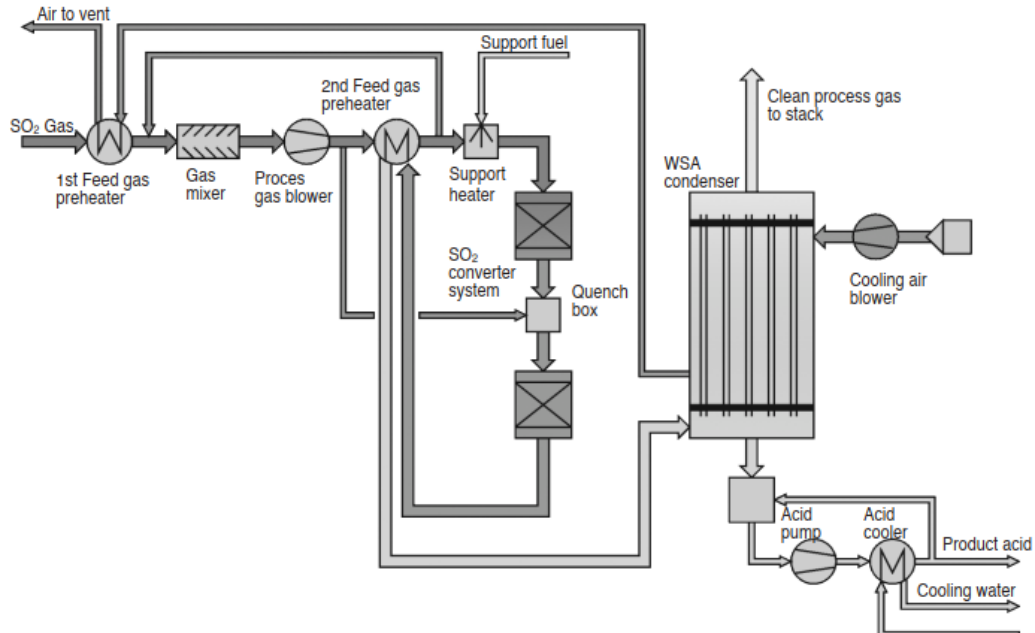


Figure 14: Traditional WSA flowsheet (Rosenberg (2006), Figure 4).

A *Compressor* was added between the WGCP and acid plant to move the gas through the WGCP and into the acid plant by overcoming the pressure drop in the WGCP. This compressor is shown in Figure 2. The gas pressure at the acid plant inlet (after the compressor) is close to ambient (0 kPag). The gas is preheated from 35 – 40 °C to above acid dewpoint (~ 170 – 180 °C) in a preheater with hot air from the condenser. The preheater is modelled as a *Simple Steady-state Rating Heat Exchanger*, requiring only the shell and tube-side pressure drops to be specified. The condenser is modelled as a *Heater*, heating ambient air, and a *Separator*, cooling the acid gas. The specified duty in the heater is the same as that required to cool the acid gas to ~80 °C. Two key considerations influenced using two different units to model the condenser. The first: the condenser acts as a heat exchanger and a separator since the cooling air is used to cool the acid gas and thereby condense out the acid mist. Secondly, as previously mentioned, this condensing reaction requires a different fluid package than the rest of the model, and two different fluid packages cannot be used in a single unit.

From the preheater, the gas is mixed with recycled process gas to provide further heating. *Tees* and *Mixers* are used to split and combine streams as and when required. Thereafter,

another *Compressor* is used to overcome the pressure drop in the acid plant, followed by a process gas heater. The process gas heater will be a gas-gas heat exchanger, heating process gas with steam. However, it is modelled as a *Heater-Cooler* set with a common duty stream to simplify sizing requirements. More recycled gas is added to the process gas, and the combined stream is further heated via indirect heat exchange with the converted process gas. These heat exchangers are modelled as a *Heater-Cooler* set, similar to the process gas heater.

The last heating step occurs in the support heater, where a combustion reaction between air and fuel is used to heat the gas. In steady-state mode, the *Simple Fired Heater* requires a fuel and air stream to produce a combustion product. These streams react independently, without affecting the inlet and outlet streams. The mixing efficiencies were specified as 100 %, and the fuel stream was specified as a mixture of propane and isobutane, typical components of liquid petroleum gas (LPG).

The heated gas is then sent to the converter. The SO_2 converting process is a two-step process, defined in Equation 1 and Equation 7. The exothermic heat of reaction of both these steps is utilised within the process. Two converter beds are separated with an interbed cooler in the catalytic converter. After the second converter bed, two more heat exchangers utilise the energy released by the exothermic reactions. The interbed heat exchanger and the heat exchanger positioned directly after the second catalyst bed heat the feed gas and cool down the reacted process gas. Similarly, the last heat exchanger heats the water feeding into a steam drum and cools the reacting gas. These cooling processes, in turn, promote the increased conversion of SO_2 to SO_3 and ultimately to H_2SO_4 , according to Le Chatelier's principle and the principles discussed in Section 2.3 (Figure 5).

The HYSYS package offers a selection of different reactors for this conversion process. The single converter unit with two heat exchangers and a steam drum was modelled as six heat exchangers and two equilibrium reactors.

When the gas exits the converter, it is sent to an air-cooled condenser. The condenser was modelled as a *Separator* with a reaction set (Equation 7) to convert the SO_3 in the gas to sulfuric acid vapour. This reaction was modelled as an equilibrium reaction using Gibbs Free Energy.

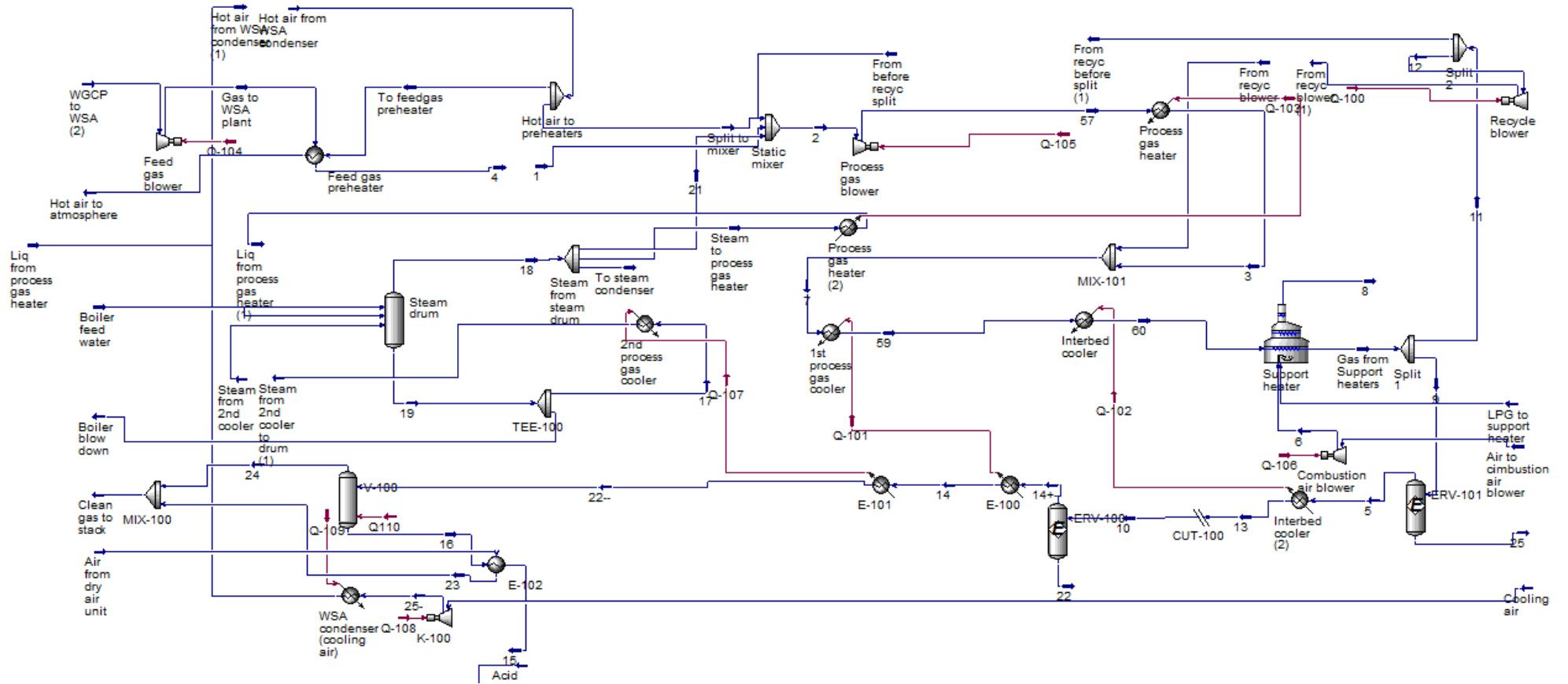


Figure 15: Steady-state WSA flowsheet.

In practise, atmospheric air enters at the top of the WSA condenser (modelled as cooling air into a heat exchanger in Figure 15), cooling and condensing the newly formed H_2SO_4 . The condensed H_2SO_4 should exit the *Separator* as a liquid. However, when modelling this *Separator* (V-100 in Figure 15), the concentrated acid vapour's temperature was reduced, but the vapour did not condense to form a liquid. A constant enthalpy *Stream Splitter* (CUT-100) was inserted before the second catalyst bed and therefore, before the condenser to allow changing the fluid package from Peng-Robinson to NRTL to allow for condensing of the acid-rich gas. This change in fluid package is required prior to the cooling of the gas to ensure any possible acid formation is captured. As the atmospheric air is used for indirect cooling, the air was not added to the *Separator* but modelled as a *Heater* with its duty stream connected to the *Separator* (V-100).

The concentrated acid is further cooled by heat exchange with cooling water; whereafter it is sent to storage (not modelled). The steady-state model of the WSA flowsheet, built in HYSYS, is shown in Figure 15.

3.3 Dynamic Model

The steady-state model set the stage for the dynamic model and further emphasized the previously mentioned complexities of an SO_2 abatement plant, such as increased heat integration and recycle streams. Therefore, it was decided to proceed with a smaller portion of the plant for this investigation. The key plant area – the acid plant – was further developed and converted into a dynamic model. The steps taken, problems incurred, and solutions made are discussed in more detail below.

3.3.1 Model Conversion

As mentioned, evaluating the entire steady-state model discussed above for its plantwide controllability would be an elaborate exercise, as the entire model would have to be converted to a dynamic model. Instead, it was decided to focus on the key plant area, the acid plant. The first step to converting the steady-state model to a dynamic one was to remove the auxiliary plant areas. After that, for the model to be a better representation of a real plant, the *Heater-Cooler* sets were replaced with (shell and tube) *Heat Exchangers*. Each *Heater-Cooler* set requiring conversion to a single *Heat Exchanger* is circled in Figure 17 with matching colours. The recycle streams that had to be connected are marked with blue arrows in Figure 17. The streams were either directly connected or, where this proved problematic to the model, *Recycle* units were used to connect the recycle streams. The connection of the recycle streams resulted in the first problem – the mass and pressure balance did not balance. The key to solving this lay in the possibility of disabling or ignoring some of the unit operations. If

a unit operation is ignored in HYSYS, it is effectively removed from the model without deleting it, meaning it is not considered in calculations. In turn, this enabled a systematic approach to evaluating portions of the model without deleting the portions that might be causing issues.

The first portion of the model focused on the two converter beds, including the upfront support heater and the two heat exchangers after each converter bed. In the steady-state model, *Adjust* units, which are similar to controllers, could be used. The *Adjusted Variable* is changed to obtain a specified target value in a *Target Variable*. An *Adjust* was used to obtain the correct amount of fuel for the *Fired Heater* to reach a specified outlet temperature. The *Fired Heater* allows setting the fuel-to-air ratio as part of the unit's design, negating the requirement for an additional *Adjust*. Another *Adjust* was used to control the temperature between the two converter beds by changing the flow ratio of the streams exiting a *Tee* (see example in Figure 16). A *Recycle* was required to connect the stream exiting the *Fired Heater* to the stream entering the first converter bed. The heat exchangers were sized expecting a low-pressure drop on both sides, and the overall heat transfer coefficient (*UA*) was estimated based on the known temperature difference over each heat exchanger.

The next portion of the model that was added/ activated was the addition of the *Tee* prior to the first process gas heater (heater after the second converter bed) to allow for a bypass of the heater to control the process gas temperature exiting the heat exchanger. The other model portions were similarly re-activated unit-by-unit to identify where *Recycle* units or *Adjusts* might be required. It was noted that using two fluid packages caused some errors in the model. The model was therefore changed to exclude the formation and condensing of acid, negating the requirement for the NRTL fluid package. The key reaction in SO_2 abatement is the catalytic formation of SO_3 which in turn reacts to form H_2SO_4 .

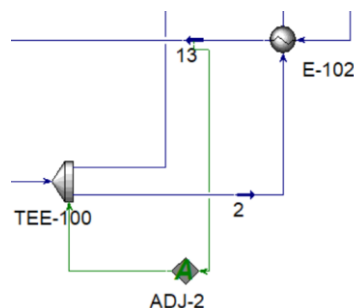


Figure 16: *Adjust* used to control temperature.

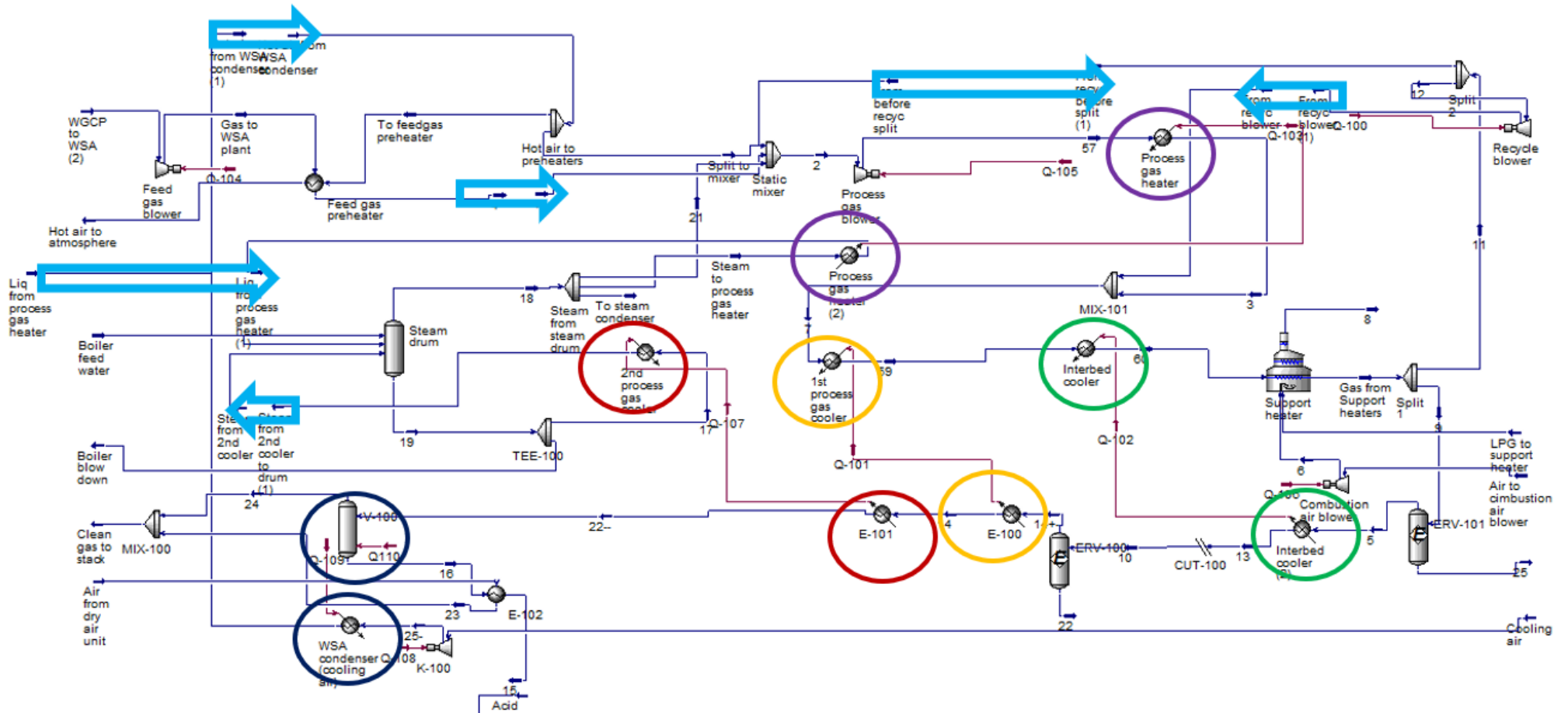


Figure 17: Steady-state to dynamic model by combining similar coloured (circled) heater-cooler pairs and connecting recycled stream (arrows).

After the steady-state model was running with the new *Heat exchangers*, *Adjusts*, and *Recycle* units, the *Dynamics Assistant* was used to start switching the model to the *Dynamic Mode*. Changes required included adding valves to the redundant (liquid streams exiting the converters) and some other streams, ticking the pressure-flow specification tick box as opposed to the fixed delta pressure box for various units, and removing the *Adjusts* and *Recycle* units. The *Dynamic Mode* model does not require *Recycle* units, as it can handle recycle streams. For the time being, *Adjusts* were completely removed, and the amount of heat, pressure, or flow ratios were manually specified. Later, controllers can be added to manage these variables.

The *Fired Heater* requires many detailed specifications regarding combustion zones to properly work in the *Dynamic Mode*. Instead of specifying or guessing all of these inputs, it was decided to use a *Heater* instead. In practice, the *Fired Heater* will likely have its own special controller system separate from the overall plant control system. The *Heater* unit in this model would adequately represent an electric heater.

The *Aspen HYSYS Help* (Aspen Technology, 2019a) function states that should no phase change be present, the *Simple End Point* model for heat exchangers should be sufficient to model the heat exchanger. The *Simple Weighted* method was used at the process gas heater (heat exchanger where steam is condensed) because the steam can condense, resulting in a phase change. Initially, the Log Mean Temperature Difference (LMTD) correction factor (F_t) was used in the heat exchangers, but the dynamic model kept showing errors due to the small F_t factor. However, it was also assumed that the effect is negligible and therefore unticked. This deselection resulted in the same results in the dynamic model without errors.

Fan curves were added to get the blowers/fans/compressors to resemble real fans. This addition provides the opportunity to specify the fan speed as a variable to be controlled instead of specifying a pressure increase.

The dynamic model was now operating adequately under steady-state conditions. However, should changes in process conditions occur, the model will likely not run optimally, as no controllers or measures are in place to reject disturbances. The plantwide control philosophy was applied to determine the possible positioning of controllers and will be discussed in Section 4. The tuning of these controllers is discussed below.

3.3.2 Dynamic Controllers

The initial controllers implemented were Proportional-Integral (PI) controllers. The controllers' responses were acceptable; therefore, the added complexity of derivative control was deemed

unnecessary. Although HYSYS has the option to *Auto-Tune* controllers, it is observed that this function often produces small gains and small integrators. The controllers can be individually and manually tuned to obtain acceptable results. The steps followed are similar to tuning an operational plant, with the added benefit of a plant without noise. A controller was used to control the feed gas flow rate. This controller will not be present in the actual plant but is used to simulate disturbances in the feed gas flow rate in the model. The steps used to tune this controller are described below, and this general methodology was used to tune any other controllers in the model.

Figure 18 shows an example of the parameters screen used when tuning a controller. The first parameter to consider is whether the relationship between the controlled variable (CV) or process variable (PV) and manipulated variable (MV) or output (OP) requires reverse or direct action control. Reverse action control is when an increase in the controlled variable (positive error) decreases the manipulated variable's output. For example, if the flow rate (CV) increases, the control valve (MV) closes to try to counteract the flow increase. Direct action control is the opposite, i.e., an increase in the controlled variable results in an increase in the manipulated variable.

The algorithm type and subtype were not changed – the default values were used. The proportional gain, K_c , and integral time constant (T_i or τ_i) were initially set to 0.1 and 0.2 min. As mentioned, only PI-control was implemented; therefore, T_d (τ_d) was not used. The other variables (b and c, in Figure 18) were set to zero.

Equation 9 illustrates the calculation of controller output (OP) for a time t using the steady state controller output (OP_{SS}), error (E) at time t , and integral (T_i) and derivative (T_d) times of the controller. The error at any time t is calculated using the setpoint (SP) and process variable (PV), as shown in Equation 10.

$$OP(t) = OP_{SS} + K_c E(t) + \frac{K_c}{T_i} \int E(t) dt + K_c T_d \frac{dE(t)}{dt} \quad 9$$

$$E(t) = SP(t) - PV(t) \quad 10$$

To tune the controller, it was set to *Automatic Mode*. Figure 19 shows an example of how controllers were tuned. The red line indicates the set point (SP) value, which was manually adjusted. The green line shows the system's response (the process variable, PV) and the blue line shows the controller output as a percentage of its range. If a positive step (increase in set point) was made, and the PV value showed an overshoot (final value was higher than the set

point)⁵, the selected gain (K_c) was too big and had to be decreased. The gain (K_c) was adjusted until the system's response (PV) matched the SP value when a step test was performed, as illustrated in Figure 19.

A wave-type response was observed where the initial integrating time constant (T_i) was too big, as seen in Figure 20. The time constant was reduced until a more stable response was obtained.

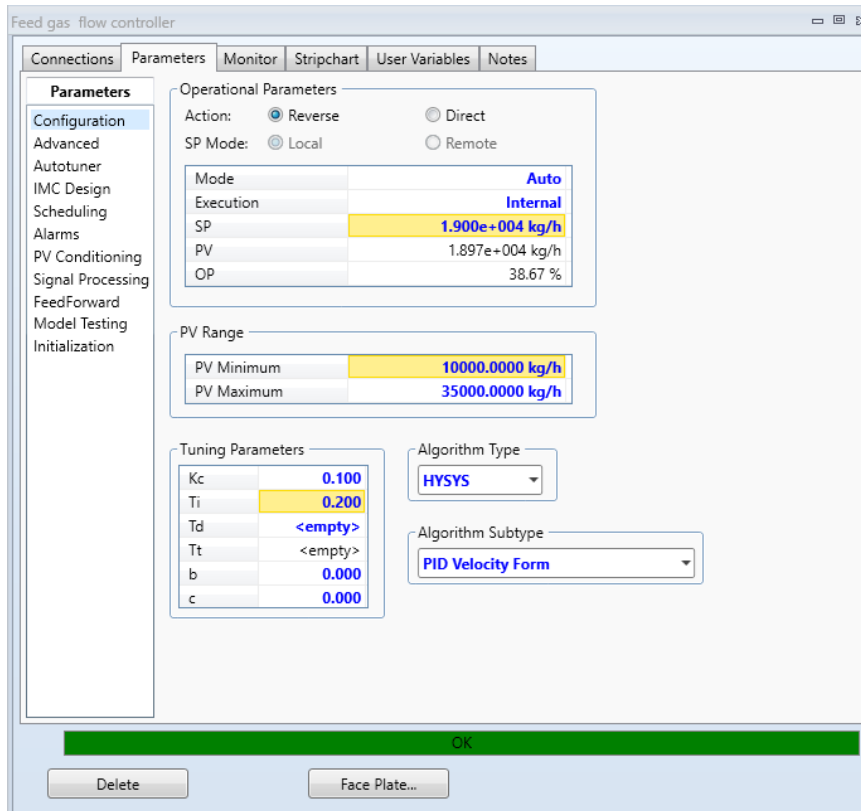


Figure 18: Feed gas flow controller – parameters.

⁵ The use of PI control will ensure that the PV value will eventually reach the SP, however this did not happen in a reasonable time.

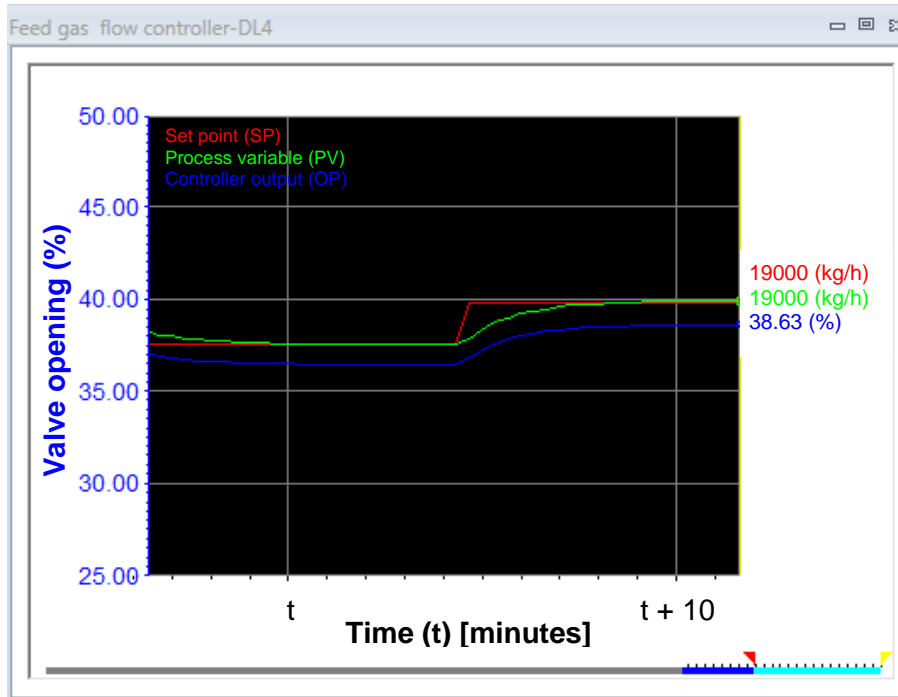


Figure 19: Step test to tune a controller.

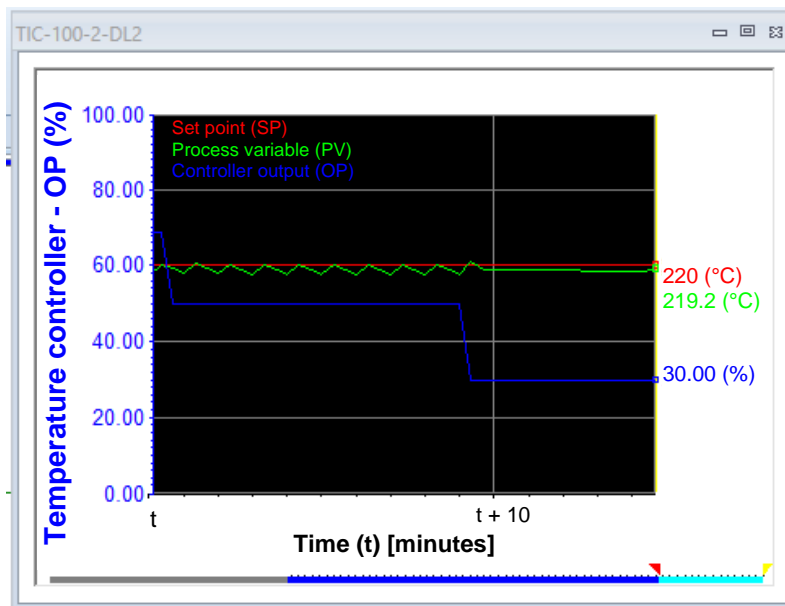


Figure 20: Example of step test resulting in wave-type system response.

When switching to *Dynamics Mode*, the *Integrator* (Figure 21) is used to specify certain integration parameters used for solving the dynamic model. Once the model is switched to *Dynamic Mode* and the *Integrator* is run, it is not advised to reset the *Integrator* as it could disturb the simulation (Aspen Technology, 2019b). Key parameters that can influence the dynamic model results are the *Acceleration*, impacting the integration step size, and the *Step*

Size, setting the integration step size. To note the effect of changing these parameters, it is important to update the *Display Interval* frequently (i.e., a small display interval).

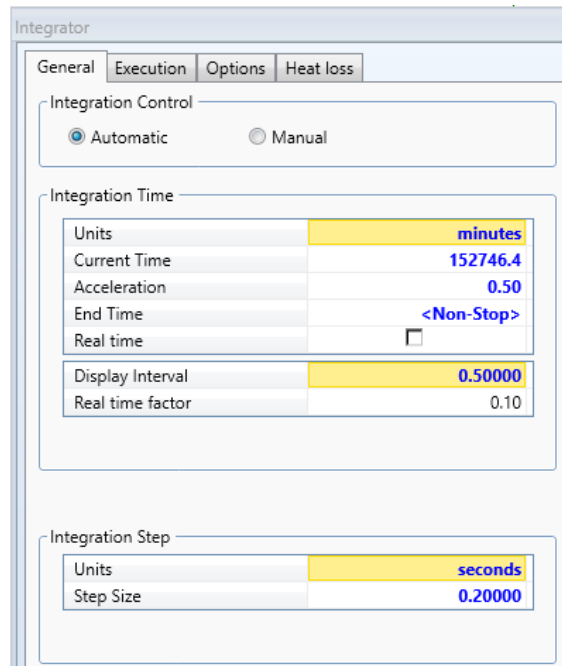


Figure 21: Dynamic integrator parameters.

The *Execution Rates* were kept at their default values, except for the *Composition* and *Flash* calculations. The default value is 10, indicating that the composition and flash calculations are executed after every 10th timestep. Since accuracy in the composition calculations is important for this plant, especially at the converters, the value was reduced to 5.

The following general options in the *Options* tab were selected (ticked):

- Rigorous non-equilibrium mixed properties – to improve the accuracy of the model.
- Use implicit check valve model – to ensure reverse flow does not occur at any timestep.
- Close component material and energy balances – as mentioned, composition is important in this plant. Therefore, it was deemed necessary that mass and energy balance calculations occur at the component level.

HYSYS has various built-in controllers available, including a *Dynamic Matrix Controller* (DMC), a type of model predictive controller (MPC). MPC is a control method by which adjustments to the input variables can be made by comparing the predictions (from an accurate dynamic model) with the current measurements. In MPC functions, the input variables are referred to as manipulated variables (MVs), the output variables as controlled variables (CVs), and the measured disturbances as disturbance variables (DVs) or feedforward variables. As MPCs rely on the predictions of the dynamic model to adjust the input variables, an accurate dynamic

model is essential. Step response models are often used for MPC predictions as they better describe stable processes with interesting dynamic interactions than simple transfer function models. The DMC model relates the dynamic step responses of the various CV-MV pairings in a MIMO model in a matrix. The individual step responses can be shown graphically, with the inputs and disturbances (MVs/DVs) in the rows and the outputs (CVs) in the columns. The MIMO step-response models and calculations can be presented using matrix-vector notation.

In HYSYS, this controller is called a *DMCplus Controller* and can interface with other Aspen *DMCplus* software to determine the dynamic interactions between dependent and independent variables. Controlled and manipulated variables are added as inputs to the *DMCplus Controller*. Optionally, feed-forward variables can also be added, which act as independent variables in the *DMCplus Controller*, i.e., the controller cannot manipulate these variables. The *DMCplus Controller* is able to perform different types of tests on the model: *Pseudo Random Binary Sequence (PRBS)*, which is easy to use for model identification; *STEP*, which is often used in practical applications or; *One-by-one*, which performs a step test in both directions on each of the variables, individually.

A *DMCplus Controller* was set up to include the possible controlled and manipulated variables. The *DMCplus Controller* was not used as a controller but rather as a method of performing the model tests and identifying the best CV-MV pairings. For the initial runs of the DMC, the default control sampling interval of 1 minute was used (as shown in Figure 22). The *Test Signal Type* of *One-by-one* was selected as it does step tests in both directions of each manipulated variable separately, simplifying the analysis of the results.

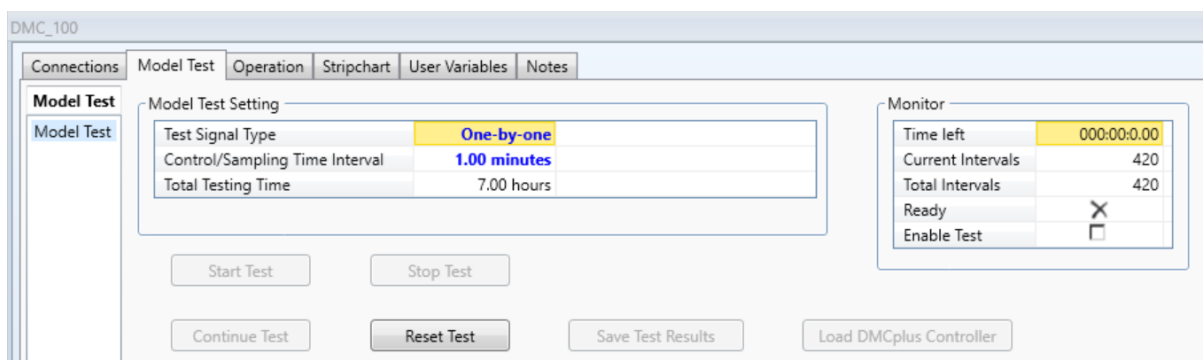


Figure 22: DMCplus Controller initial model test.

Figure 23 shows an example of the initial results: a step test of the feed gas flow rate (bottom blue curve) and the corresponding response of the conversion in one of the catalysts beds (top red curve). The system appeared to respond with an instantaneous step, not resembling the expected first-order (or second-order) step responses. The majority of the other controlled

variables showed similar results. At first, this was attributed to some problem in the model or how the model and controller interacted, but as the results on the strip charts from the same runs did not show these spikes, further investigation was required.

As the dynamic model ran without issues, the setup of the dynamic model was identified as a possible cause. At first, the acceleration of the *Integrator* was increased, but the change in results was minimal: the response was still near instantaneous, not resembling a first-order step response. Changing the integrating time step did not resolve the issue either. However, looking at the integrating time step of the overall *Integrator* prompted the re-evaluation of the *DMCplus Controller* set-up: the default controller sampling interval of 1 minute is an order of magnitude larger than the *Integrator* step sizes. Therefore, the controller does not record/sample at the required frequency to adequately capture the system's response.

The controller's sampling frequency was increased to an interval of 0.02 minutes (1.2 seconds), and the subsequent results were more aligned with the expected response, as shown in Figure 24.

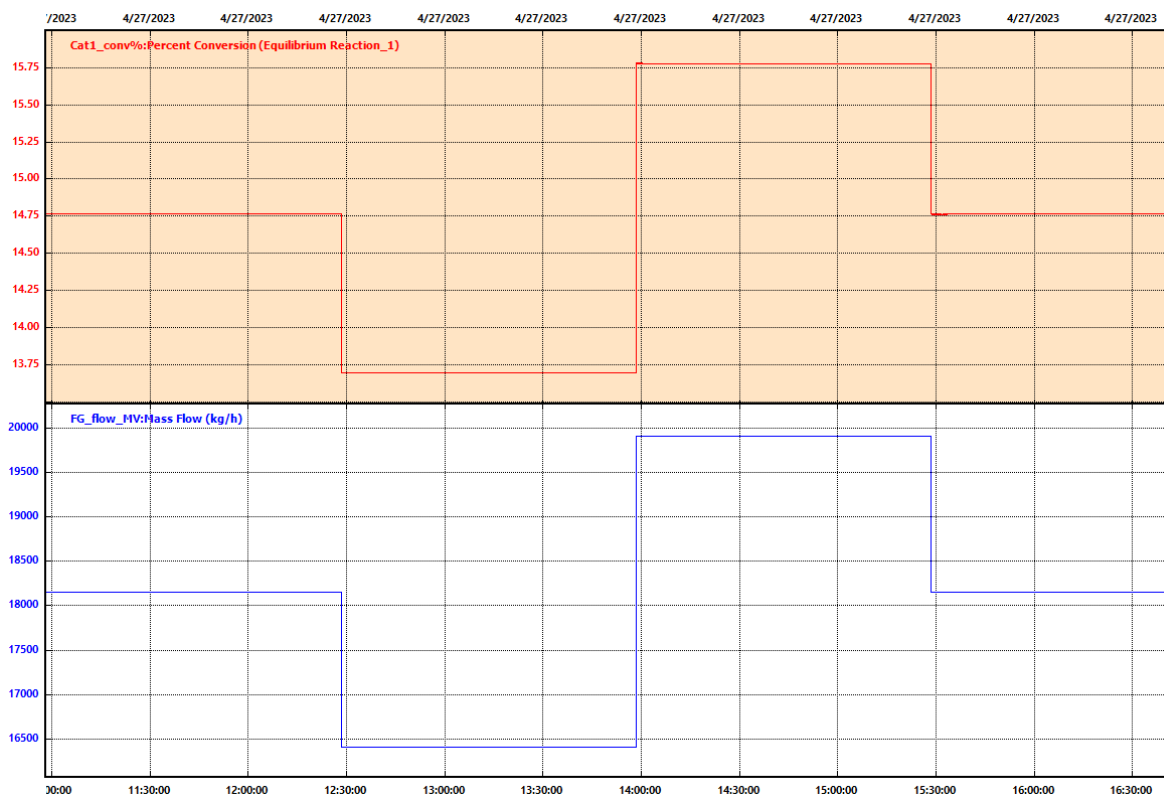


Figure 23: Step test results – initial.

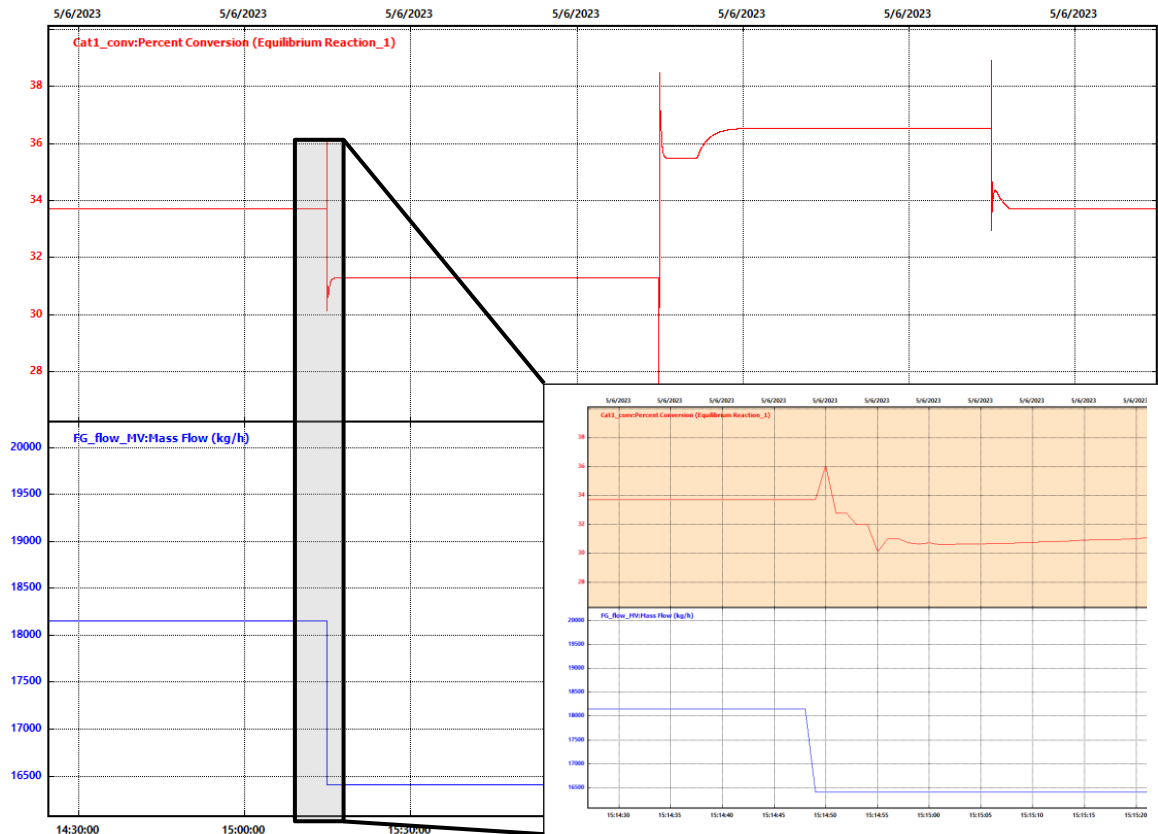


Figure 24: Step response – increased sampling frequency.

When implementing the *DMC Controller*, it was noted that some of the recorded measurements had shown the incorrect units and values; for example, when trying to record the temperature of the stream going into the interbed cooler, a value of 1.6×10^6 kmol / h was reported by the *DMC Controller* instead of a value of about 460 °C. This was due to the measurement specified not being a calculatable variable of the stream. If the temperature was instead referred to as the inlet temperature of the heat exchanger and thereby referenced a temperature connected to the heat exchanger instead of the stream, it could be calculated, and therefore, it was correctly recorded.

Another issue that had to be resolved was a large time delay (dead time) of about 30 minutes, as shown in Figure 25. This was attributed to too much hold-up at some pieces of equipment. To narrow down where this excess hold-up could be in the system, the temperature and flow at the outlet of the different units were recorded, and a step test was conducted. Measuring the values at each step allowed for quick identification of the unit where the hold-up or delayed response first occurs. This delay was seen to be around the process gas heater. Upon further investigation, the steam line valve was identified as the unit with the excess hold-up. Due to the high pressure and high-temperature steam, the line size at the valve has a greater impact on the linear velocity of, for example, a gas in a comparatively big duct. The standard line size

of 50 mm specified by HYSYS resulted in a lower linear velocity for a given flow rate and a small pressure drop. The flow rate through the valve is influenced by both the valve's inlet and outlet pressures via the valve equation (Aspen Technology, 2019b). Reducing the line size to 25 mm increased the linear velocity by four times ($v \propto \frac{1}{d^2}$), leading to an improved pressure balance and a much reduced hold-up/delay.

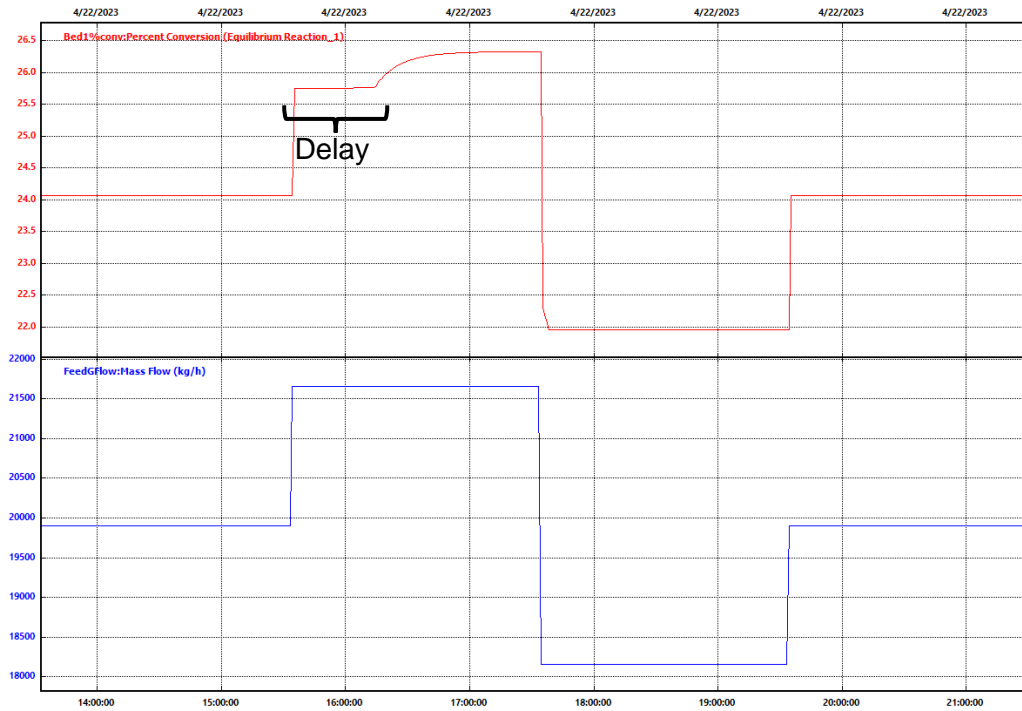


Figure 25: Step response – long time delay.

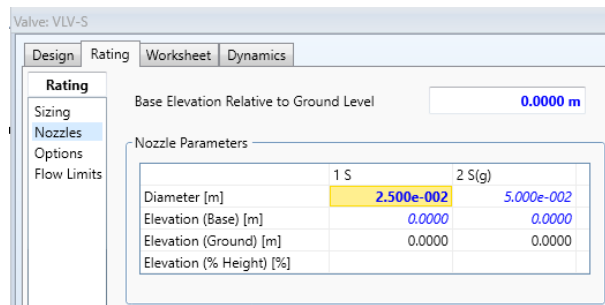


Figure 26: Steam valve nozzle parameters.

4 Results and Discussion of the Plantwide Control Application

4.1 Choice of Methodology

Larsson & Skogestad (2000) proposed a nine-step procedure to approach the plantwide control problem. Although that procedure will not be followed for this analysis, it will be compared to the seven-step top-down, bottom-up approach used by Skogestad (2002). The nine-step procedure's first step is to identify the control objectives and process constraints. Identification of the objectives is considered an important step as upfront identification of the overall objective of the plantwide control strategy can inform the subsequent decisions required. For example, keeping the overall objective in mind can aid in identifying and selecting the primary controlled variables to achieve the overall objective. However, in 2002 Skogestad (2002) listed the selection of the primary controlled variables as step 1 of a seven-step procedure instead of identifying the control objective first as in the nine-step procedure (Larsson & Skogestad, 2000). In 2004, the seven-step procedure (Skogestad, 2002) was expanded to include defining the operational objectives prior to selecting the primary controlled variables (Skogestad, 2004).

This study will follow the seven-step top-down, bottom-up approach first described by Skogestad (2002) but will consider the identification of the control objective before identifying the process variables (Skogestad, 2004)

4.2 Step 1: Identification of Process Variable

The main objective of the acid plant is to achieve the highest possible conversion of SO_2 to SO_3 and, subsequently, H_2SO_4 . Secondary control objectives include minimising temperature fluctuations (leading to cyclical behaviour, which can cause fatigue stress in mechanical equipment), keeping the off-gas temperature above the acid dew point temperature and minimising operational costs. The operational cost of the plant is primarily influenced by the power consumption of the fans/blowers, the external heating required before the converter (i.e., fuel consumption or, in this case, electrical power consumption) and cooling water usage (excluded in this model). The steam used for heating and cooling effectively exists in a closed system; therefore, the consumption thereof will not influence the operation cost function.

4.3 Step 2: Selection of Manipulated Variable

The second step (Larsson & Skogestad, 2000, Skogestad, 2002) aims to identify which variables are available to manipulate and control the primary variables identified in the previous step. This is often best executed by doing a degrees of freedom analysis. However, as plants get larger performing this analysis becomes more and more difficult.

Jensen & Skogestad (2009) used a simplified method of identifying the available degrees of freedom of a complex plant. The method assigns degrees of freedom based on the type of unit operation and number of feed streams. This method was employed to identify this plant's available steady-state degrees of freedom. As the feed stream cannot be controlled and will be regarded as a disturbance variable, no degrees of freedom will be assigned. The hot air and steam feed streams are each assigned a degree of freedom, The splitters account for four more degrees of freedom, and the blowers are each assigned another degree of freedom. Although there are five heat exchangers, the ones with steam and hot air do not contribute to steady-state degrees of freedom. For the two heat exchangers, after the two converter beds, a degree of freedom is lost by accounting for the bypass as part of the splitter degree of freedom. Therefore, the degrees of freedom for this plant is 10. The ten manipulated variables in Table 5 will therefore be adequate to account for all 10 degrees of freedom. The steady-state values reported in Table 5 have not been optimised and result in an overall conversion of 79.1 % of SO₂. To improve the conversion and obtain ~98 % conversion, the inlet temperature to each catalyst bed must be controlled / optimised.

Table 5: Key variables.

Variable	Unit	Description	Steady-state value
Available Manipulated Variables			
EH_p	kJ / h	Power/ fuel flow rate	352 452 (98 kW)
9FG	kg / h	Hot gas to second process gas cooler (by controlling bypass 1BP-1)	18 830 (bypass: 287)
12FG	kg / h	Hot gas to interbed cooler (by controlling bypass 2BP-2)	14 720 (bypass: 4 397)
FA001_sp	rpm	Feed gas blower fan speed	2 037
FA002_sp	rpm	Process gas blower fan speed	1 800
FA003_sp	rpm	Recycle gas blower fan speed	1 250
S	kg / h	Steam flow rate	549
C	kg / h	Hot air flow rate	19 080
1R	kg / h	Gas recycled	628
3R	kg / h	Gas to mixer	331
Controlled Variables			
SO2%_1	%	SO ₂ conversion in Reactor 1	48.3
SO2%_2	%	SO ₂ conversion in Reactor 2	59.6
Disturbance Variables			
F	kg / h	Feed flow rate	18 158
F_SO2	Vol%	Inlet composition – SO ₂	3.0
F_H2O	Vol%	Inlet composition – H ₂ O	7.0

In Figure 27, potential key controlled, manipulated and disturbance variables have been identified.

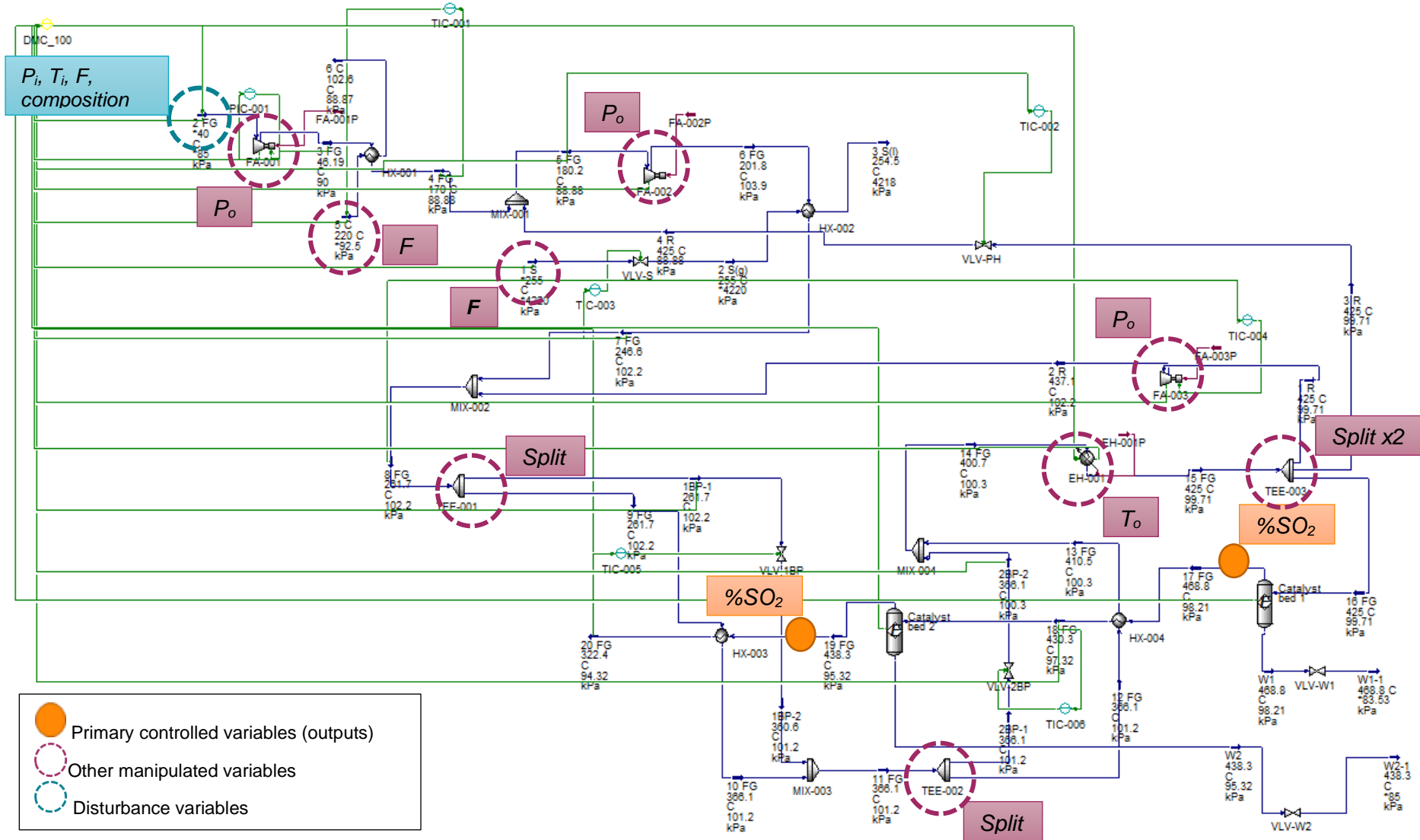


Figure 27: Dynamic model – variables used for control.

The *DMCplus Controller* was used to perform step tests on the dynamic model – each of the identified manipulated and disturbance variables was individually stepped, and the response of each possible controlled variable was recorded. These step tests aim to determine which of the primary variables should be controlled by evaluating the effect of disturbances (introducing active constraints) and the effect or economic loss of using constant set-points for certain variables. Using constant set points for the primary controlled variables aims to attain self-optimizing control by realising an acceptable loss without having to control or re-optimize when disturbances occur (Skogestad, 2000).

It was difficult to change (step) the feed gas composition to see the effect of compositional variation on the system. To do this, feed streams with different compositions would have to be mixed in varying ratios to create the actual feed stream. This would have required an additional controller in the model to simulate a disturbance in feed composition. For the purpose of this study it was deemed as unnecessary but can be incorporated into future models. The manipulated variables used in the *DMCplus Controller* and the values used for the initial step tests are listed in Table 6. In some cases, the original values differ from that reported in Table 5; these variables had to be adjusted to allow for the step sizes (Table 6) to be made in each direction (for example, to ensure that a negative valve opening is not specified as a result of stepping the valve -20 % from its original opening of 10 %).

In the model (and actual plant) it is relatively easy to evaluate the effect of fan speeds on the system as these can be changed with a setting (i.e., in the control system, change the fan speed). However, the flow rates cannot be changed as easily as the fan speeds (i.e., there is no ‘flow rate button’ in the control system), and therefore valves are required to manipulate the flow rates, both in the model and in the physical system. The streams and the associated valves that influence their flow rates are listed below:

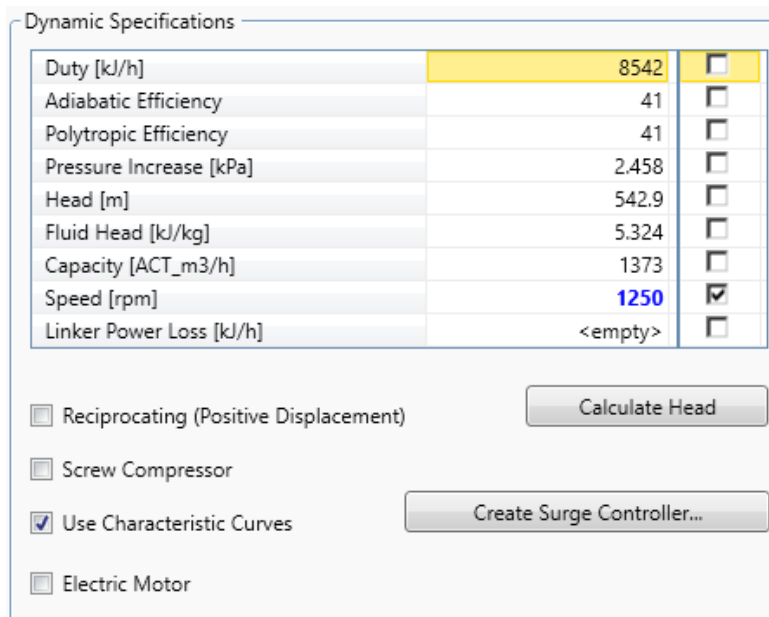
- F (feed gas flow) – none. As this is a feed stream in the model, HYSYS has the capability of setting the flow rate without a controller or valve.
- 9FG (gas to second process gas cooler) – VLV-1BP. The valve regulates the flow in the bypass line and, thereby, indirectly manages the flow through the heat exchanger. This valve is required in the bypass line to ensure the pressure balance over the heat exchanger and the bypass line works out.
- 12FG (gas to interbed cooler) – VLV-2BP. This valve-stream configuration operates similarly to the previous configuration mentioned between 9FG and VLV-1BP.
- S (steam) – VLV-S. The valve on the steam line regulates the steam flow rate.
- C (hot air) – none. Like the feed gas flow rate, this stream’s flow rate is changed directly (as an input) in HYSYS.

- 1R – none. The mass flow rate of this stream is specified as a hardcoded input.
- 3R – VLV-PH. This valve controls the flow of hot recycle gas to MIX-100.

The fans' speed does not need a valve or other method of controlling it, i.e., it can be specified directly in the *DMCplus Controller*, given that the speed is selected as a specification for the given fan (see Figure 28). As the speed setpoint changes, the fan's operating point shifts on the characteristic curves and consequently, the other parameters of the fan change.

Table 6: *DMCplus Controller* step test setup.

Manipulated Variable	Unit	Initial Value	Amplitude (%)	Step size
FG_flow ⁶	kg / h	18 158	5.0	1 750
EH-001T	C	425.0	5.0	21.25
VLV-PH	%	26.7	20.0	20
1R	kg/h	702	3.0	150
FA-003	rpm	1 250	15.0	187.5
FA-001	rpm	2 037	10.0	203.7
FA-002	rpm	1 800	15.0	270
VLV-S	%	66.5	10.0	10
5C	kg / h	19 080	10.0	3 731
VLV-1BP	%	30.0	20.0	20
VLV-2BP	%	38.2	20.0	20



Dynamic Specifications

Duty [kJ/h]	8542	<input type="checkbox"/>
Adiabatic Efficiency	41	<input type="checkbox"/>
Polytropic Efficiency	41	<input type="checkbox"/>
Pressure Increase [kPa]	2.458	<input type="checkbox"/>
Head [m]	542.9	<input type="checkbox"/>
Fluid Head [kJ/kg]	5.324	<input type="checkbox"/>
Capacity [ACT_m3/h]	1373	<input type="checkbox"/>
Speed [rpm]	1250	<input checked="" type="checkbox"/>
Linker Power Loss [kJ/h]	<empty>	<input type="checkbox"/>

Reciprocating (Positive Displacement) Calculate Head
 Screw Compressor
 Use Characteristic Curves Create Surge Controller...
 Electric Motor

Figure 28: Dynamics specification of blowers.

The manipulated, disturbance, and controlled variables differ significantly in magnitude, and the effect of one manipulated variable cannot quantitatively be compared to that of another. For example, changing a valve opening by a value of 10 (10 out of 100 possible change) and a

⁶ Feed gas flow is a disturbance variable.

fan speed by 10 (10 out of 3 200 possible change) and comparing both effects on the controlled variables will give skewed results. Therefore, to simplify comparisons between the different variables, the input and output variables in Table 7 were scaled according to the method described by Skogestad & Postlethwaite (2005). This method entails dividing each variable by its maximum anticipated / permitted change. For disturbances, this is the largest anticipated change in disturbance and for inputs, the maximum permitted input change.

The scaled steady-state gain, i.e., the change in output divided by change in input or disturbance, as shown in Equation 11, for the final SO₂ % and total power consumption for a step down in the manipulated (or disturbance) variable (-MV) and a step up in the manipulated (or disturbance) variable (+MV) are given for of each of the manipulated (disturbance variable in the case of the feed gas flow rate) variables in Table 7.

$$G = \frac{\Delta y}{\Delta u} \quad 11$$

Table 7: Scaled steady-state gains.

Manipulated Variable	Unit	SO ₂ [%] (-MV)	SO ₂ [%] (+MV)	Duty [kJ/h] (-MV)	Duty [kJ/h] (+MV)
FG_flow ⁷	kg / h	-0.09	0.17	-42.12	-41.06
EH-001T	°C	0.49	0.54	-16.48	-0.89
VLV-PH	%	0.00	0.00	-0.46	-
1R	kg / h	0.00	0.00	0.00	0.00
FA-003	rpm	-0.23	-0.09	-19.91	-6.59
FA-001	rpm	-0.06	-0.10	-9.35	-4.74
FA-002	rpm	-0.05	-0.05	-12.27	-6.55
VLV-S	%	0.06	0.06	7.07	2.05
5C	kg / h	0.04	0.03	4.67	0.88
VLV-1BP	%	-0.01	-0.01	-0.90	-
VLV-2BP	%	0.07	0.07	-5.32	-

The time delay (dead time) of each manipulated variable on the change in final SO₂ concentration and the total duty is given in Table 8 **Error! Not a valid bookmark self-reference.**. The time delays are very small (less than 11 s) irrespective of the manipulated variable, indicating a fast response to changes in the manipulated/disturbance variables. For this study the dead time was therefore not used to determine manipulated and controlled variable pairings.

The results reported in Table 7 are more easily analysed when looking at it visually. The effect on final conversion by stepping each of the manipulated/ disturbance variables is shown in Figure 29. In Figure 29, each manipulated variable is step-tested consecutively, and the resulting movement in the final SO₂ concentration for each step test is shown. Here it is clear

⁷ Feed gas flow is a disturbance variable.

that a change in outlet temperature of the electric heater (inlet temperature to the first converter) and, by implication, the electric heater's duty has the most prominent effect on the final conversion achieved. FA-003's speed has the second largest effect on the conversion. These visual results correlate with that reported in Table 7.

Table 8: Dead time (in seconds).

Manipulated Variable	Unit	SO ₂ [%]	Duty [kJ/h]
FG_flow ⁷	kg / h	2.4	1.2
EH-001T	°C	8.4	0
VLV-PH	%	2.4	2.4
1R	kg / h	8.4	2.4
FA-003	rpm	8.4	2.4
FA-001	rpm	2.4	2.4
FA-002	rpm	2.4	2.4
VLV-S	%	8.4	10.8
5C	kg / h	8.4	8.4
VLV-1BP	%	8.4	2.4
VLV-2BP	%	6.0	2.4

It is observed that the steady-state gain achieved when stepping up is not necessarily the same as when stepping a variable by the same amount in the opposite direction. This behaviour makes sense when considering the system's physical properties: increasing the converter bed inlet temperature will not have an equal but opposite effect on the conversion as decreasing the temperature. This ability to capture non-linearity in the process is another advantage of using a model to determine the plantwide control strategy.

The opposite effect is evaluated to consider the manipulated variables that can be specified to have constant setpoints and thereby achieve some degree of self-optimising control (i.e., achieves an acceptable loss by implementing a constant setpoint). The manipulated variables with little to no effect on the primary controlled variables can likely be set to constant set points without incurring significant economic losses. When considering the final SO₂ conversion, the variables that might be set to constant setpoint are 1R (hot gas recycled from the support heater outlet to the process gas heater outlet), VLV-PH (hot gas recycled to the mixer to heat the feed gas), and VLV-1BP (bypass around HX-003), as these variables have the smallest effect on the final SO₂ conversion.

Considering the results in Table 7 and Figure 30, these same variables have little effect on the system's total duty (total energy consumption by FA-001, FA-002, FA-003, and EH-001); therefore, we can use constant set points for these variables. Using constant setpoints for these three variables leaves seven remaining degrees of freedom.

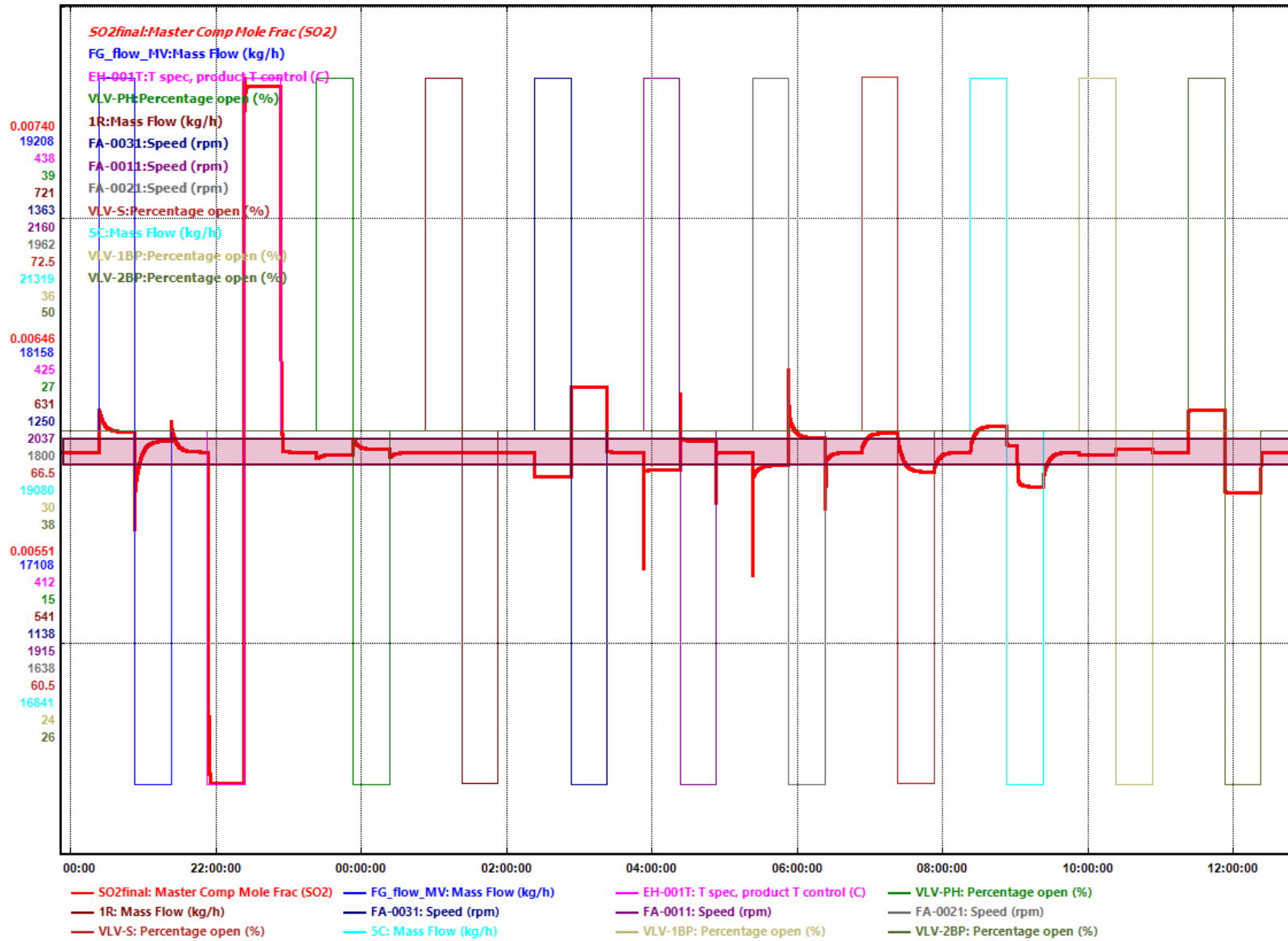


Figure 29: Effect of step tests on final SO₂ concentration.

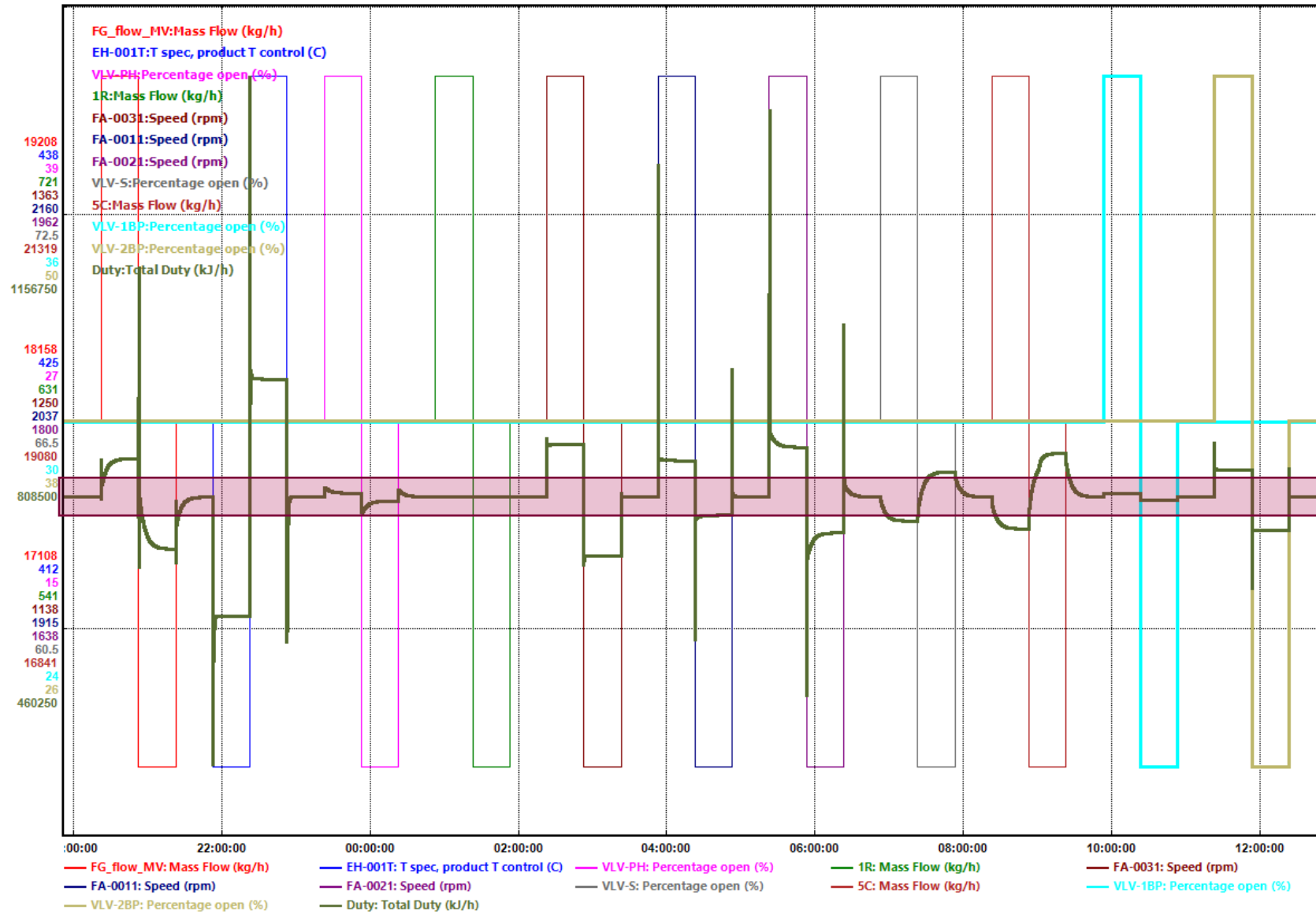


Figure 30: Total duty during step tests.

4.4 Step 3: Setting Production Rate

Deciding where to set the production rate is a very important decision as it impacts the structure of the control system in the bottom-up design. The analysis often informs this selection and results from the preceding step. Certain constraints in the system can also influence the choice of manipulated variables (Larsson & Skogestad, 2000).

From Table 7, it is evident that the final SO₂ concentration is most significantly impacted by changes in the first converter's inlet temperature, as this manipulated variable produces the largest steady-state gain. Another important consideration in selecting where the production rate will be set is the overall operation of the plant. Ideally, the chosen manipulated variable should ensure stable operation, smooth transitions, and disturbance rejection.

A controller (XIC-100) was added to manipulate the first converter's inlet temperature (EH-001T) to keep the final SO₂ concentration constant. Comparing Figure 29 and Figure 31, it is evident that manipulation of the first converter inlet temperature effectively keeps the final SO₂ concentration constant. The consequent effect on the total duty is seen in Figure 32, where the general response is the same as in Figure 30.

4.5 Step 4: Regulatory Control

The bottom-up design follows the more traditional control design procedure by first looking at essential controls and then implementing further control to optimise the system. The regulatory control layer aims to stabilise the plant and provide local disturbance rejection by using simple controllers, such as PID controllers. The secondary controlled variables need to be identified to implement this control layer. These variables will either be used in stabilising control loops to manage drifting away from the nominal plant operation, or they will be used to manage disturbances impacting the primary controlled variables (Skogestad, 2004, Larsson & Skogestad, 2000, Luyben *et al.*, 1997).

When selecting the secondary controlled variables, operational constraints have to be considered. Luyben *et al.* (1997) mention that environmental considerations and product quality can influence the control constraints. However, by controlling the emissions (final SO₂ concentration) as part of Step 3, the quality of the final product and environmental concerns have been addressed.

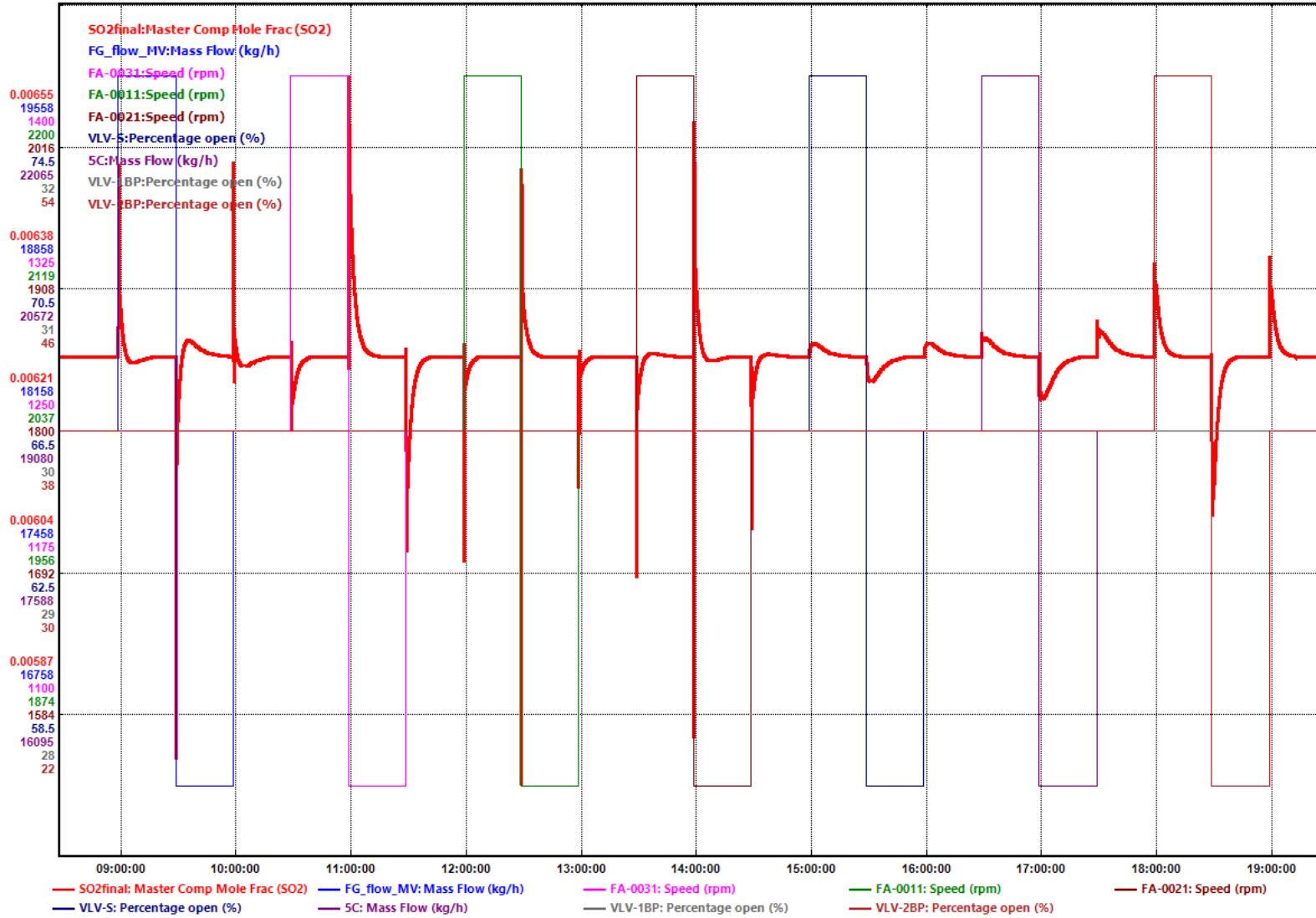


Figure 31: Final conversion response when stepping MVs while controlling converter inlet temperature.

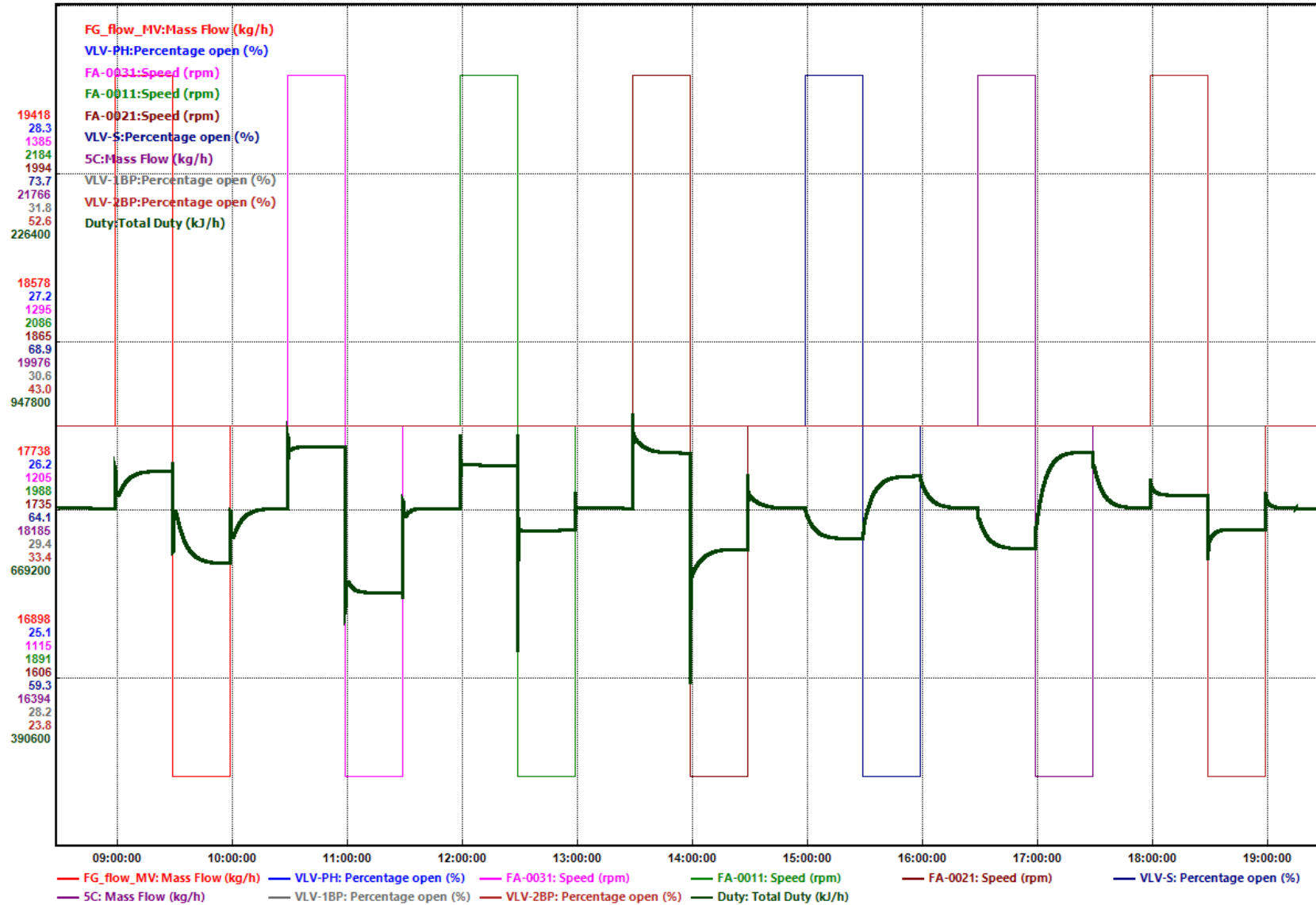


Figure 32: Effect on Total Duty when controlling the final SO₂ concentration.

The feed gas flow rate (disturbance variable) significantly affects the system's total duty and, thereby, the operating cost. This effect is illustrated in Table 7, where it is evident that the scaled gain of the disturbance variable is larger than any of the manipulated variables' gains when comparing the total duty of the system. Controller XIC-100 has been implemented; therefore, this controlled system's response will be considered for further analyses.

The disturbance (feed gas flow rate) also has a significant effect on the preheater's (HX-002) outlet temperature as well as the first process gas heater's (HX-003) outlet temperature (tube side), as seen in Figure 33. HX-003's tube side outlet temperature can be regarded as a disturbance to the downstream process, either managed by downstream processes/controllers or the current system. The impact of HX-003's outlet tube side temperature on the current plant is also insignificant. It was therefore decided to consider HX-002's outlet temperature first. HX-002's outlet temperature is controlled by the amount of steam fed to the heat exchanger. TIC-003 is activated, which aims to control the outlet temperature by adjusting the steam flow rate. Controlling the steam flow rate and, thereby, HX-002's outlet temperature improves the rejection of the disturbance caused by fluctuations in the feed gas flow rate and stabilises the plant operation regarding total duty. Furthermore, in Figure 34, less variation is observed in the tube side outlet temperature of HX-003.

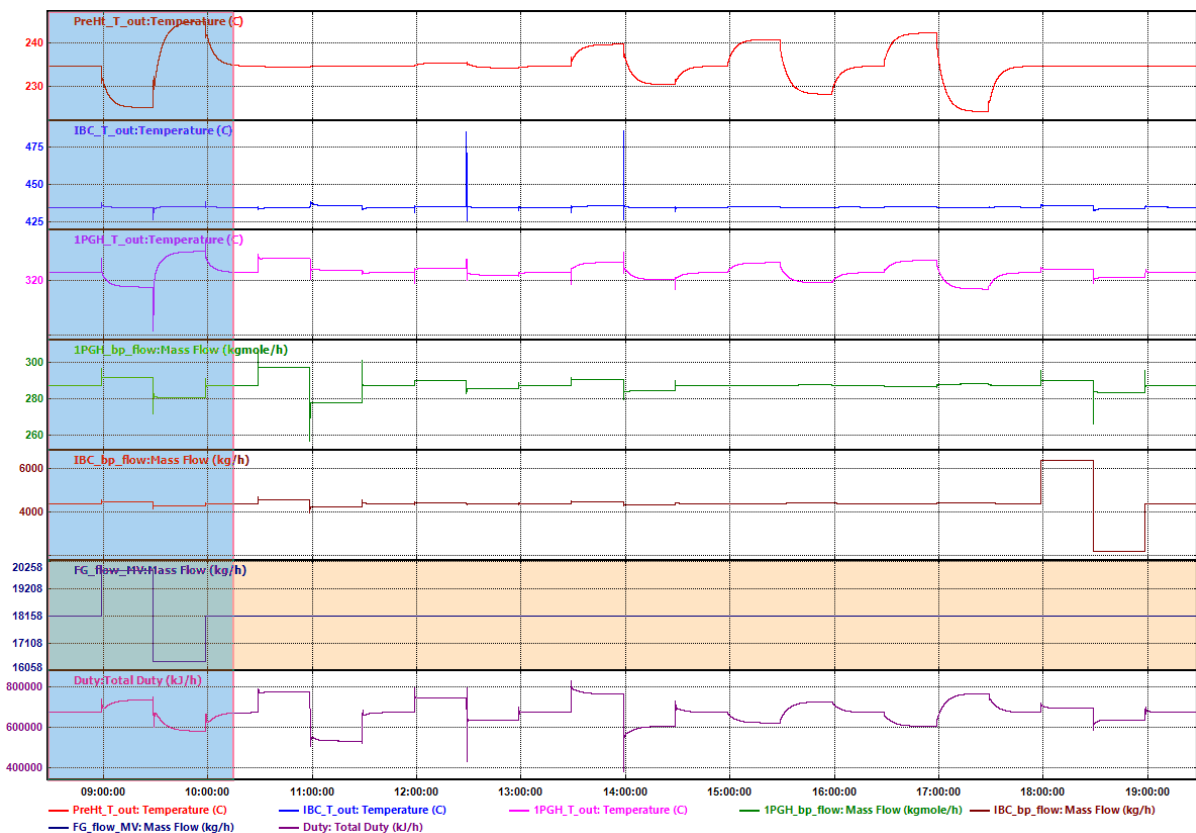


Figure 33: Effect of disturbance variable on other process variables.

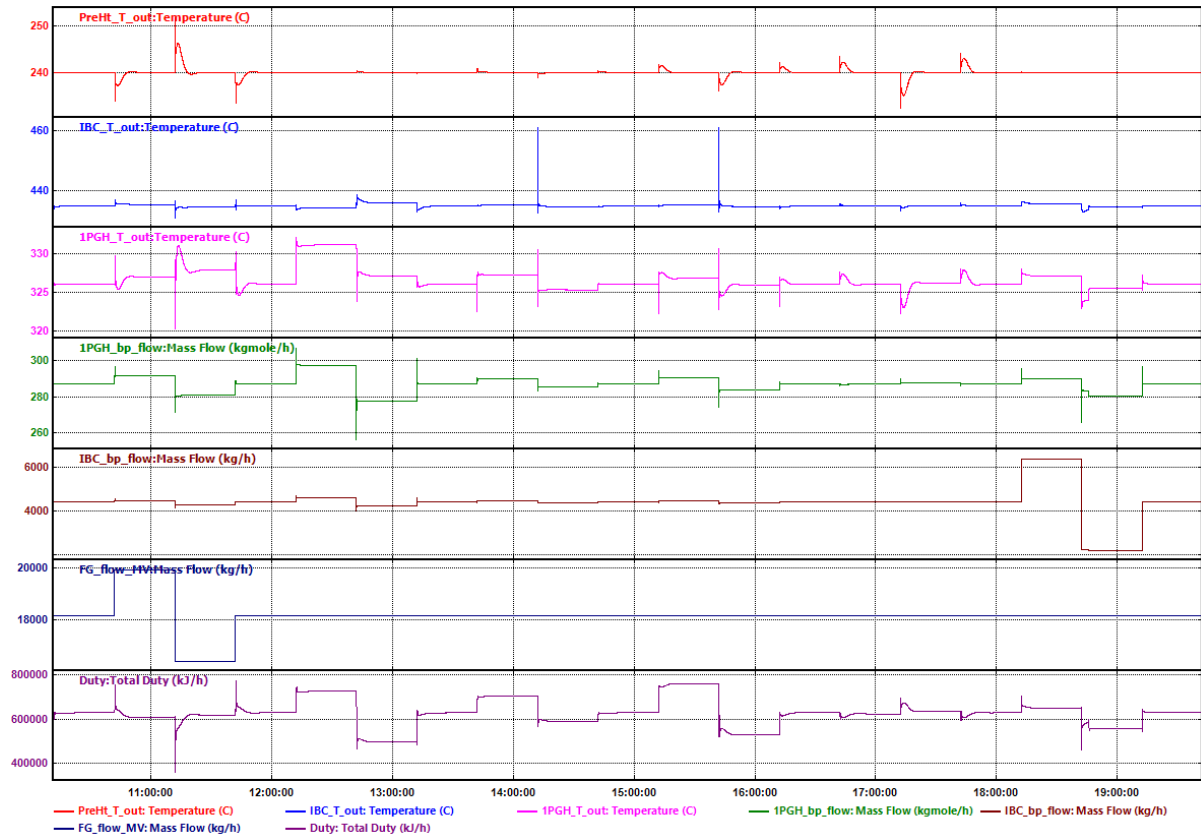


Figure 34: Effect of disturbance variable, when controlling steam flow rate.

The total duty comprises the duty of the three fans and the duty of the support heater. In Figure 35, the individual response of each of these variables was considered, where the electric heater contributes the most to observed fluctuations in the total duty. This contribution is due to its weighted contribution to the total duty. Furthermore, it is observed that although FA-003 contributes the least to the total duty, as it has the lowest individual duty, it is the most susceptible to fluctuations in the process. The electric heater's duty is determined by the temperature difference over it, and thus the inlet temperature and outlet temperature (determined by XIC-100).

After implementing TIC-003, controlling the steam flow rate and HX-002's outlet temperature, the effect of the remaining five manipulated variables (5 DOF) on the total duty and final SO₂ concentration is shown in Figure 36 and Figure 37, respectively. The three fans have the largest effect on the total duty, and the condenser flow rate has the smallest effect. Similarly, steps in the setpoints of the three fans result in the largest overshoot in the SO₂ concentration (Figure 37).

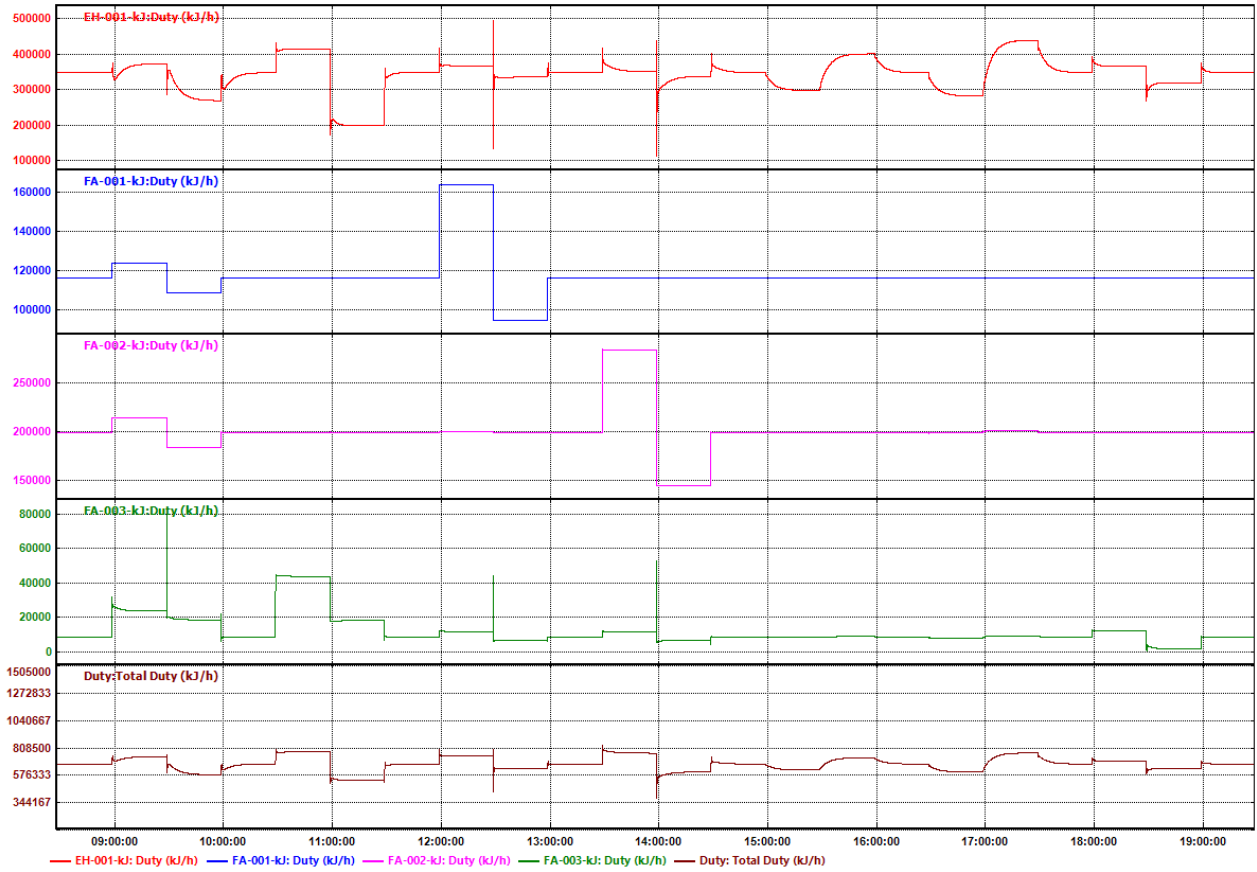


Figure 35: Step response of CVs contributing to total duty to a disturbance change.

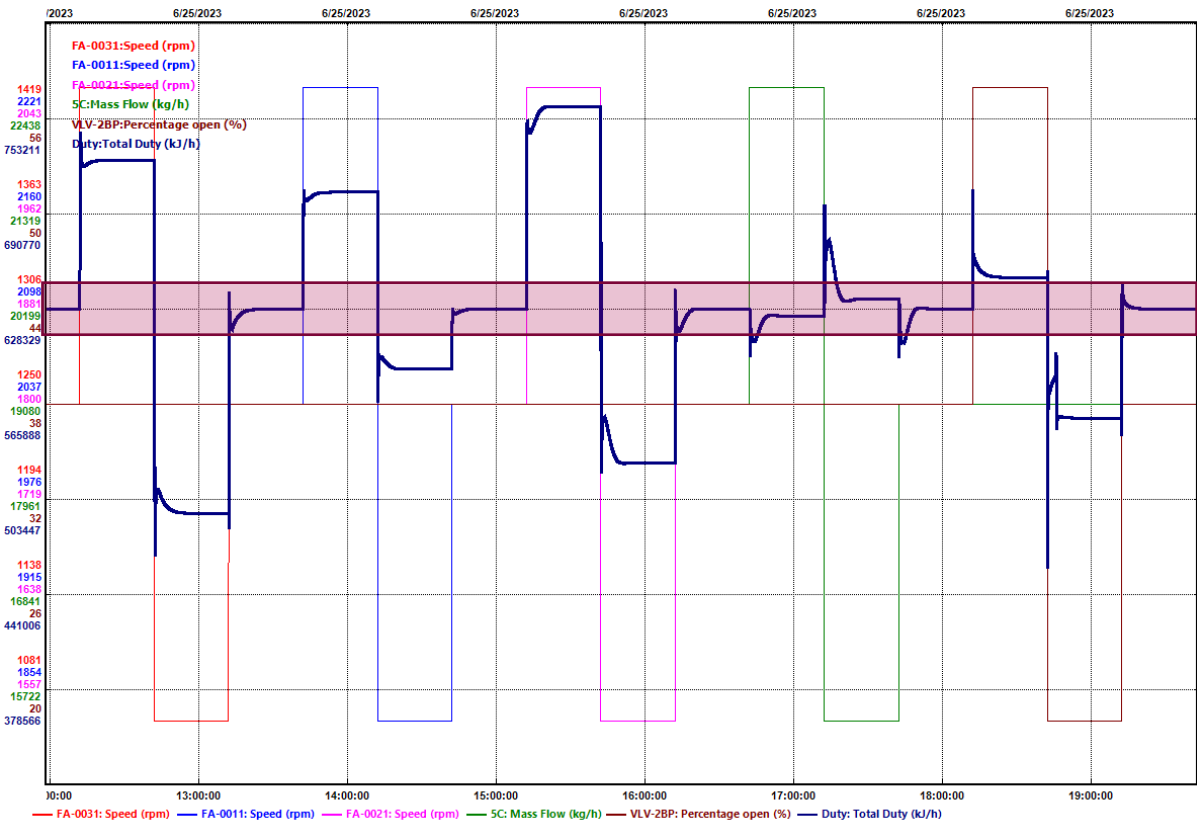


Figure 36: Effect of remaining 5 MVs on the total duty.

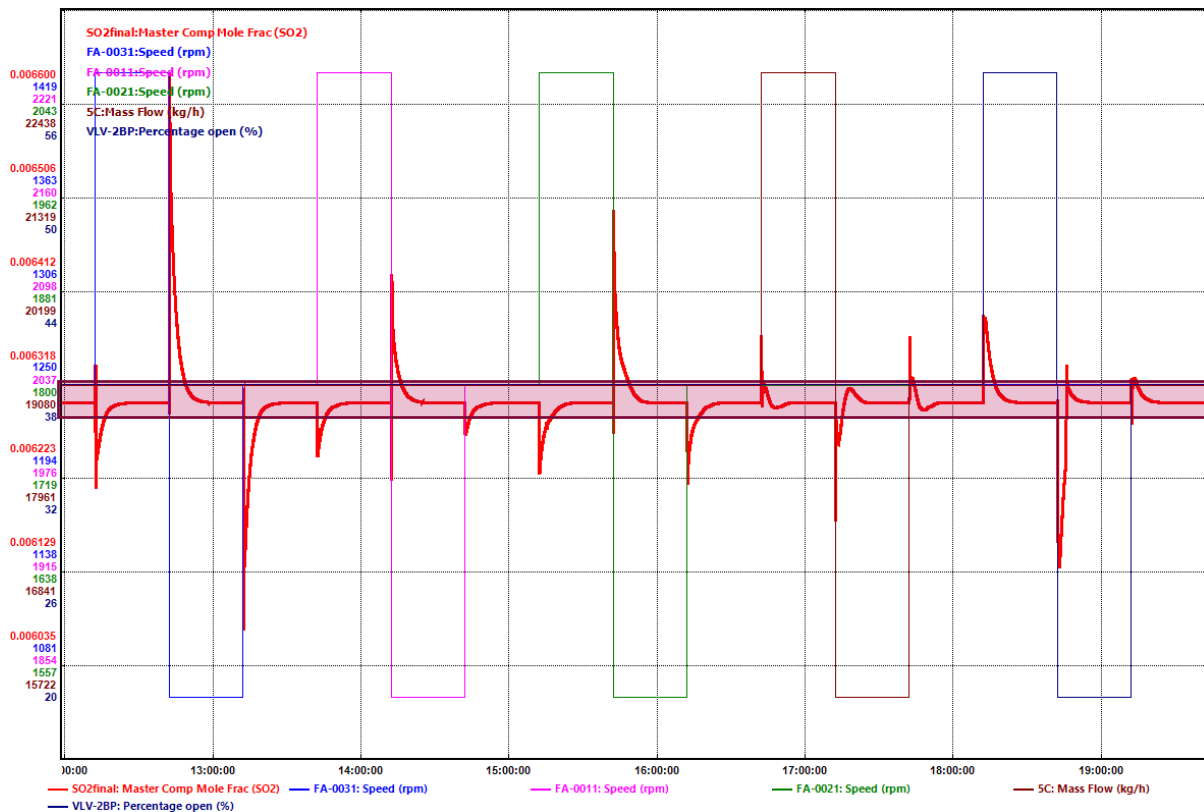


Figure 37: Effect of remaining 5 MVs on the final SO₂ concentration.

To further reduce the fluctuation in total duty and, at the same time, reduce fluctuations in the tube side outlet temperature of HX-003, another regulatory control loop is considered. Figure 38 shows the step responses of the remaining 5 DOFs on the total duty, electric heater's duty and HX-003's outlet temperature. FA-003's fan speed significantly impacts both HX-003's temperature and the electric heater's duty. FA-002's fan speed influences the total duty but not the electric heater's duty. This impact is thus purely due to the increased power required when operating at a higher fan speed.

Controller TIC-004 was switched on to control the temperature of stream 8FG (see Figure 39) as this stream is closer to FA-003 and will influence the temperature of stream 20 FG (HX-003's outlet temperature). The result of this decision is seen in Figure 40, where we see that by controlling stream 8FG's temperature, the temperature of stream 20FG also remains constant. However, there is no visible or significant effect on the total duty.

The four remaining degrees of freedom are the fan speeds of FA-001 and FA-002, the hot air flow rate and the bypass around HX-004. As a regulatory measure, the hot air flow rate will be used to control the exit temperature of HX-001 to above the acid dewpoint temperature. This is required to ensure that downstream equipment is not susceptible to or damaged by corrosion due to acid condensing out of the process gas stream.

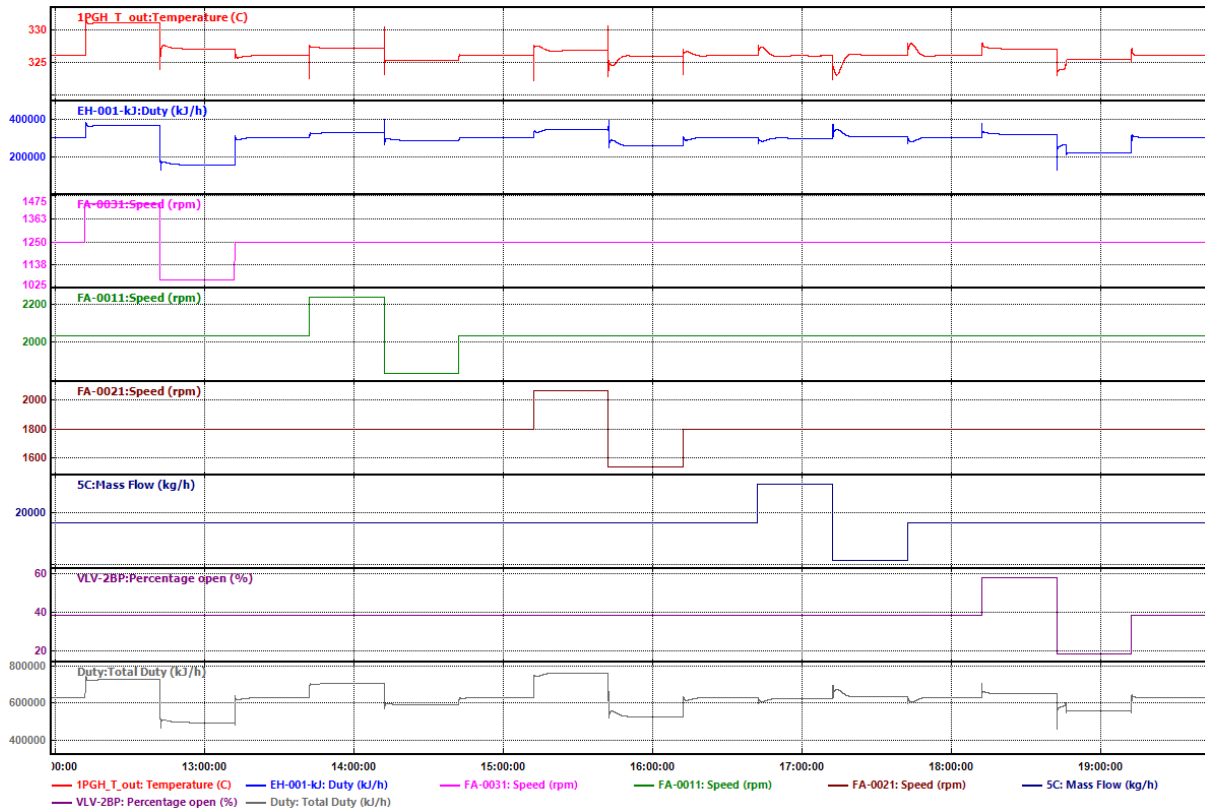


Figure 38: Effect of remaining DOFs on duty and HX-003's outlet temperature.

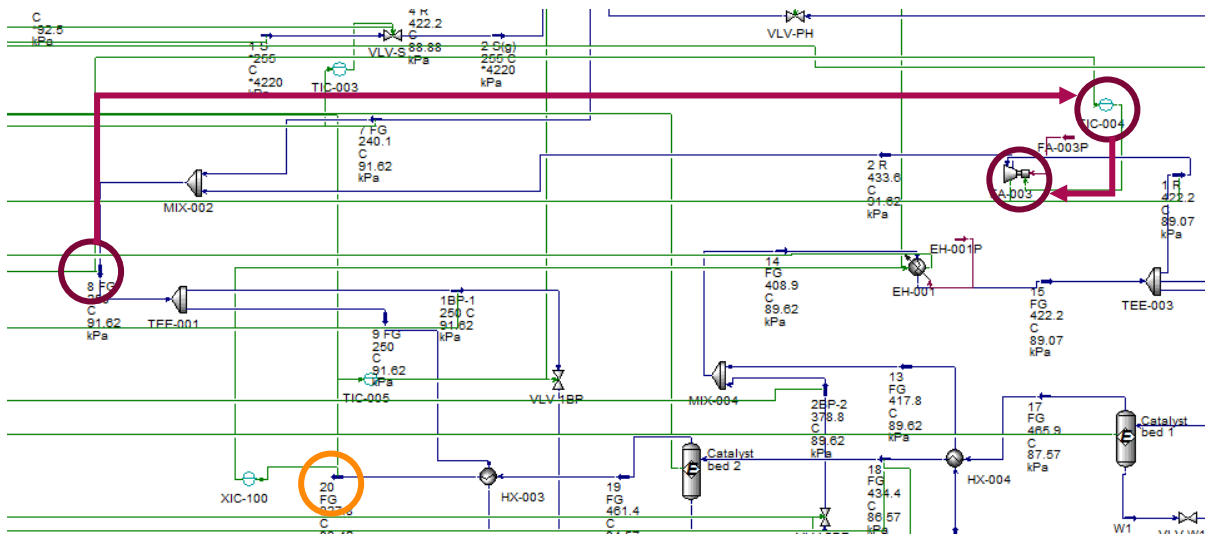


Figure 39: Using MV FA-003 fan speed to control stream 8FG temperature.

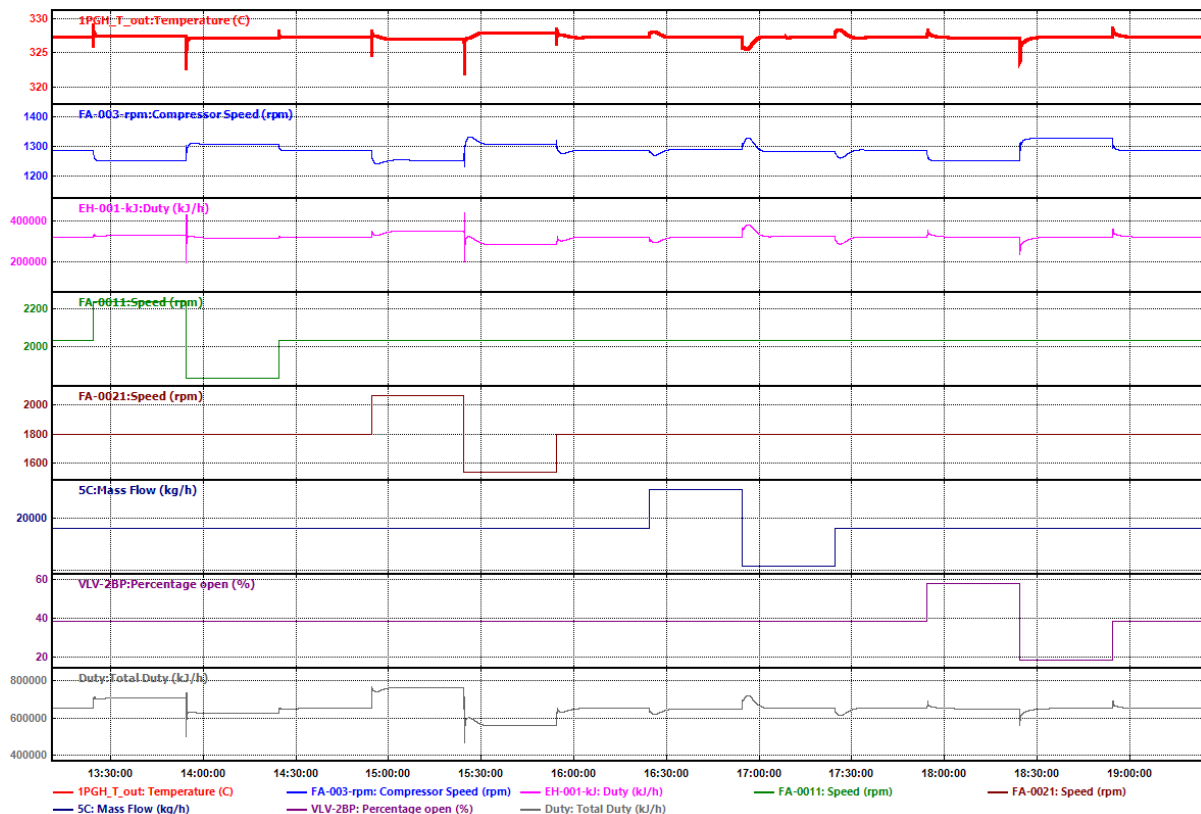


Figure 40: Step tests when MV FA-003 fan speed is used to control 8FG’s temperature.

TIC-001 is implemented, controlling the outlet temperature of HX-001 to above 175 °C. Technically, this temperature would need to be calculated based on the concentration of SO₂, SO₃, and H₂O in the feed stream. However, since we cannot add changes in the composition as disturbances, the need for the calculation is redundant. A manual input value was used to illustrate the implementation of the plantwide control strategy. The effectiveness of this controller should also be tested against disturbances in the feed gas temperature. As it is not possible to test this disturbance, it is assumed by the rejection of the increase in feed gas flow rate as well as a slight change in temperature (due to heat of compression when changing FA-001 speed) that the controller performs adequately. The temperature control is illustrated in Figure 41.

4.6 Step 5: Supervisory Control

The supervisory layer aims to utilise the remaining degrees of freedom to maintain the primary control variables at their optimal setpoints. The two methods usually used in this layer are decentralised control and multivariable control. Decentralised is ideal when constraints are static, and the process does not have too much interaction. Multivariable control is preferred when the constraints are active, i.e., continuously changing and when the process has lots of interaction.

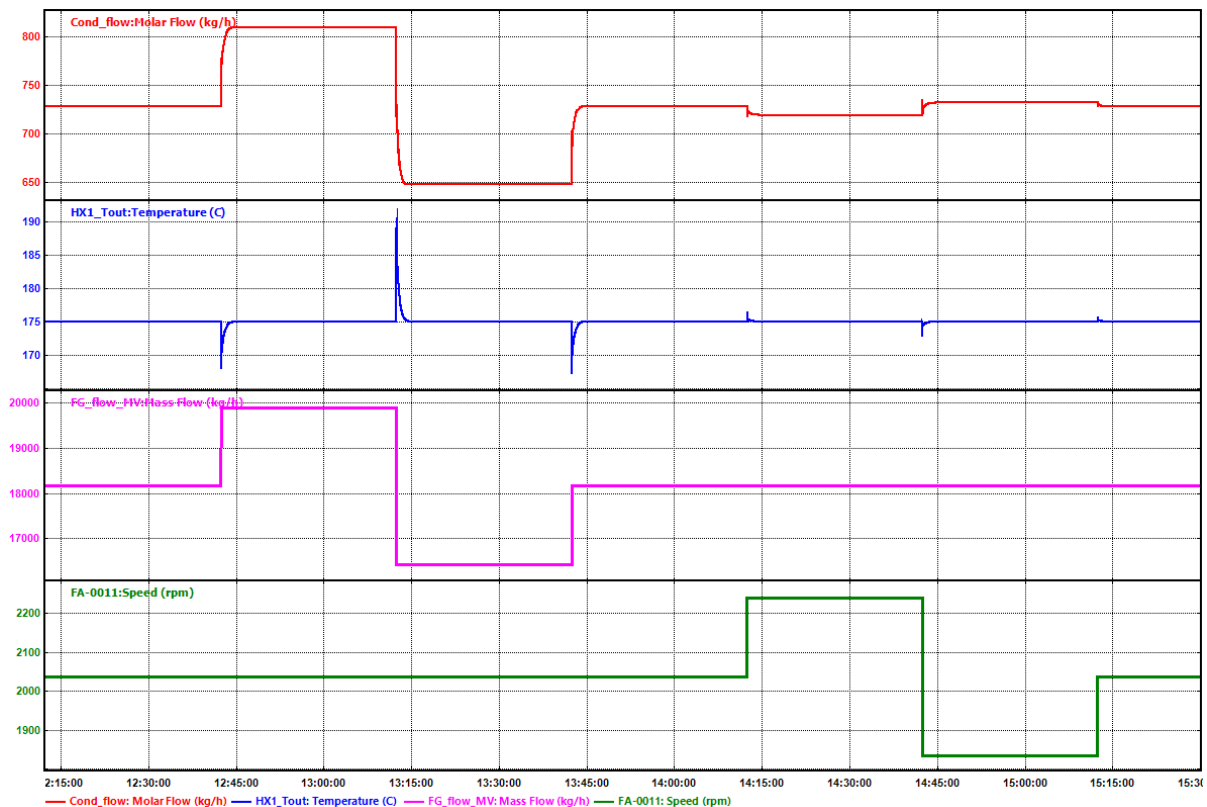


Figure 41: Temperature control (above acid dewpoint) by changing hot air flow rate.

As mentioned, FA-001 is typically used to move the process gas through the upstream system. For this plantwide design, the fan will therefore be set to achieve a constant outlet pressure.

Controllers from the regulatory layer that can be used or adjusted by the supervisory layer are the TIC-004 (adjusts the fan speed of FA-003 to control the temperature of 8FG) and TIC-003 (controls the steam flow rate and thereby the outlet temperature of HX-002). The three manipulated variables with constant set points (1R, VLV-PH, VLV-1BP) can be optimised or adjusted before implementing the supervisory controller. The final SO₂ concentration is limited by legislation and environmental compliance and should, therefore, not be adjusted or changed.

An advanced control method is readily available as the *DMCplus Controller* was used to perform the model tests. Therefore, model predictive control can be implemented using the dynamic matrix controller to control the MIMO system. The MPC system can be implemented on top of a regulatory control layer, utilising the controllers from the regulatory layer mentioned above. This helps minimise performance losses as the multivariable control policy has access to the setpoints of the regulatory controllers (Juliani & Garcia, 2017, Skogestad, 2002).

In Figure 42, a block flow diagram of an MPC system is shown. The dynamic model can be used to predict the current values of the output variables (controlled variables, such as the final SO₂ concentration). These values are compared to that of the actual process/ plant, and the differences, the residuals, provide feedback to a Prediction block. At each sampling instance, two types of calculations are performed using the predictions: setpoint and control calculations. Constraints on both the MVs (inputs) and CVs (outputs) can be included in both types of calculations (Seborg *et al.*, 2010).

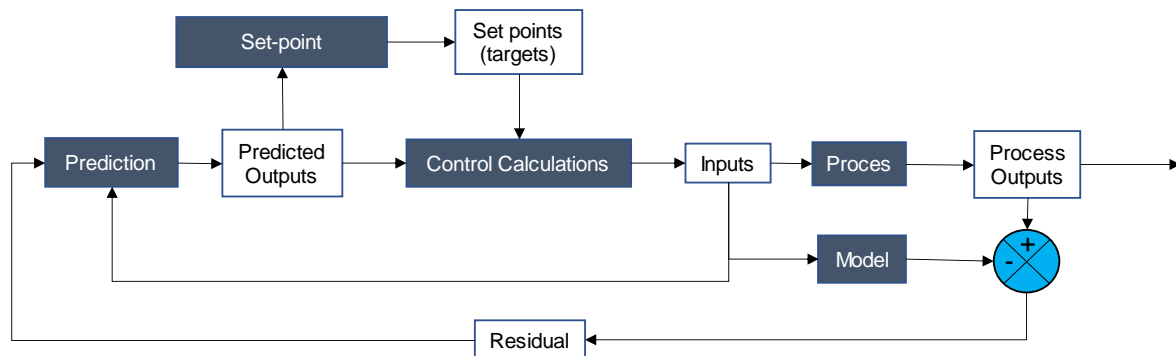


Figure 42: Block flow diagram of MPC.

The setpoint calculations provide the targets for the control calculations and are calculated from an objective function. MPC, therefore, relies on real-time optimisation of a linear objective function based on a steady-state model of the process. As part of the top-down approach, the objective of the plantwide control was to maximise the conversion/ minimise the final SO₂ concentration. The setpoint calculations will be based on the controllers identified in the regulatory layer. The varying process conditions can influence the constraints and, thereby, the optimal setpoint values of the model. Constraints applicable in this plant/model include ensuring the fans do not enter surge conditions and keeping the gas temperature above the acid dewpoint temperature.

4.7 Step 6: Real-Time Optimisation

Real-time optimisation (RTO) considers continuously computing and implementing the optimal set points for the controlled variables. To find this optimal operating point, the active constraints and costs of running the plant should be considered (Skogestad, 2004). Given that this plant does not represent an actual installed plant, optimisation of the set point values has little value at this stage of the model development.

Typical real-time optimisation problems can solve nonlinear and linear objective functions, even in multivariable optimisation cases. For real-time optimisation, steady-state models are usually used as the plant is meant to operate at steady-state. The RTO calculations/iterations

are only initiated when the plant is operating at steady-state, i.e., key measurements are within permissible limits. Optimisation software, such as software from AVEVA, Yokogawa, and Honeywell, to name a few, is available for implementing RTO. The RTO iterations include a step for data validation and updating process parameters that form part of mass and energy balances, such as heat exchanger fouling coefficients. After this step, operating and economic data are used as input to determine the new optimum set points. The new setpoints will be implemented only if the process is operating at the same steady state as before the calculation was initiated and if the new setpoints are statistically different (Seborg *et al.*, 2010).

One shortcoming of MPC is that it relies on a linear objective function of a steady-state model, where not all objective functions are linear, and a plant rarely operates under steady-state conditions. The model predictive controller mentioned in Step 5 provides a manner of real-time optimisation as it calculates the sequence of control moves (changes to the inputs) to move the predicted response to its setpoint optimally. Larsson & Skogestad (2000) described different control architectures used in plantwide control, one of which is the multilayer control architecture. This architecture has algorithms that connect higher-level controllers, such as RTOs, to lower-level controllers, such as MPCs, with or without a coordination layer. The interaction between the regulatory layer, MPC, and RTO is depicted in Figure 43. The coordination layer manages information from both levels and finds feasible local references for the MPC that correlate with the global solution calculated by the RTO.

When the MPC is implemented in an online plant, the economic and control objectives and the variability in process parameters should be evaluated. Implementing an RTO can be beneficial if the process variables are subject to large variations. Similarly, if the operation is such that it has energy consumption, it might require RTO to optimise the fuel vs electricity consumption based on utility rates.

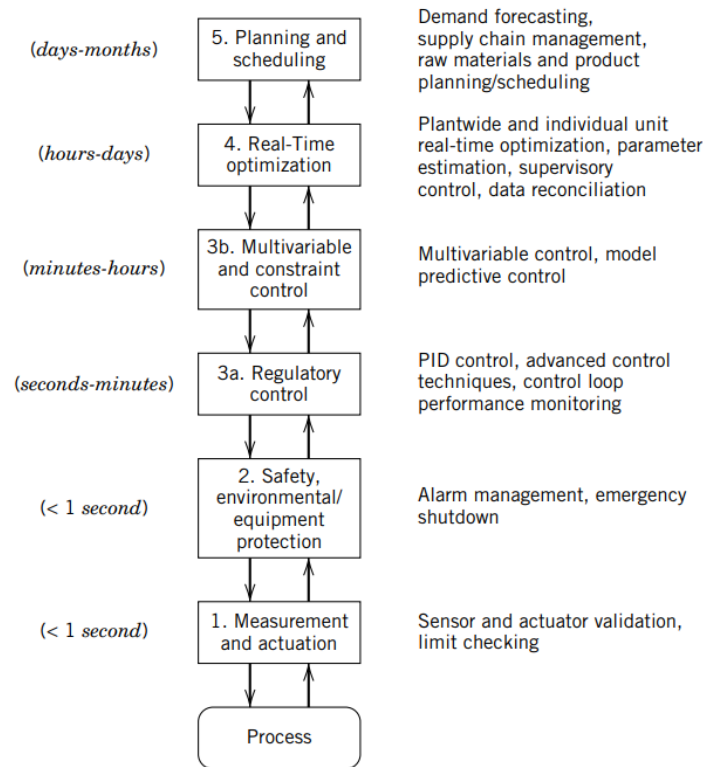


Figure 43: Process control and optimisation levels (adapted from Seborg *et al.* (2010), Figure 19.2).

4.8 Step 7: Model validation

Skogestad (2002 and 2004) describe this model validation step as validating the selected control structure using a nonlinear dynamic simulation. However, in this case, the nonlinear dynamic simulation was used to develop the control model instead of using a purely mathematical approach. The combination of controlled and manipulated variables has been proven to work in the dynamic HYSYS model and the results described in the preceding steps.

The open loop step responses recorded in the HYSYS *DMCplus Controller* during the step tests were imported to Aspen's *DMC Builder*, as shown in Figure 45 to Figure 47. The parameter trials were set up as shown in Figure 44. The finite impulse response (FIR) is simple and fast and can easily fit higher-order data (Aspen Technology, 2019b). Originally, the prediction, frequency uncertainty and time uncertainty were selected for the 30-minute time to steady state case. However, the uncertainty plots indicated too much uncertainty, and these selections were changed to the 10-minutes to steady state case. The FIR algorithm could be applied to the recorded data as the step tests were carried out individually – similar to single-input-single-output (SISO) models. The subspace models, on the other hand, are suitable for multiple-input-multiple-output (MIMO) models and calculate parametric state-space models (Aspen Technology, 2019b).

Subspace Trials

+ Add
 ✎ Edit
 ✕ Delete
 Template: Select a Template ...
 ✎ Edit
 Grouping:

	Time to Steady State	Oversample	Max Order	Prediction	Uncertainty	Time Uncertainty
	15	1	30	<input type="checkbox"/>	<input type="checkbox"/>	<input type="checkbox"/>
	30	1	30	<input type="checkbox"/>	<input type="checkbox"/>	<input type="checkbox"/>

FIR Trials

+ Add
 ✕ Delete

	Time to Steady State	Coefficients	Smoothing	Prediction	Uncertainty	Time Uncertainty
	10	15	5	<input checked="" type="checkbox"/>	<input checked="" type="checkbox"/>	<input checked="" type="checkbox"/>
	20	30	5	<input type="checkbox"/>	<input type="checkbox"/>	<input type="checkbox"/>
	30	60	5	<input type="checkbox"/>	<input type="checkbox"/>	<input type="checkbox"/>

Figure 44: Parameter trial setup for open loop step responses.

Figure 45 shows the unadjusted open-loop step responses. In contrast, in Figure 46, the *Typical Move* option was selected, which implements a function similar to scaling by showing the relative magnitudes in step responses for a certain controlled (output) variable. No corner flag is visible on any of these figures, indicating that the system response is stable and no integrating states are present (Aspen Technology, 2019b).

A bode frequency and time uncertainty plot (red) with a 2-sigma uncertainty band (green) is shown in Figure 48 and Figure 49, respectively, for each input-output variable pair. The output signal-to-noise ratio is shown in blue on the frequency uncertainty plot (Figure 48). There is no visible frequency uncertainty band on any input-output variable pair.

The *DMC Builder* software automatically determined the typical move but was overridden where this calculation differed from the step size recorded in Table 6. Applying the typical move makes it easier to see the manipulated variables that have little or no effect on the possible controlled variables. Figure 47 shows the open loop responses, with the typical move

enabled but of only the grade A, B, and C results. In Figure 47, it is clear 1R does not affect any of the possible controlled variables, confirming the decision to fix its setpoint (Section 4.5). In Figure 49 1R also shows has a large time uncertainty band with all controlled variables. It is evident that selecting the pairing of SO₂ concentration and electric heater temperature is the clear decision, as the electric heater is the only MV that impacted the SO₂ concentration (with a grade higher than C).

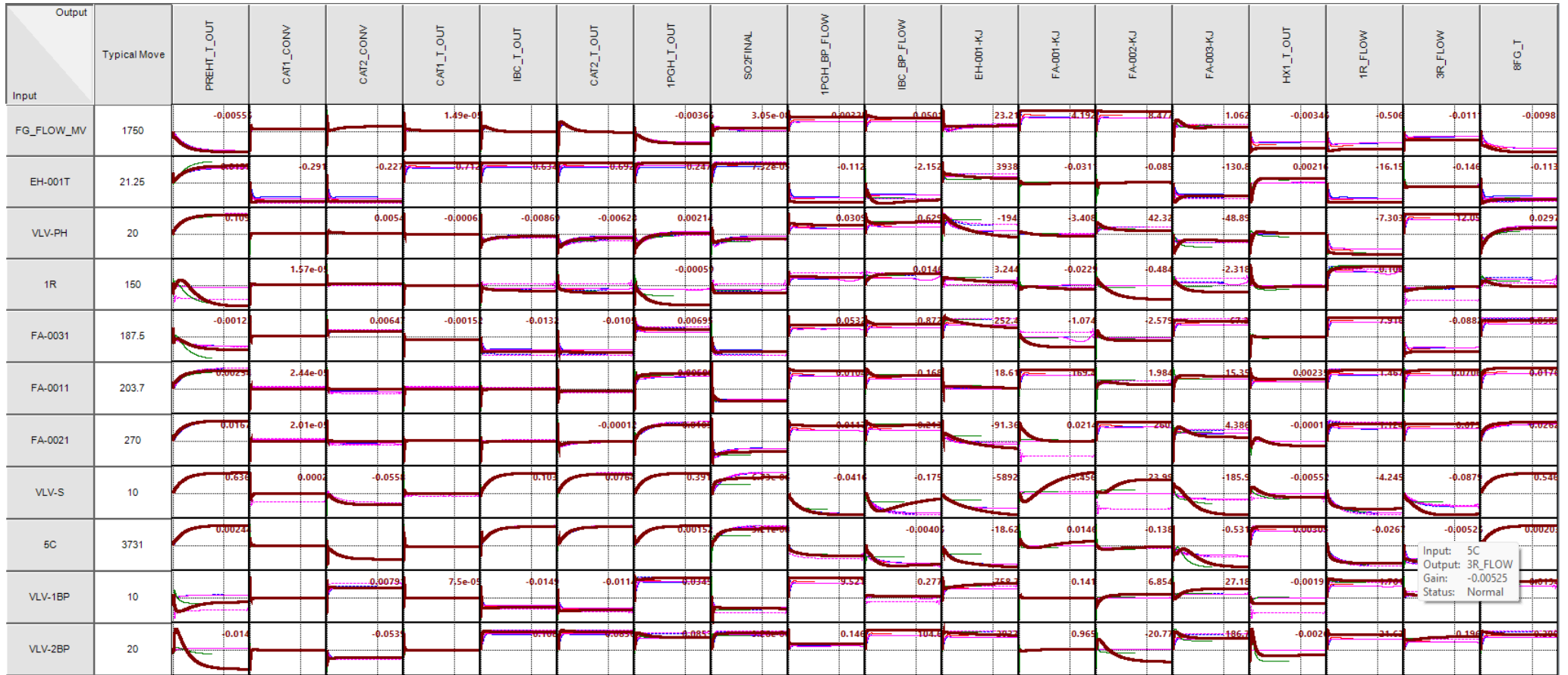


Figure 45: Open loop step response of manipulated variables (SISO) – typical move disabled.

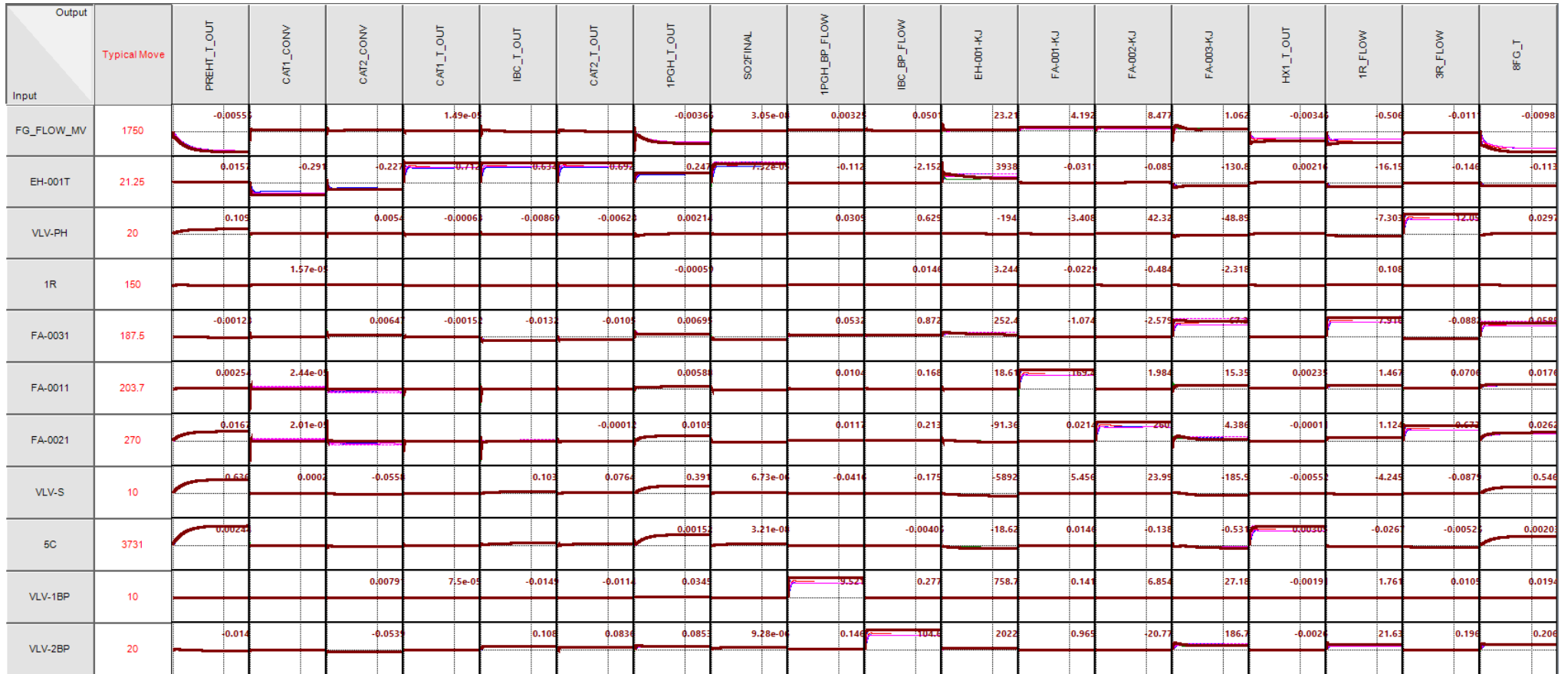


Figure 46: Open loop step response of manipulated variables (SISO) – typical move enabled.

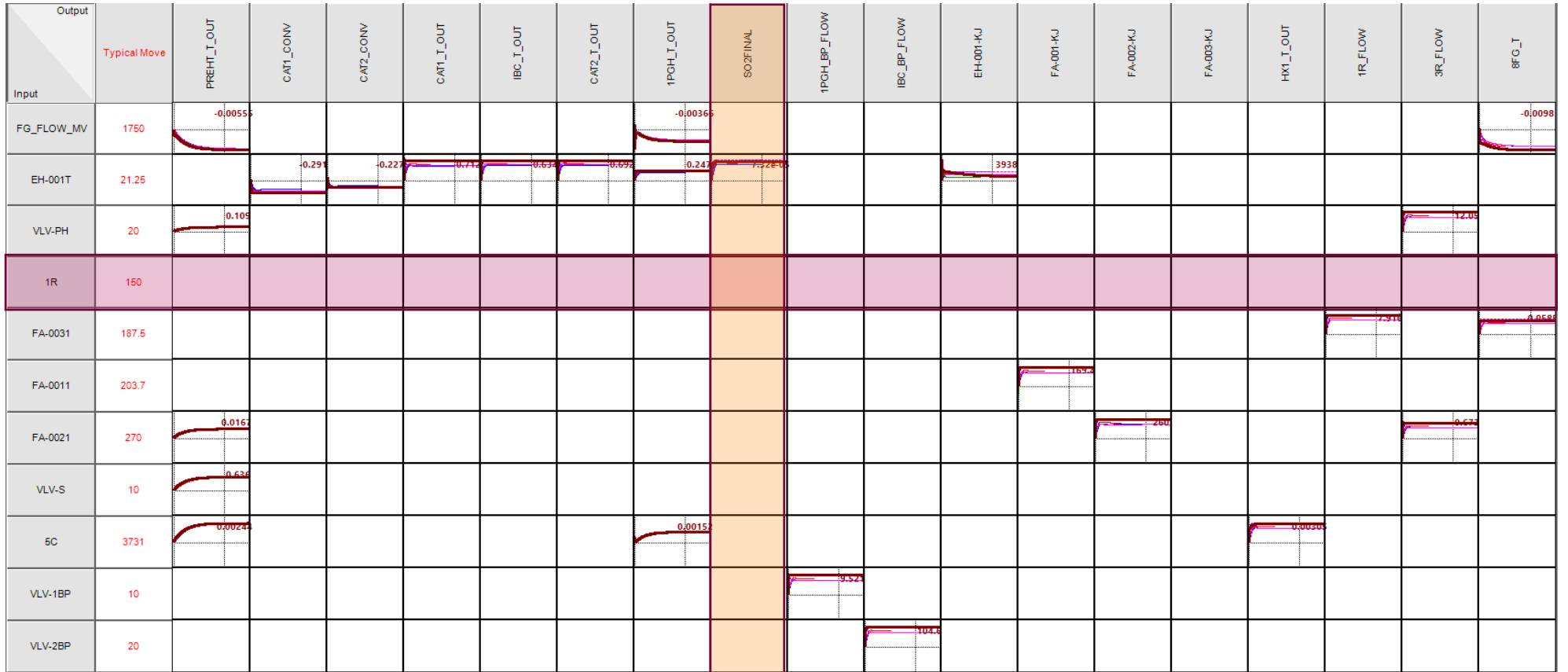


Figure 47: Open loop step response of manipulated variables (SISO) – typical move enabled, only grades A-C.

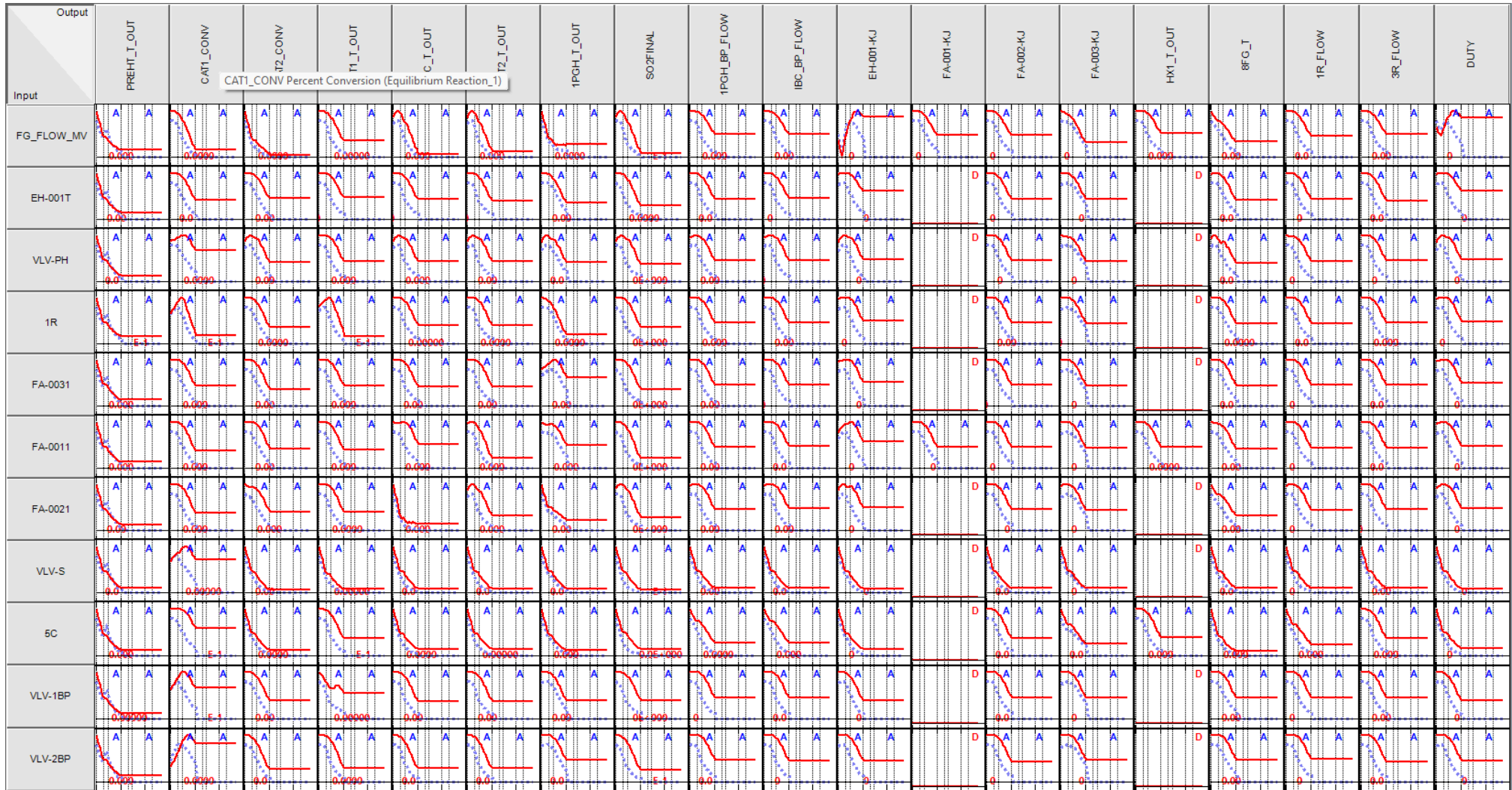


Figure 48: Frequency uncertainty of the open loop step response using FIR parameter trials with 10 minutes to steady state.

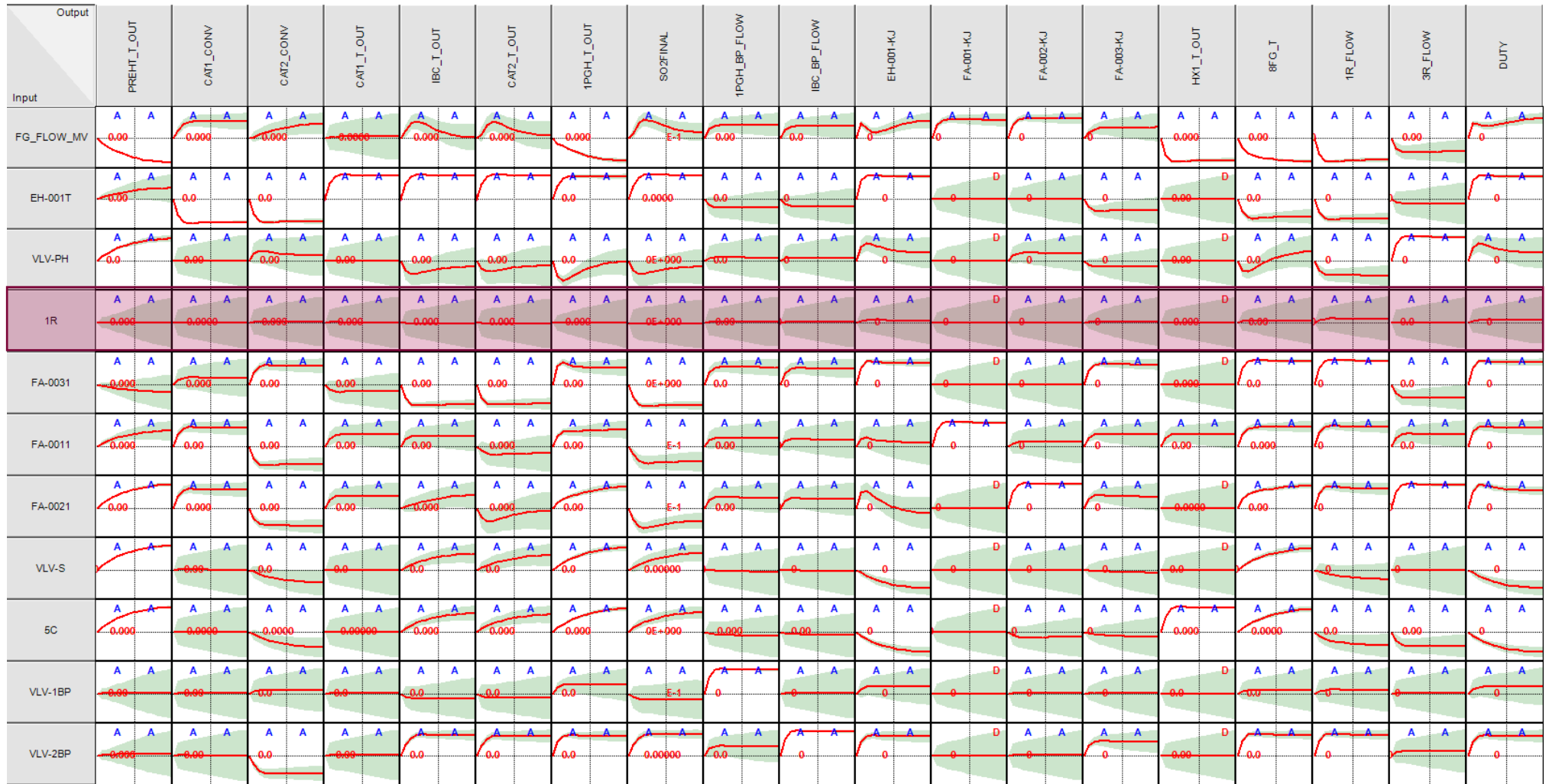


Figure 49: Time uncertainty of the open loop step response using FIR parameter trials with 10 minutes to steady state.

5 Conclusion and Recommendations

Implementing the methodology described by Skogestad (2004) to determine the pairing of controlled and manipulated variables in an acid plant provided a systematic approach to solving the plantwide control problem. Using a simulated dynamic model from the start provided a means of continually validating decisions, such as the choice of controlled and manipulated variables. Using the dynamic model effectively negated the requirement for an iterative process, i.e., having to go back and re-evaluate some of the previous decisions made after the validation was done in steps 6 or 7.

The simulated model removed the necessity for complex mathematical functions and relied less strongly on experience to a certain extent. The simulated model also enabled the opportunity to evaluate the dynamic unit-to-unit interactions. Therefore, the dynamic model could be used to consider the combination of various control combinations and evaluate their effects without the risk of causing damage to an actual plant and without the influence of noise. This approach of using a dynamic simulation model to implement a plantwide control model has the following benefits:

- Providing a link between steady-state optimisation and process control.
- Continuous validation of the decisions made is a less iterative procedure.
- Consideration of self-optimising control.
- No complex mathematical analysis
- Improves fundamental understanding of the process and interactions in the process.
- Possibility to apply the solution to similar plants with minimal adjustment.
- The opportunity of implementing DMC or MPC models to live plants (software dependent).
- Considers control and operation of the plant and the overall (plantwide) control objective.

This is a simplified model of an acid plant, and many other measurements and controls might be required in an operating plant, such as vibration and condition monitoring of fans. Future work can include calibrating this model to an operational plant and comparing the results. As this is only a portion of the plant, further development of the simulation may be required to include noise and other disturbances identified in the operational plant.

This model can be further developed to encompass more upstream, downstream and/ or auxiliary plant areas. Thereafter, the plantwide control methodology can be applied to see whether there are any changes in the controlled and manipulated variable pairings.

6 References

Aspen (2019a), "Aspen HYSYS Help", 11. Aspen Technology, Inc.

Aspen (2019b), "DMC Builder Help", 11. Aspen Technology, Inc.

Jensen, JB, and Skogestad, S (2009), "Steady-state operational degrees of freedom with application to refrigeration cycles" *Industrial & Engineering Chemistry Research*, 48 (14), 6652-6659.

Jones, R (2005), "An overview of South African PGM smelting" *Nickel and Cobalt 2005: Challenges in Extraction and Production*, 44th Annual Conference of Metallurgists.

Juliani, R, and Garcia, C (2017), "Plantwide control: a review of design techniques, benchmarks and challenges" *Industrial & Engineering Chemistry Research*, 56 (28), 7877-7887.

King, MJ, Davenport, WG, and Moats, MS (2013), *Sulfuric Acid Manufacture - Analysis, Control, and Optimization*, Elsevier.

Larsson, T, and Skogestad, S (2000), "Plantwide control - a review and a new design procedure" *Modeling, Identification and Control*, 21.

Lausch, HR, Wozny, G, Wutkewicz, M, and Wendeler, H (1998), "Plant-wide control of an industrial process" *Chemical Engineering Research and Design*, 76 (2), 185-192.

Luyben, ML, Tyreus, BD, and Luyben, WL (1997), "Plantwide control design procedure" *AIChE Journal*, 43 (12), 3161-3174.

Martínez-Sánchez, O, Gómez-Castro, FI, and Ramírez-Corona, N (2022), "Plantwide control of a biodiesel production process with variable feedstock" *Chemical Engineering Research and Design*, 185, 377-390.

Mbohwa, C, and Mabiza, J (2015), "Environmental impacts assessment of the cleaning of plant off-gas in the recovery process of PGM at the Anglo American Platinum LTD, South Africa", paper presented at *International Conference on Operations Excellence and Service Engineering*, 2015, Orlando, Florida, USA.

Rosenberg, H (2006), "Topsoe wet gas sulphuric acid (WSA) technology—an attractive alternative for reduction of sulphur emissions from furnaces and converters", paper presented at *International Platinum Conference 'Platinum Surges Ahead'*, 2006.

Schlesinger, ME, King, MJ, Sole, KC, and Davenport, WG (2011), *Extractive Metallurgy of Copper*, 5th edition, Elsevier.

Seborg, DE, Mellichamp, DA, and Edgar, TF (2010), *Process Dynamics and Control*, 3rd edition, John Wiley & Sons.

Shen, F, Ye, L, Guan, H, and He, Y (2023), "Enhanced control structure design for an industrial off-gas system: Simple reconfigurations benefit the economy" *Heliyon*, 9 (1), e12934.

Skogestad, S (2000), "Plantwide control: the search for the self-optimizing control structure" *Journal of Process Control*, 10 (5), 487-507.

Skogestad, S. 2002. "Plantwide control: Towards a systematic procedure." In *Computer Aided Chemical Engineering*, edited by Johan Grievink and Jan van Schijndel, 57-69. Elsevier.

Skogestad, S (2004), "Control structure design for complete chemical plants" *Computers & Chemical Engineering*, 28 (1), 219-234.

Skogestad, S, and Postlethwaite, I (2005), *Multivariable Feedback Control: Analysis and Design*, 2nd edition.